Cellular Atlas of Laryngeal and Vocal Fold Embryogenesis, Maturation and Aging

By

Tadeas Lunga MD

A dissertation submitted in partial fulfillment of requirements for the degree of

Doctor of Philosophy

Communication Sciences and Disorders

at the

University of Wisconsin – Madison

2024

Date of final oral examination: 4/26/2024

The dissertation is approved by the following members of the Final Examination Committee:
Susan L. Thibeault, Professor, Surgery
Nathan V. Welham, Professor, Surgery
Christina M. Kendziorski, Professor, Biostatistics and Medical Informatics
Deneen M. Wellik, Professor, Cell & Regenerative Biology
David O. Francis, Associate Professor, Surgery

ACKNOWLEDGEMENTS

First and foremost, I would like to express my deepest gratitude to my mentor, Dr. Susan Thibeault, for her unwavering support throughout my research and medical career. Dr. Thibeault, you are a shining example of how hard work pays off, and I am incredibly grateful for your guidance and the opportunity you have given me. I am committed to carrying forward the lessons I have learned from you into my future as a physician-scientist, and I will make sure to uphold your reputation with honor.

Secondly, I would like to thank my parents, Vlasta and Pavel. Your unwavering support and belief in me have been the bedrock of my journey to becoming a scientist. This work is as much a testament to your sacrifices and encouragement as it is to my dedication.

I am also immensely grateful to my beloved wife, who has been by my side throughout the entirety of my PhD journey. We met in this very program, and her steadfast support and understanding have been my anchor through the highs and lows of this pursuit.

I dedicate this work to my grandmother, who unfortunately passed away during my PhD. Her love, wisdom, and unwavering belief in me continue to inspire me every day.

I am very thankful to my committee members Drs. Wellik, Francis, Kendziorski, and . Welham. Your support and encouragement have been invaluable to me throughout this journey.

Lastly, I would like to express my gratitude to Elliot Xie, a PhD student in Dr. Kendziorski's laboratory. Without him, I would not have been able to finish this project.

Finally, I would like to thank my lab members. You are a great group, and I have truly enjoyed working with you, from our research collaborations to our lunch breaks. The past five years have been filled with fun memories, and I wish each of you the very best on your future journeys.

TABLE OF CONTENTS

LIST OF FIGURES

LIST OF ABBREVIATIONS

VF	vocal fold
VFs	vocal folds
scRNA-seq	single-cell RNA sequencing
Epi	epiglottis
TC	thyroid cartilage
CC	cricoid cartilage
AC	a pair of arytenoid cartilages
IA	transverse/oblique interarytenoid muscles
LCA	lateral cricoarytenoid
PCA	posterior cricoarytenoid muscles.
CT	cricothyroid muscle
TA	thyroarytenoid muscle
LP	lamina propria
SLLP	superficial lamina propria
HA	hyaluronic acid
DLLP	deep layer of lamina propria
VFFs	vocal fold fibroblasts
ECM	extracellular matrix
PGE2	prostaglandin E2
Ar	alar cartilage
SCA	superior cricoarytenoid muscle
Ep	epithelium
RP	respiratory primordium

RD	respiratory diverticulum
PPhF	primitive pharyngeal floor
4PP	fourth pharyngeal pouch
PLPh	primitive laryngopharynx
BPB	bronchopulmonary buds
EL	epithelial lamina
E	embryonic
LG	laryngeal groove
TEF	tracheoesophageal fistula
MRI	magnetic resonance imaging
IPF	interstitial pulmonary fibrosis
HCC	hepatocellular cirrhosis
HNSCC	head and neck squamous cell carcinoma
W	week
P	postnatal
H&E	hematoxylin and eosin staining
BMPC	basement membrane producing cell
PBEC	proliferating basal epithelial cell
NPBEC	nonprolifetating basal epithelial cell
SBEC	suprabasal epithelial cell
SEC	secretory cell
CC	ciliated cells
EPMP	early proliferative mesenchymal progenitors

Ch	chondroblasts
ST	stromal cells
FB	fibroblasts
MSC	muscle stem cell
SMC	skeletal muscle cell
SMMC	smooth muscle cell
MG	macrophages
NEC	neuroendocrine cells
SchC	Schwann cells
BVEC	blood vessel epithelial cell
LVEC	lymphatic vessel epithelial cell
FACS	fluorescence-activated cell sorting
RNAish	RNA in-situ hybrididization
DEG	differntally expressed genes
A	arytenoid cartilage
UMI	unique molecular identifiers
CPM	counts per million
PCA	principal component analysis

ABSTRACT

Introduction

Embryogenesis, maturation, and aging of the larynx and vocal folds (VF) are intricate processes crucial for voice production. Structural variations in VF mucosa across different age groups, from newborns to the elderly, predispose individuals to age-associated voice disorders. Treatment options for these disorders remain limited due to gaps in understanding the cellular and genetic processes underlying these structural changes. To address these gaps, our study aimed to identify and comprehend the cellular heterogeneity of VF across the lifespan using single-cell RNA sequencing. In addition, we aimed to identify differentially expressed genes across lifespan and developmental trajectories and relationships between different cell populations.

Methods

We used the Bl6 mouse strain, harvesting larynges at various embryonic (E) and postnatal (P) stages. Tissues were processed into single-cell suspensions, and cDNA libraries were prepared and sequenced. Data underwent quality control, normalization, integration, and clustering with annotations based on differentially expressed genes (DEG). In addition, we performed pseudotime trajectory analysis for epihelial and mesenchymal cell populations. We also performed DEG analysis across timepoints for major epithelial, mesenchymal, and immune cell populations.

Results

Clustering identified 23 major cell populations, including epithelial, mesenchymal, endothelial, immune, and neuronal populations. Epithelial clusters included basement membrane-producing cells (BMPC), proliferating basal epithelial cells (PBEC), nonproliferating basal epithelial cells (NPBEC), suprabasal epithelial cells (SBEC), ciliated epithelial cells (CC), and secretory epithelial cells (SEC). Mesenchymal clusters included early proliferating mesenchymal progenitors (EPMP), stromal cells, fibroblasts (FB), chondroblasts, chondrocytes, smooth muscle cells, and skeletal muscle cells. Immune cell clusters comprised macrophages (MG), dendritic cells, neutrophils, and lymphocytes. Endothelial cells and neuronal clusters were also identified. Cell complexity increased from embryonic stages to adulthood, peaking between adolescence and adulthood before declining. Prenatal stages showed predominance of mesenchymal populations. Postnatal stages showed an increase in epithelial populations. In later postnatal stages there was an influx of immune cells specifically neutrophiles and pro-inflammatory macrophages. The DEG analysis across timpoints revealed functional maturation of epithelial cells starting 4W of age in PBEC, NPBEC, and SBEC. FB showed collagen production maturation between E18.5 to 4W. Trajectory analysis revealed EPMP gave rise to chondroblasts, fibroblasts, and skeletal muscle cells. The PBEC was a precursor to major differentiated cell populations such as SBEC, SEC, and CC. Lastly, we revealed multiple subtypes for major cell populations such as BMPC, PBEC, NPBEC, SBEC, SEC, EPMP, FB, and MG.

Conclusion

Our single-cell atlas reveals the cellular heterogeneity of VF and laryngeal tissue throughout development. Major cell populations were established early, with mesenchymal populations predominantly in embryonic stages and epithelial cell populations in postnatal development.

Epithelial cells mature at 4W. FBs mature earlier between E18.5 to 4W. The cell atlas of laryngeal and VF development across lifespan serves as a benchmark for designing novel engineered-based strategies for VF tissue restoration and/or replacements, differentiation trajectories, cross species tissue comparison and translational research focused on age-, gene-, and population-specific treatment options.

CHAPTER ONE: INTRODUCTION

Background and Significance

Voice disorders can affect any age group from neonates to the elderly (Bainbridge et al. 2017). The underlying causes across the lifespan differ by age group; neonates can develop voice disorders secondary to congenital malformations whereas elderly due to age-related degenerative changes to the vocal fold (VF) mucosa (Martins et al. 2016). The 12-month prevalence of voice disorders is 6% - 7%, 7% - 8%, and 20% - 29% in young-to-middle-aged adults (18-44), middle-aged adults (44-64) and elderly (65+), respectively (Bainbridge et al. 2017). Vocal impairment negatively impacts psychological, social, and occupational function, ultimately diminishing the quality of life (Murry and Rosen 2000; Merrill, Anderson, and Sloan 2011). While treatment options have improved, medical and behavioral treatment for voice disorders is not yet age-specific and precise specific to cellular and molecular targets.

VFs lie within the larynx, which is situated at the crossroads of the respiratory and digestive tracts. Apart from phonation, VFs protect the airway during swallowing and abduct during breathing. Laryngeal and VF development across the lifespan is complex and highly understudied. It initiates *in utero,* when the larynx and VF gain their shape and begin to function, and continues postnatally when the larynx and VF increase in size and undergo morphological changes throughout the process of maturation that is necessary for proper phonation (Ximenes Filho et al. 2003; Hartnick, Rehbar, and Prasad 2005; Hirano, Kurita, and Sakaguchi 2009; Boudoux et al. 2009; Roberts, Morton, and Al-Ali 2011; Kuhn 2014a; Lungova and Thibeault 2020). An improved understanding of how VF tissue develops is necessary to improve our understanding of biological, cellular, and molecular processes that are activated at

specific stages of the laryngeal and VF development. This knowledge will be foundational to tailor age-specific treatment strategies for voice disorders across the lifespan.

Several studies have focused on the characterization of laryngeal and VF development in humans and murine models (Zaw-Tun and Burdi 1985b; Sañudo and Domenech-Mateu 1990; Hartnick, Rehbar, and Prasad 2005; Tabler et al. 2017; Lungova et al. 2015a; 2018; Mohad et al. 2021). Human studies have evaluated laryngeal and VF morphology using classic Hematoxylin & Eosin staining at defined key stages of laryngeal embryonic and postnatal development (Gatti, MacDonald, and Orfei 1987; Sañudo and Domenech-Mateu 1990; Zaw-Tun and Burdi 1985b; C. M. Sapienza, Ruddy, and Baker 2004; Hartnick, Rehbar, and Prasad 2005; Miklaszewska et al. 2010; Fayoux et al. 2008). Studies using murine models have defined major morphogenetic events that occur during murine laryngeal/VF embryogenesis. These events were correlated with human embryonic development to confirm that both species progress through similar developmental stages. Moreover, studies using transgenic mice elucidated the mechanistic roles of key genes and signaling pathways in normal and aberrant VF development and VF-associated congenital diseases (Tabler et al. 2017; Lungova et al. 2018; Mohad et al. 2021). A recent study by Wendt et al. 2022 provided a global characterization of genes and signaling molecules that are expressed at different stages of murine laryngeal/VF embryogenesis and postnatal maturation by bulk RNA sequencing (bulk RNA seq) as compared to the developing trachea and esophagus. Bulk RNA seq delivers average global gene expression profiles of thousands of cells but is not able to capture gene expression of individual cells or specific cell types (Li and Wang 2021). Therefore, there is still a paucity of data that characterize all cell populations that reside in the laryngeal/VF mucosa and supporting structures, their functional and developmental relationships

and their contribution to laryngeal and VF morphogenesis and postnatal maturation (Wendt et al. 2022).

Comprehensive characterization of cell populations in organs is possible using advanced single-cell RNA-sequencing (scRNA-seq) technologies. This technology is capable of detecting heterogeneity among individual cells, specific cell types, to delineate cellular reciprocal interactions, and to establish cellular maps (Mereu et al. 2020; Hwang, Lee, and Bang 2018; Chen et al. 2021; Karlsson et al. 2021). One important application of scRNA-seq is to create high-resolution catalogs of all cells in a tissue of interest, known as a cell atlas. Cell atlases are key sources for the discovery of new diagnostic markers and therapeutic targets which could ultimately improve precise/early diagnosis and treatment outcomes (Tang et al. 2019). Cell atlases are transforming our understanding of biology, health, and disease (Panina et al. 2020).

The aim of this dissertation project, utilizing scRNA-seq technology, was to provide a comprehensive characterization of the cell populations that contribute to the embryonic and postnatal development of the murine larynx and VFs including age-related degenerative changes in the VF mucosa while establishing the first murine cell atlas of laryngeal and VF development across the life span. These findings will serve as a valuable reference for the evaluation of functional prognosis and treatment outcomes in congenital laryngeal/VF malformations and age-associated VF disorders. Further, the results will serve as a benchmark for developing age-specific treatments for voice disorders across the lifespan and designing bioengineered VF mucosa for VF tissue restoration and replacement.

Human Laryngeal and Vocal Fold Structure and Function

Human Laryngeal Anatomy and Function

The larynx is situated in the anterior portion of the neck above the trachea. It serves as a passageway between the upper and lower airways. The VFs are housed within the larynx. The functions of the larynx are to act as a sphincter that protects lower airways and lungs from foreign materials, to maintain an open airway during breathing and to serve as a sound source for voice production facilitated by the VFs (Sapienza and Hoffman 2020; Lungova and Thibeault 2020). The laryngeal framework is comprised of cartilages, extrinsic and intrinsic laryngeal muscles, ligaments and moveable joints (Sapienza and Hoffman 2020). Laryngeal cartilages include the epiglottis (Epi), thyroid cartilage (TC), cricoid cartilage (CC), a pair of arytenoid cartilages (AC) which rock on the CC to facilitate VF motion (Lungova and Thibeault 2020). Human specific cartilages compared to mice are cuneiform and corniculate cartilages. (Lungova and Thibeault 2020).

Laryngeal cartilages provide attachment points for laryngeal muscles. Laryngeal muscles are skeletal in origin that voluntarily control VF adduction for voicing and swallowing and VF abduction for breathing. VF adduction is facilitated by transverse/oblique interarytenoid muscles (IA) and lateral cricoarytenoid (LCA) whereas VF abduction is controlled by the posterior cricoarytenoid muscles (PCA). The cricothyroid muscle (CT) works as a VF tensor (Lungova and Thibeault 2020). The thyroarytenoid muscle (TA, also known as vocalis muscle) forms the deepest portion of the VFs. TA muscle was shown to play a role in anterior VF adduction (Yin and Zhang 2014).

Human VF Histology

The VFs are musculomembranous paired tissues that stretch between the TC and ACs. The unique composition of the VF mucosa is essential for vocal quality and when damaged can lead to significant dysphonia. VF mucosa is protected by a multilayered non-keratinizing stratified squamous epithelium that can withstand high amounts of shear stress and serves as a barrier to irritants and microorganisms (Gray et al. 2000; Levendoski, Leydon, and Thibeault 2014). The epithelial layer connects to the lamina propria (LP) via the basement membrane. Hirano et al. divided the lamina propria into three layers superficial, intermediate and deep LP based on extracellular matrix (ECM) organization. The superficial layer of LP (SLLP) also known as Reinke's space has a viscous and gelatinous texture that has a limited concetration of collagen and elastin fibers (Gray et al. 2000c; Kuhn 2014). The intermediate layer of LP (ILLP) contains mostly elastin and hyaluronic acid (HA). Elastin is present in three forms within the LP – oxylatan, elaunin, and elastic fibers (Gray et al. 2000; Moore and Thibeault 2012). Elastin plays a pivotal role in VF vibration because it provides VF LP the ability to stretch and recoil without a deformation (Moore and Thibeault 2012). HA provides shock adsorption and viscosity (Ward, Thibeault, and Gray 2002). The deep layer of LP (DLLP) is rich in collagen fibers, specifically collagen I and III, which provides strength and support. DLLP attaches to the vocalis muscle. According to the body-cover theory postulated by Hirano the stratified squamous epithelium and SLLP form the VF cover and DLLP with the TA (vocalis muscle) form the body (Hirano 1974). ILLP is considered a transitional layer. Overall, the density of LP changes from a jelly-like structure to stiffer layers allowing the production of mucosal wave that occurs during the VF vibration (Lungova and Thibeault 2020; Kuhn 2014b).

Human Voice Production

VF vibration modulates airflow through the glottis and produces a buzzing tone (a sound source) which is filtered by the vocal tract and subsequently shaped by speech articulators to generate a recognizable voice and speech (Zhang 2016; Bailly et al. 2018). VF vibration is enabled by the layered structure of the LP specifically; the VF cover glides over the body from the inferior to the superior surface of VFs. The average fundamental frequency of VF vibration for males ranges from 100 to 150 Hz, whereas for females it ranges from 180 to 250 Hz (Zhang 2016b; Gunter 2004). The fundamental frequency is perceived as pitch and is determined by the mass and tension of the VFs and air pressure during vibration (Lungova and Thibeault 2020). VF mass and tension are typically regulated via muscle contraction and relaxation of the various laryngeal muscles (TA, PCA, PCA, CT). For example, increased tension in VF is achieved by CT muscle contraction which leads to an increase in fundamental frequency (pitch). In addition, VF mass can be influenced by the increased epithelial thickness and ECM composition of VF LP. VF mucosa undergoes significant mechanical stress during VF collision, thus intense VF vibration over prolonged periods also known as phonotrauma, is a major risk factor for developing benign VF lesions such as VF nodules (Levendoski, Leydon, and Thibeault 2014b).

Cell populations of Human Adult Larynx and VF Epithelium

The luminal surface of the VFs is covered by a protective layer of stratified squamous epithelium (Fig. 1) which forms a physical barrier against injury and microorganisms. Approximately 5-10 epithelial layers make up the adult VF surface (Levendoski, Leydon, and Thibeault 2014a). The epithelium is composed of the basal layer that contains less differentiated proliferating cells that exit the cell cycle as they migrate toward the lumen and stratify (Fig. 1).

The luminal cell layer contains terminally differentiated cells (Fig. 1) that slough off the surface during mechanical abrasion when VF approximate and collide during a phonatory cycle (Levendoski, Leydon, and Thibeault 2014b). The same type of epithelium is found in mechanically exposed tissues such as the esophagus, vagina, and oral cavity (Squier, Monographs, and 2001 n.d.). Epithelium on the surface of VFs transition into pseudostratified columnar epithelium cranially (at the laryngeal vestibule) and caudally, at the subglottis. The pseudostratified epithelium is the main type of epithelium in the upper respiratory tract and is composed of ciliated columnar cells and mucous secreting goblet cells (Knight and Holgate 2003). Goblet cells are found also on the surface of false VFs and subglottis (Kutta et al. 2002).

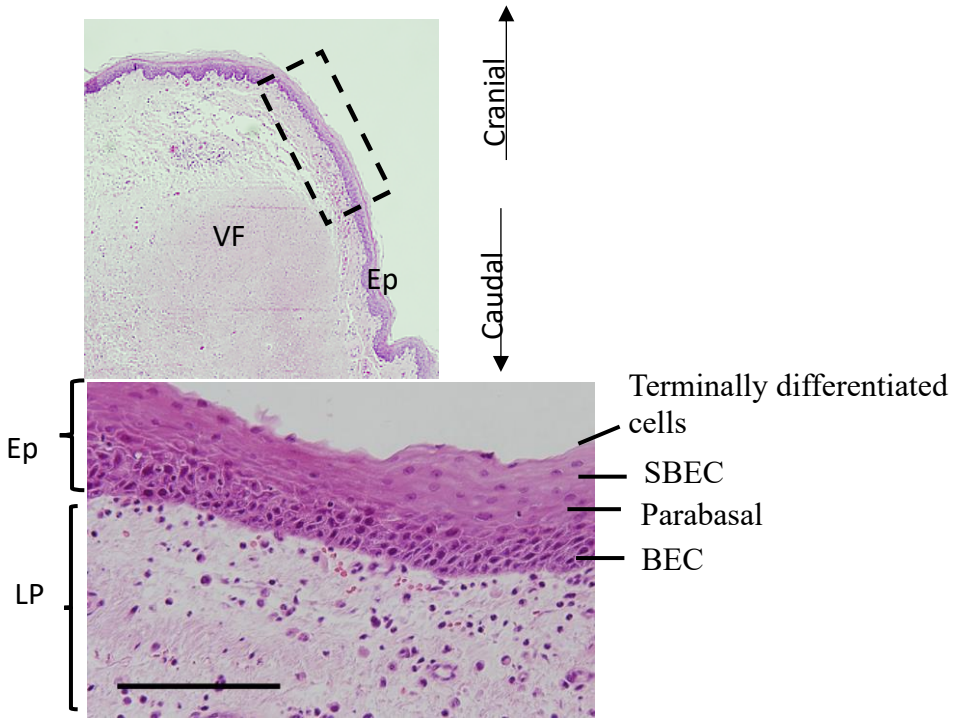

Figure 1: Laryngeal and vocal fold epithelium. *Hematoxylin-eosin staining of stratified squamous epithelium lining the true vocal folds showing the basal, parabasal, suprabasal cell layers and terminally differentiated cells. BEC, Basal Epithealial Cells; SBEC, Suprabasal Epithelial Cells; Ep, Epithelium; LP, Lamina Propria; VF, Vocal Fold.*

Individual cells in the VF epithelium are connected by various types of cell junctions. Cell junctions are protein complexes that provide cell adhesion, cell communication, and epithelial barrier properties (Gill et al. 2005). There are three groups of cell junctions; tight, anchoring, and communicating junction, named based on their function (Gill et al. 2005). To withstand mechanical forces and serve as a protective layer, the luminal layer of cells is joined by tight junctions which are composed of proteins called occludins forming complex zonula occludens. Tight junctions are the main determinant of epithelial permeability via the paracellular pathway. Anchoring junctions include desmosomes and hemidesmosomes. Their function is to maintain epithelial integrity by creating cell-to-cell connections (Levendoski, Leydon, and Thibeault 2014b). Desmosomes connect adjacent cell membranes, whereas hemidesmosomes connect the basal layer to the basal membrane. Their function is essential for stabilizing epithelial sheets during vibration. Communicating junctions also known as gap junctions form intercellular channels that allow for signaling between adjacent cells by exchanging small signaling molecules or changing ion gradients.

The larynx is a highly responsive sensory organ that triggers protective mechanisms such as cough, swallowing, and apnea in response to chemical, mechanical, and thermal stimuli (Jetté et al. 2020). Chemicals can trigger responses in both intraepithelial nerve fibers and in specialized chemosensory cells that could be scattered in VF epithelium or organized into taste buds (Jetté et al. 2020). Taste buds in humans are comprised mostly of taste cell types II (bitter, sweet, umami) and III (acid responsiveness). These structures are highly innervated in order to quickly trigger a protective response.

Cell populations of Human Adult Vocal Fold Lamina Propria

Human adult VF LP is predominantly made of extracellular matrix (ECM), such as HA, collagen, and elastin. As mentioned above, the ECM characteristics of LP are crucial for its vibratory properties specifically exquisite viscoelasticity that supports high-frequency oscillation and voice production (Y. Kishimoto et al. 2016). The cells responsible for the maintenance and production of ECM are called fibroblasts (Fig. 2). The LP also contains rare populations of cells that are critical for its function namely immune cells that take part in the mucosal immune responses and endothelial cells/pericytes lining the blood vessels.

VF fibroblasts (VFFs) are essential for regulating tissue homeostasis and driving regeneration and structural reorganization during wound healing (Y. Kishimoto et al. 2016b). VFFs are responsible for synthesizing glycosaminoglycans, proteoglycans, elastin, and collagen molecules (King et al. 2012). During nonpathologic wound healing VFFs acquire a contractile myofibroblast phenotype to achieve wound closure and afterward undergo apoptosis during the final stage of wound healing (Y. Kishimoto et al. 2016). Based on their cell surface markers, immunophenotypic characteristics, and differentiation potential VFFs are considered mesenchymal stem cells in VF LP (Hanson et al. 2010). Fibroblasts are described as having a spindle-shaped morphology; however, they are a heterogeneous population with organ-dependent transcriptional diversity based on their anatomical position (Rinn et al. 2006). The epigenetic influence of mechanical forces on VFFs plays a role in maintaining a unique environment. In comparison to other fibroblasts isolated across the body, VFFs are enriched in transcription factors and genes that regulate pluripotency, ECM composition, migration, proliferation, and differentiation which makes them capable of rapidly responding to the constantly changing vibratory environment (Li et al. 2016; Foote et al. 2019). In addition, VFFs

are indirectly involved in regulating host immune responses. In vitro studies using normal VFFs and diseased VFFs derived from VF scar/benign lesions cocultured with macrophages, have revealed that there is paracrine communication between VFFs and macrophages through secretion of cytokine and chemokine molecules depending upon the origin of the VFFs (King et al. 2012). VFFs from VF polyps show increased expression of proinflammatory cytokines compared to VFFs isolated from normal VF tissue. Moreover, prolonged bacterial inflammation, vocal abuse, or gastroesophageal reflux can also influence VFFs behavior such that VFFs express inflammatory cytokines, chemokines, and lipid mediators such as IL-6, IL-8, INF-Gamma, and prostaglandin E2 (PGE2). This VFF behavior can recruit and activate tissue macrophages which promotes chronic inflammation in the VF mucosa and stimulates the environment for benign VF lesions such as VF polyps (King et al. 2012).

Other cell types described in the VF LP include immune cells predominantly tissue macrophages Macrophages can rapidly respond to endogenous stimuli that are generated following tissue injury or infection. Macrophages exhibit plasticity. Upon activation from an injury stimulus/infection, they can differentiate into either M1 type which is pro-inflammatory or M2 type exhibits anti-inflammatory properties (alternative activation) (King et al. 2012; Nakamura et al. 2022). The classically activated M1 macrophages exhibit enhanced anti-microbial activity and secrete high levels of pro-inflammatory cytokines such as IL-1, IL-6 and IL-23 (Mosser and Edwards 2008). They provide defense against infection. M2 macrophages are generated in the presence of IL-4. The function of M2 macrophages is to secrete anti-inflammatory cytokines such as IL-10 and IL-4 to promote wound healing and contribute to the production of the ECM as they can the activate conversion of VFF into myofibroblasts. In response to injury, during the early inflammatory stage of wound healing the macrophages adopt

M1 phenotype that gradually shifts into M2 by 14 days post-injury. The two markers of both phenotypes can co-exist in one macrophage and can exist occasionally during wound healing. The balance between M1 and M2 types has a critical role in regulating inflammation and tissue remodeling and scar formation in the injured tissue. If the balance is disturbed, overexpression of the M1 type can lead to host tissue damage and prolonged healing whereas dysregulation of M2 type can lead to excessive tissue fibrosis and hypertrophic scar formation (Mosser and Edwards 2008).

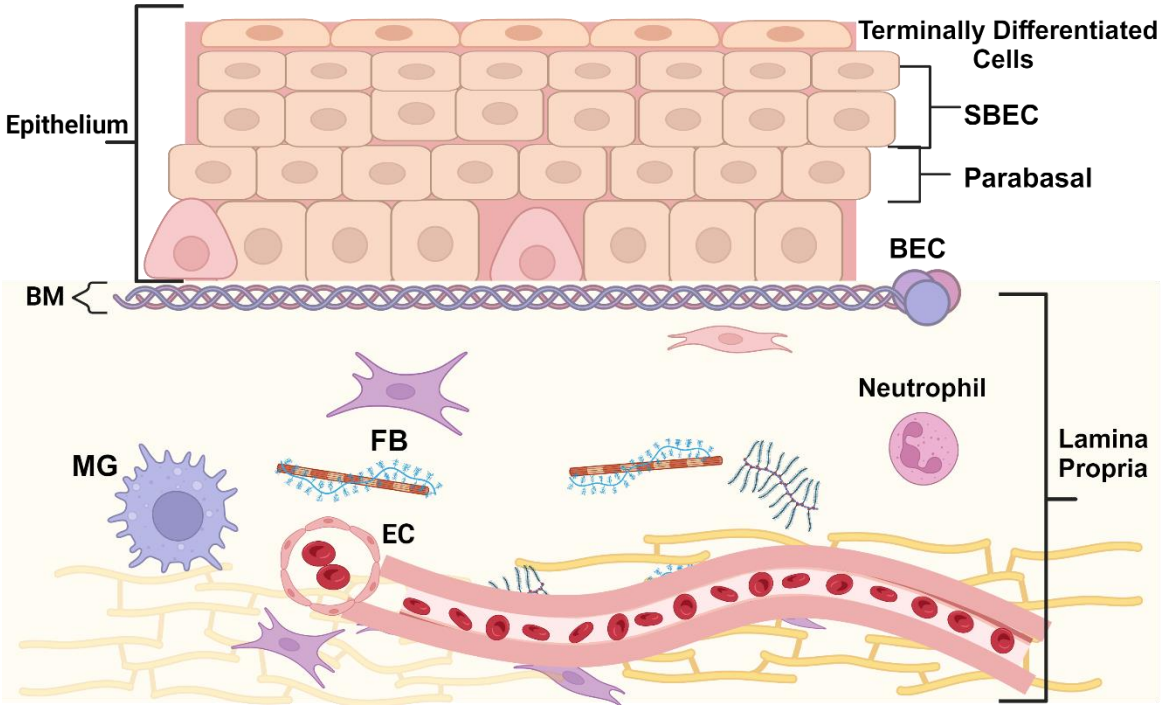

Figure 2: Human vocal fold lamina propria. *Schematic illustration showing different cell types in the lamina propria including fibroblasts, macrophages, neutrophils, endothelial cells lining the blood vessel. EC, Endothelial Cells, MG, macrophages; FB, fibroblasts; BM, Basement Membrane; SBEC, Suprabasal Epithealial Cells; BEC, Basal Epithelial Cells. Created with BioRender.com*

The third type of cell described in VF mucosa is endothelial, which forms a single cell layer that lines blood vessels. Blood vessels enter the anterior and posterior part of the VF and run parallel to the VF edge. The vascular structure of VF is unique to prevent hypoxia and

trauma to blood vessels during vibration (Sato 2018). The SLLP is less vascularized than the deeper layers of the VFs. The most abundant type of blood vessel in the SLLP is capillary. The capillary wall is made up of endothelial cells that are attached to the basal lamina. The endothelial cells are surrounded by supporting cells called pericytes (Sato 2018). The functions of pericytes are synthesis, mechanical support, protection, differentiation, and capillary contraction. Reinke's edema is characterized by increased capillary permeability and fragility specifically, the endothelium has many fenestrae with thickened basal membrane, and the pericytes do not support and protect the capillary wall (Hirano and Sato 1999).

Murine Models in Voice Research

Mouse as a Model in Voice Research

Murine models are nowadays frequently used in VF research despite their differences in vocalization. Mice utilize ultrasonic vocalization for social communication with a fundamental frequency range between 100 and 120,000 Hz (Premoli, Memo, and Bonini 2021). Several theories attempted to explain the mechanism for ultrasonic production. The most recent theory is called the edge-tone model, such that ultrasound voicing is produced with a ventral pouch (air sac-like cavity) located above the VFs (Riede, Borgard, and Pasch 2017). The edge of the pouch is supported by the alar cartilage opposite the glottal exit. During voicing, airflow interacts with the alar edge of the ventral pouch allowing for resonance within the pouch.

Advantages of the murine model over traditionally used animal models in voice research include low maintenance/cost, short and defined gestation period (usually around 18.5 days), a large number of offspring, and most importantly the amenability for genetic manipulation (Thomas et al. 2009; Yamashita, Bless, and Welham 2009b). Moreover, murine VF exhibit

similar morphology, function, and progression through developmental stages which make them a good model for studying cellular and molecular mechanisms of laryngeal/VF embryogenesis, postnatal VF mucosal regeneration and biomechanical studies (Griffin et al. 2021; Lungova and Thibeault 2020).

Murine Laryngeal Anatomy and Vocal Fold Histology

Like humans, a murine laryngeal framework is composed of laryngeal cartilages - Epi, TC, CC and pair of AC with intrinsic laryngeal muscles such as LCA, PCA, CT and TA that perform similar function as their human counterparts. A unique feature in rodents include the presence of alar cartilage (Ar) that is positioned above the VFs and is attached to the TC. The alar cartilage participates in ultrasonic vocalization in rodents. In addition, there is a thin pair of muscles called superior cricoarytenoid (SCA) muscles that connect the dorsal surface of the AC and CC. SCAs assist with the VF approximation similar to transverse and oblique interarytenoid muscles in humans.

The histologic structure of murine VFs is similar to humans. VFs are lined with–non-keratinizing stratified epithelium (EP) which has a lower number of layers compared to humans (approximately 3 layers). Basal epithelial cells are anchored to the basement membrane with suprabasal cell cells stratifying as they move apically. Murine EP also contains taste cells type II that have a lower degree of innervation compared to human (Jetté et al. 2020). The murine LP is simple without obvious layering. The structure of ECM consists mostly of collagen type I and tropoelastin/elastin fibers with similar distribution to humans. Murine VF LP also contains VFFs embedded in ECM, immune cells (tissue macrophages) and endothelial cells lining blood vessels (Yamashita, Bless, and Welham 2009a; Lungova and Thibeault 2020).

Laryngeal and Vocal Fold Embryonic and Postnatal Development in Mice and Humans

Overview of Laryngeal Development in Humans

Development of vertebrate embryos can be described using a standardized system called Carnegie Stages (Hill 2007). There are a total of 23 stages during embryonic development which correlate to gestational weeks as following; stage 11 = week 4; stage 12 = week 4; stage 13 = week 5; stage 14 = week 5; stage 15 = week 5; stage 16 = week 6; stage 17 = week 6; stage 18 = week 7; stages 19-23 = weeks 7-8 (Hill 2007). The first sign of respiratory development in humans is noted during stage 11 with epithelial thickening along the ventral aspect of the foregut known as the respiratory primordium (RP) (Rubin, Sataloff, and Korovin 2014). At stage 12, the site of origin of the respiratory diverticulum (RD) is called the primitive pharyngeal floor (PPhF) (Rubin, Sataloff, and Korovin 2014). The RD is a ventral out pocketing of foregut lumen that extends into RP. The cephalic part of the RD eventually becomes the subglottic region of the human larynx (Zaw-Tun and Burdi 1985a; Kakodkar, Schroeder, and Holinger 2012). The PPhF is separated from the floor of the fourth pharyngeal floor (4PP) by a segment called primitive laryngopharynx (PLPh) (Zaw-Tun and Burdi 1985a). The caudal part of the RD gives rise to bilateral projections called bronchopulmonary buds (BPB) which will develop into the lower respiratory tract. Pharyngeal mesoderm causes compression of cephalic region of respiratory diverticulum eliminating the foregut lumen, which results in development of an epithelial lamina (EL). The mesoderm elongates into an epiglottic and two arytenoid swellings in the PhF at the level of the 4PP (Zaw-Tun and Burdi 1985a). During stage 16, the laryngeal cecum is formed in the region between arytenoid swellings and the epiglottis, as the EL obliterates the primitive laryngopharynx (PLPh) (Kakodkar, Schroeder, and Holinger 2012).

During stages 17-18, the cecum descends up to the level of the glottis (Kakodkar, Schroeder, and Holinger 2012). During stage 21, the EL separates cephalocaudally, forming the laryngeal vestibule which is continuous with the subglottic cavity. A bilateral pouch is formed in the caudal region of the cecum which then ascends to give rise to the VFs. The laryngeal cartilage and intrinsic muscles are developed from the pharyngeal mesoderm which surrounds the laryngeal cavity (Zaw-Tun and Burdi 1985a).

Overview of Laryngeal and Vocal Fold Embryonic Development in Mice

Initiation of murine laryngeal development occurs at embryonic (E) day 9.5 and is similarly to humans closely associated with the formation of the RD (Herriges and Morrisey 2014; Lungova and Thibeault 2020). The laryngeal field is similarly situated between the 4PP and the cranial portion of the RD. 4PP contains the laryngeal groove (LG), an opening, that further elongates and gives rise to the PLPh with prospective VFs (Henick 1993; Lungova and Thibeault 2020). Lungova et al. 2018, defined five major stages of the murine laryngeal/VF morphogenesis that include: 1) laryngeal field specification at E9.5; 2) formation of the PLPh and apposition of lateral walls at E10.5; 3) formation of EL due to approximation and fusion of lateral walls with prospective VFs at E11.5; 4) EL recanalization from E13.5-18.5 and 5) onset of VF epithelium stratification, and maturation of the LP, laryngeal cartilages and muscles (Lungova et al. 2018). These findings have shown that the EL is a temporal structure, unique to the VFs, that temporarily blocks the entrance into the lower airways, therefore, it needs to disintegrate and open forming the laryngotracheal tube.

Mechanistic studies that have focused on the early stages of laryngeal morphogenesis reveal that specification of the laryngeal field is regulated by *Shh* (Tabler et al. 2017). Genetic

inactivation of *Shh* in transgenic mouse models causes failure of lateral wall approximation and laryngeal agenesis (Lungova et al. 2015b). Similarly, the process of EL recanalization is controlled genetically e.g. via *Wnt/beta-Catenin Yap/Hippo* signaling pathways with the help of mechanical load created by amniotic fluid that constantly flows through the developing VFs down into lungs and backward (Lungova et al. 2018; Mohad et al. 2021; Lungova et al. 2020). Overexpression of Yap due to conditional inactivation of *Lats1 and 2* leads to failure in differentiation of VF basal epithelial cells that accumulate in the laryngeal lumen and prevent successful VF separation. This condition resembles laryngeal atresia. Similarly, conditional deletion of *Beta-Catenin* in VF epithelial progenitors leads to incomplete VF separation resembling mild and severe cases of laryngeal webs (Lungova et al. 2018). Both conditions can be life threatening causing severe respiratory distress and problems with voicing across the lifespan (Lungova and Thibeault 2020).

A recent study by Wendt et al. 2022 analyzed laryngeal, tracheal and esophageal expression profiles over time by bulk RNA seq. All three organs share the same origin in the anterior foregut through interactions between anterior foregut endoderm and the surrounding splanchnic mesoderm (L. Han et al. 2020). Hence, congenital malformations of these organs such as esophageal atresia, tracheoesophageal fistula (TEF), congenital laryngeal webbing and/or laryngeal cleft occur often together. Wendt et al. 2022 identified 3,472 differentially expressed genes shared across all three tissues during prenatal and postnatal stages of development. Between E10.5 and E13.5, the authors showed that shared genes across all three tissues were enriched for neurogenesis namely genes associated with pathfinding and targeting axons such as bHLH transcription factor and LIM homeobox transcription factor. In addition, this period was accompanied by the downregulation of gene sets for cell proliferation such as *Shh, Trim71,*

Bnc1, *Lef1*, *Bex4* and *Tert*. At E13.5 to E18.5; the organs are characterized by a tripartite organ process of laryngotracheoesophageal septation and EL recanalization. This process is accompanied by epithelium stratification, intrinsic muscle differentiation and chondrification in the newly formed larynx. Hence, transcriptome in those stages was enriched for muscle processes, epithelium development, motor-driven movement and extracellular matrix organization. *Wnt*, *Notch*, and *Fgf* pathways were found to be responsible for epithelium stratification while cartilage and muscle development were associated with genes *Sox9*, *Col11a2* and *Col2a1* (Table 1).

Postnatal Changes to the Larynx and Vocal Folds in Humans

After birth, the human larynx undergoes postnatal changes in position, size and histology. In a newborn, the TC is attached to the hyoid bone and the larynx is located at the level C3 – C4 cervical vertebrata. The larynx separates from the hyoid bone and descends to C6 by the age of 5 and C7 around 15 – 20 years of age. In the neonate, the epiglottis is in close apposition to the uvula and soft palate. The higher position of the infant larynx allows for a tighter oral seal to improve sucking (Fried, Kelly, and Strome, 1982). Also, the high position of the larynx makes neonates obligate nose-breathers. The laryngeal descendance leads to longer vocal tract and a decrease in the fundamental frequency (Fried, Kelly, and Strome, 1982). The neonatal larynx is conical in the transverse dimension and a cylindrical shape in the anterior-posterior dimension. A study by Kahane 1977, examined the morphological changes in dimensions of prepubertal and pubertal laryngeal in ages 9 –18. The prepubertal larynges in both sexes share similar dimensional characteristics. With puberty, the male larynx dimensions change substantially to develop into an adult male larynx. The differences between prepubertal female larynx and adult female larynx requires less growth per unit time, compared to males, to reach maturity. By

puberty, there is a clear sexual dimorphism in the larynx. The male larynx is significantly bigger in all aspects than female specimens (Kahane, 1978). Histological changes include ossification of laryngeal cartilages with the onset of ossification in TC and CC during the mid-twenties and in ACs at the age of thirty.

Human VFs undergo prominent changes in length and histology. In infants, the VF length is approximately 6-8mm and increases to approximately 12-17 mm and 17 – 23 mm in the adult female and male, respectively. Histologically, newborn VF LP has characteristic monolayered organization that lacks mature three-layered structure. The concentration of HA in newborns is increased and evenly distributed throughout the VF LP unlike in adults where HA is predominantly located in the SLLP (Schweinfurth and Thibeault 2008; Kuhn 2014; Ira 1974; Hartnick, Rehbar, and Prasad 2005). Histologic findings of infant monolayered VF LP has been confirmed by high-resolution magnetic resonance imaging (MRI) in a study by Kishimoto et al. 2021 (A. O. Kishimoto et al. 2021). Infants to one year of age start to produce longitudinal fibers in response to crying stimuli. From 3 to 5 years of age there is an increase in the longitudinal fiber forming a visible mature ILLP which is similar to that in adults. However, the SLLP is not yet differentiated making pediatric VFs susceptible for hoarseness. The differentiation of SLLP and DLLP occurs after the age of 10. The layered structure of LP presumably reflects the complexity of phonatory function (Ishii et al. 2000). However, the exact mechanism of VF LP maturation is still not yet known (Infusino et al. 2013).

Due to increasing life expectancy, voice disorders in elderly population are on the rise (Beatriz et al., 2021). Elderly patients suffer from age-related dysphonia also known as presbyphonia (Rapoport, Meiner, and Grant 2018). Presbyphonia is diagnosis per exclusion made in the absence of other laryngeal disease (Rosow and Pan 2019). Aging voice is associated

with a weak, hoarse, breathy, strained and low-pitched voice (Takano et al. 2010). On stroboscopic imaging, common findings are VF bowing with reduced mucosal wave, VF atrophy and incomplete VF closure. Histologically, the SLLP gets thinner with significantly reduced concentration of HA making the tissue less viscoelastic (Kuhn 2014). There is increased cross-linking between elastin fibers (impairing their ability to recoil) and high concentration collagen I fibers in DLLP of VF LP thereby reducing elastic properties and pliability (Kuhn 2014; Moore and Thibeault 2012). In addition, there is a decreased axon diameter, axonal loss and laryngeal muscle atrophy (Seino and Allen 2014).

Postnatal Changes to the Larynx and Vocal Folds in Mice

After birth, the murine larynx and VFs also undergo postnatal changes in size and histology similar to humans. A study by Griffin et al 2021, evaluated the murine laryngeal and VF geometric dimensions, biomechanics, and cellular proliferation from early prenatal development (starting E13.5) to postnatal stages such as P0 (newborn) and adulthood (6 – 8 weeks). Analysis of results reveals quadratic growth in laryngeal length, transverse diameter, dorsoventral diameter, and VF internal length (Fig, 7b). Internal VF thickness grows linearly and VF stiffness increases quadratically throughout development. The differences between pre-and post-natal stiffness are concomitant with the switch from the aqueous environment to the air interface when the amniotic fluid is resorbed, and the newborn pups take their first breaths (from E18.5 to P0). The authors further demonstrated that in the postnatal stages, the increase in laryngeal and VF dimensions/stiffness is not associated with increased cell proliferation, but rather with cell differentiation and subsequent ECM deposition. Histologically, during postnatal murine LP maturation, HA density decreases significantly with age as opposed to the collagen

density (Abdelkafy et al. 2007). Postnatal maturation of the murine VF epithelium is marked by a change from two layers (a basal and suprabasal cell layer) at birth to three or four layers in adulthood (Lungova et al. 2015). Basal cells lose their columnar shape and become cuboidal. The more apical suprabasal layers terminally differentiate and become progressively more squamous towards the luminal surface of the VF (Lungova et al. 2015).

From Microscopy to Single-Cell RNA-Sequencing and Cell Atlases

Creating cell atlases has been a long goal in the field of biology in order to comprehensively characterize different cell populations contributing to physiology, development,and disease (Quake 2022). Efforts started with a morphologic characterization of tissues and small organisms using optical and electron microscopy (Quake 2022; Cajal 1911; Fawcett 1966). Since morphologic features of cells under a microscope are not very precise to differentiate among individual cells, the introduction of targeted polyclonal/monoclonal antibodies has enabled to detect various cells based on their specific nuclear, cytoplasmic or cell-membranous protein markers. The discovery of protein-specific antibodies led to the establishment of Fluorescence-Activated Cell Sorting (FACS). FACS revealed that morphologically similar cells can vary dramatically at their molecular level. The desire to have even deeper knowledge about cells has led to analyze single cells using gene expression (transcriptome) profiling (Quake 2022).

Initial efforts in transcriptome analysis were accomplished with gene expression microarrays. The limitations of this technology were a low throughput of cells, time-consuming and laborious tissue processing and more importantly, it only analyzed the transcriptome with the use of known RNA probes. Bulk RNA seq was a breakthrough in transcriptome analysis, which made the process simpler and allowed for the analysis of new RNA sequences present in a

sample. However, it also required to average genetic expression across thousands of cells together, providing low resolution into cellular composition and could not distinguish whether gene expression changes were due to strong response in a few cells or weaker across all cells (Wilbrey-Clark, Roberts, and Teichmann 2020). Despite its limitations, bulk RNA seq had broad utilities, especially in cancer biology such as classification, biomarkers, disease diagnosis, and optimizing therapeutic treatment (X. Li and Wang 2021). ScRNA-seq was the first technique to analyze individual cells in a sample based on their gene expression without the need to average their genetic expression across all cells in a sample. Since its first introduction in 2009, technological development has improved the scale, accuracy and sensitivity of scRNA-seq. ScRNA-seq can provide the cellular makeup of complex and dynamic systems. This technique has allowed for 1) the characterization of unique cell populations in different organs, 2) transient cellular states 3) studying cellular communication and 4) the establishment of lineage trajectory reconstitution. By 2014, scRNA-seq was used to discover new blood cell types. Since then, the development of single-cell atlases expanded rapidly.

Cell Atlas is a comprehensive reference catalog of all cells (depending on studied species) based on their stable properties and transient features as well as their locations and abundances for tissue of interest (Regev et al. 2017). It is a map that shows relationships among cells and their developmental trajectories (Regev et al. 2017). Cell Atlases provide a precise understanding of normal physiology and disease mechanisms (Lindeboom, Regev, and Teichmann 2021). They also serve as an important platform to investigate new diagnostic tools, regenerative medicine approaches and drug discoveries.

So far scRNA-seq allowed for the creation of cell atlases for the developing human heart, small intestine, lungs, pancreas, and more (Asp et al. 2019; Fawkner-Corbett et al. 2021;

Travaglini et al. 2020; Enge et al. 2017). In laryngology, scRNA seq was used to evaluate the composition of only human anterior mucosal VFs, in patients undergoing gender-affirming surgery. The analysis revealed important cell types such as epithelial, stromal, muscle, secretory, submucosal, neuronal and immune cells. VFs were collected from middle-aged adults. This to our knowledge a first try that shed further light on human VF cellular heterogeneity(Laitman et al., 2024).

In clinical practice, scRNA-seq has refined the treatment approach for idiopathic pulmonary fibrosis (IPF) by discovering and subsequently targeting specific immune cells that drive the progression of IPF (Keener 2019). ScRNA-seq is also a valuable tool in cancer research. It has allowed for the characterization of the complex tumor environment in hepatocellular carcinoma (HCC), head and neck squamous cell carcinoma (HNSCC) and lung cancer, etc. (Lvyuan Li et al. 2021). Cell heterogeneity within a tumor is one of the main reasons for treatment failure. Thus, understanding cell heterogeneity is important to improve treatment strategies via the personalized medicine (Lvyuan Li et al. 2021).

Collectively, scRNA-seq and cell atlases provide fundamentals for studying different stages of laryngeal/VF development, homeostasis and age-related degenerative processes. In embryonic development, the areas of interest are to elucidate molecular mechanisms behind 1) differentiation of the epithelium and the establishment of EL, 2) differentiation and origin of mesenchymal structures and 3) potential involvement of epithelial/mesenchymal structures in EL recanalization 4) origins of neurogenesis and axonal invasion into developing VF and lastly 5) origins of VF vasculature (Lungova and Thibeault 2020). From the clinical perspective, the knowledge obtained from scRNA-seq could improve genetic testing, better prenatal counseling, insights into disease pathophysiology, and ultimately treatment strategies.

There is a need to thoroughly characterize cellular changes responsible for laryngeal/VF maturation and aging. Areas of interest include understanding all cell types and molecular pathways responsible for 1) postnatal maturation of VF epithelium, 2) postnatal maturation of VF LP from neonatal monolayered LP to mature and organized LP in adults, and 3) degenerative changes in the VF mucosa associated with aging. From the clinical perspective, this knowledge is necessary to develop age-specific treatment approaches and to serve as a benchmark for designing engineered-based strategies for VF tissue restoration and replacement.

Aim and Hypothesis

The aim of this dissertation was to comprehensively characterize changes in cellular and molecular heterogeneity of the murine larynx/VF throughout the embryogenesis, postnatal maturation, and tissue aging whereby creating a shareable cellular atlas of murine laryngeal and VFs across the lifespan. We hypothesized that the VF and laryngeal cellular complexity will increase from early embryonic stages to adulthood. Early stages of embryonic development will be accompanied by mostly progenitor cells giving rise to mature cell populations that appear postnatally. In the aging group, VF tissue may undergo degeneration (cell death) resulting in a decrease in cell complexity and immune cells infiltration. We anticipated an increased role of macrophages in tissue debris removal and enhanced local immune response. To test our hypotheses we harvested laryngeal and VF tissue from embryonic stages E11.5, E13.5, E15.5, and E18.5 and across postnatal stages such as P0, P4W, P12W, P1year, and P1.5year. These stages correlate to significant developmental stages in humans such as E11.5 EL formation, E13.5 – onset of EL separation, E15.5 – the middle of EL recanalization, E18.5 – the end of EL recanalization, P0 – newborn, 4W – adolescent, 12 W – young adult, 1 year – middle -aged adult

and 1.5 – elderly (Graber et al. 2015; Shoji et al. 2016; Lungova and Thibeault 2020). The resultant cell atlas of laryngeal and VF development across lifespan serves as a benchmark for designing novel engineered-based strategies for VF tissue restoration and/or replacements, cross species tissue comparison and translational research focused on age-, gene- and population-specific treatment options.

CHAPTER TWO: MATERIALS AND METHODS

Study Design

The objective of this dissertation was to create a murine cellular atlas of laryngeal and VF embryogenesis (embryonic day E11.5, 13.5 15.5, and 18.5), postnatal (P) maturation (P0, 4W, 12 W), and aging (1 and 1.5-year-old) using single-cell RNA sequencing (Fig. 3). The single-cell atlas was accompanied by Hematoxylin and Eosin (H&E) staining to evaluate changes in the tissue morphology.

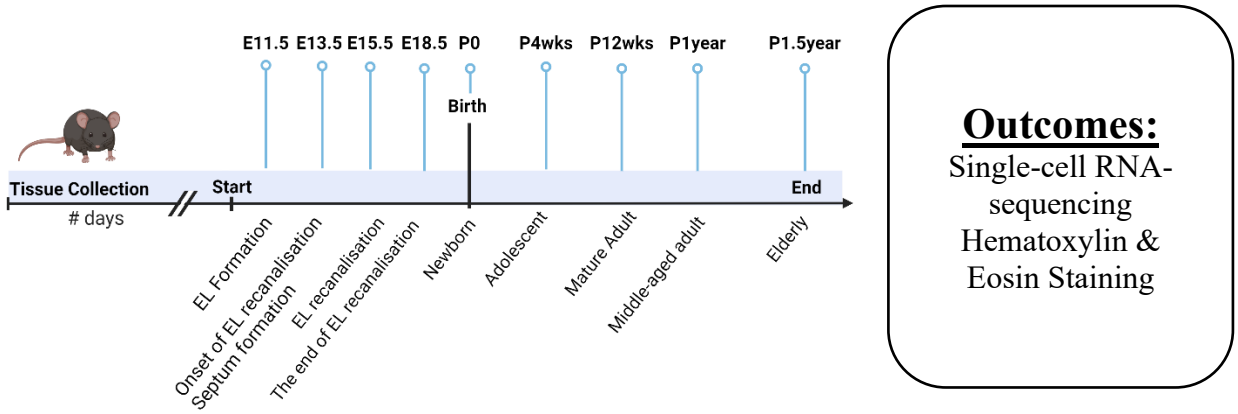

Figure 3: Schematic illustration of experimental design. *Created with BioRender.com*

Mouse Model

All animal studies were performed with approval from the Animal Care and Use Committee at the University of Wisconsin-Madison. Wild-type C57BL/6J (JAX Stock #000664) mice were obtained from the Jackson Laboratory. This is a well-established murine model to study embryogenic development, maturation, and aging in other organs (Apelo et al. 2016; Gardner et al. 2016; Joanisse et al. 2016).

Laryngeal and Vocal Fold Dissections

Embryonic and Newborn Laryngeal Dissections

To study embryonic and newborn (P0) stages of laryngeal development, one male and two females were mated in a mating cage. When vaginal plugs were found; the pregnant were designated as embryonic (E) day 0.5. Pregnant females were euthanized at E11.5 E13.5, E15.5, and E18.5 5 through CO2 asphyxation and cervical dislocation. To access the murine uterus with amniotic sacs, the midline laparotomy was done (Fig. 4A). Next, the murine uterus with embryos was removed from the abdomen (Fig. 4B). Individual embryos were separated using microscissors (Fig. 4C). Embryos were removed from the amniotic sacs using microscissors and put on ice until motionless and unresponsive to touch (Fig. 4D). Individual embryos has two sacs such as yolk sac and the amniotic sac. Murine embryos were sacrificed via decapitation. The same euthanasia technique was used in postnatal P0 pups (newborn), the female was not euthanized. Murine embryonic and newborn larynges were dissected out based on a protocol outlined in Fig. 4E-I. For simplicity, the E15.5 stage dissection is described. The instruments used were two insulin needles (Exel – 29 1/2 G 50 Units). The tip of the needle was bent to 90 degrees. The adjusted needle tip is sufficient to go through the tissue as it is soft and fragile. The adjusted insulin tip has two functions, the side of the tip is for cutting and the tip is for precise microdissecting and securing the tissue block from moving. The first cut was done in between the maxilla and mandible parallel to the mandible (Fig. 4D). The cut went through the cheek and skull to separate the skull with maxilla from the neck region. The skull base remained attached to the neck region. To secure the embryo in place while cutting, the body was held gently with tissue tweezers. The second scalpel cut is made below the hind limbs (Fig. 4E). Position the embryo on the base created with the second cut. The remaining skull base was removed to

expose the pharynx with the laryngeal vestibule (Fig. 4F). The superior view under the microscope displayed from anterior to posterior – mandible, tongue, pharynx with laryngeal vestibule, posterior pharyngeal wall, and the spinal cord (Fig. 4G). Next, three cuts with the adjusted insulin needle were made laterally from the laryngeal vestibule on the right and left side and between the larynx and the spinal cord (Fig. 4G). Gently cut through the tissue. The tongue-laryngo-tracheal complex was isolated (Fig. 4H). The tongue was removed from the laryngo-tracheal complex (Fig. 4H). Lastly, the larynx was separated from the trachea (Fig. 4I).

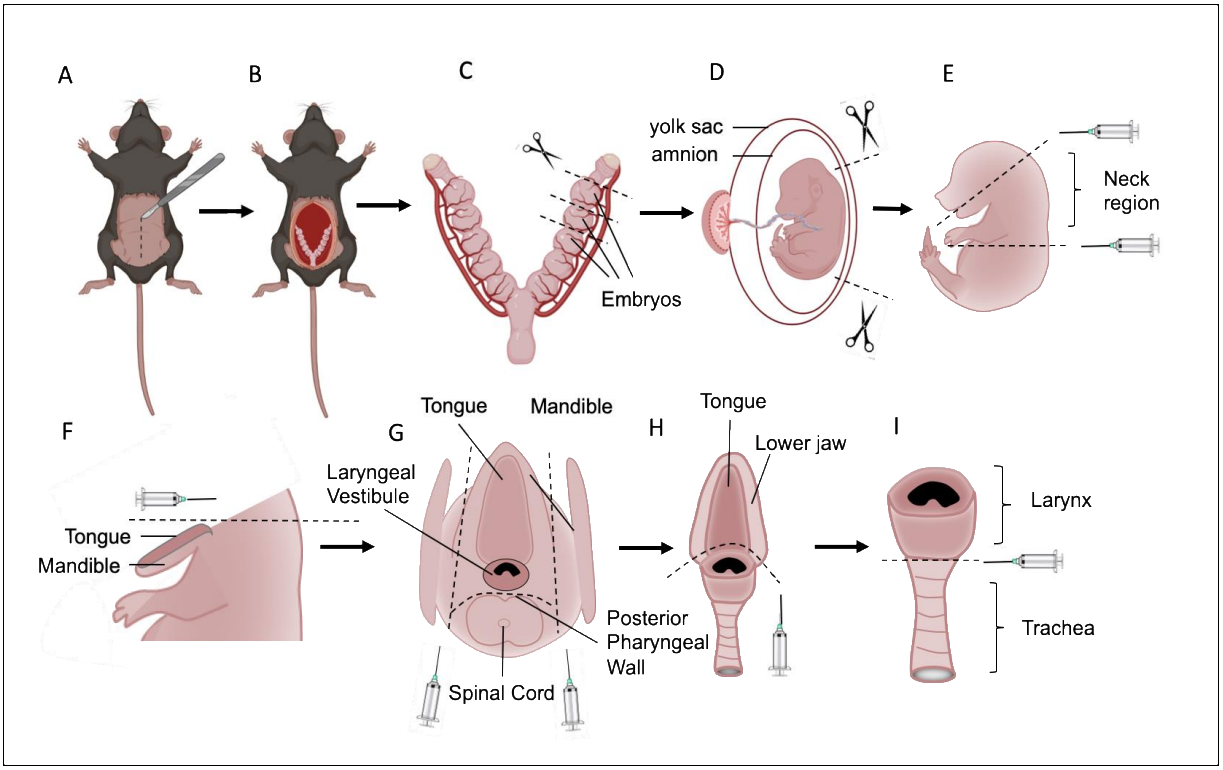

Figure 4: Dissection protocol for embryonic and P0 larynx. *Created with BioRender.com*

Postnatal Laryngeal and VF Dissections

To harvest postnatal (4W onward) murine larynges, mice were euthanized in a CO2 chamber with cervical dislocation. First, a mid-anterior neck incision through skin and subcutaneous tissue was made from the lower jaw to the sternum (Fig. 5A). The freed skin with subcutaneous

tissue was removed. The exposed submandibular glands were lifted with forceps and removed to visualize the larynx and trachea (Fig. 5B-C). Subsequently, cuts were carried through the oral cavity and lower jaw laterally along the visible larynx and trachea on the right and left side to loosen the complex of tongue-larynx-trachea-esophagus from surrounding tissue (Fig. 5D-G). The complex of the tongue-larynx-trachea-esophagus was transferred into DPBS in a 15ml tube and put on ice. The larynx was microdissected from surrounding tissue under the microscope (Fisher Scientific Stereo Zoom Microscope, Waltham, MA, USA) based on a protocol outlined in Fig. 6A-E. Once the larynx was cleared of surrounding tissue it was transferred onto a green polyester platform and secured with two needles (Fig. 6F-G). The posterior laryngotomy was made to access the VFs (Fig. 6H-I). VFs were cut out with micro scissors on each side while holding onto the right or left vocal fold tissue with tweezers (Fig. 6J-K). Once the VFs were dissected out, they were transferred into 300 microliters of Dulbecco's Modified Eagle Medium (DMEM) (D5796, Sigma-Aldrich) in a sterile petri dish sitting on ice.

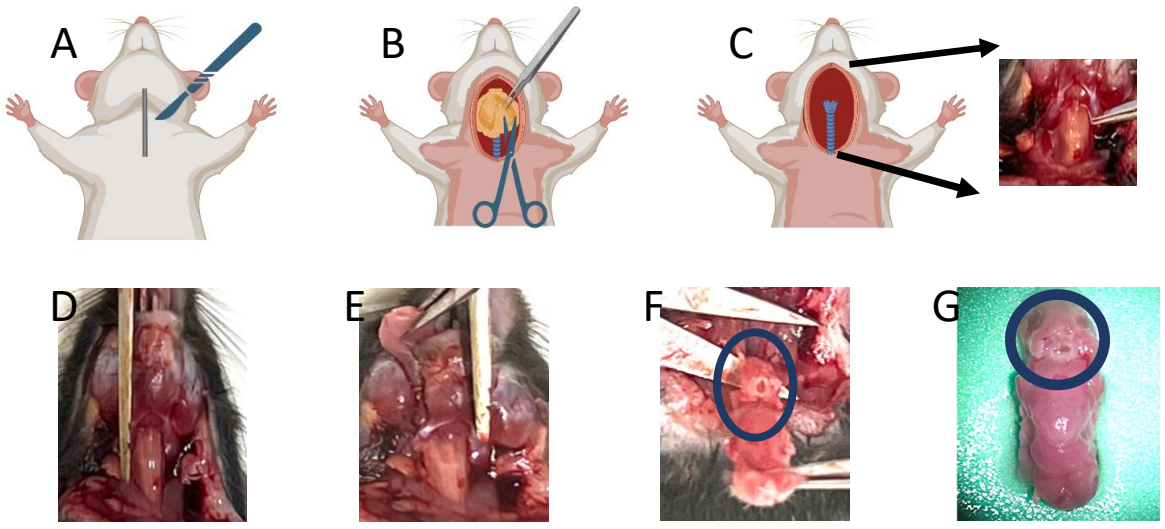

Figure 5: Adult laryngeal dissection protocol. (*A) Mid-anterior neck incision through skin and subcutaneous tissue, (B) Exposure of submandibular glands (yellow) and their removal. (C)Exposure of larynx and trachea (blue) on a schematic and a photo (D) Scissor-cut through the lower jaw lateral to the larynx on the right, (E) Scissor-cut through the lower jaw lateral to the larynx on the left, (F) Removal of tongue-larynx-trachea-esophagus complex, (G) tongue-larynx-trachea-esophagus complex on a photo. Created with Biorender.com*

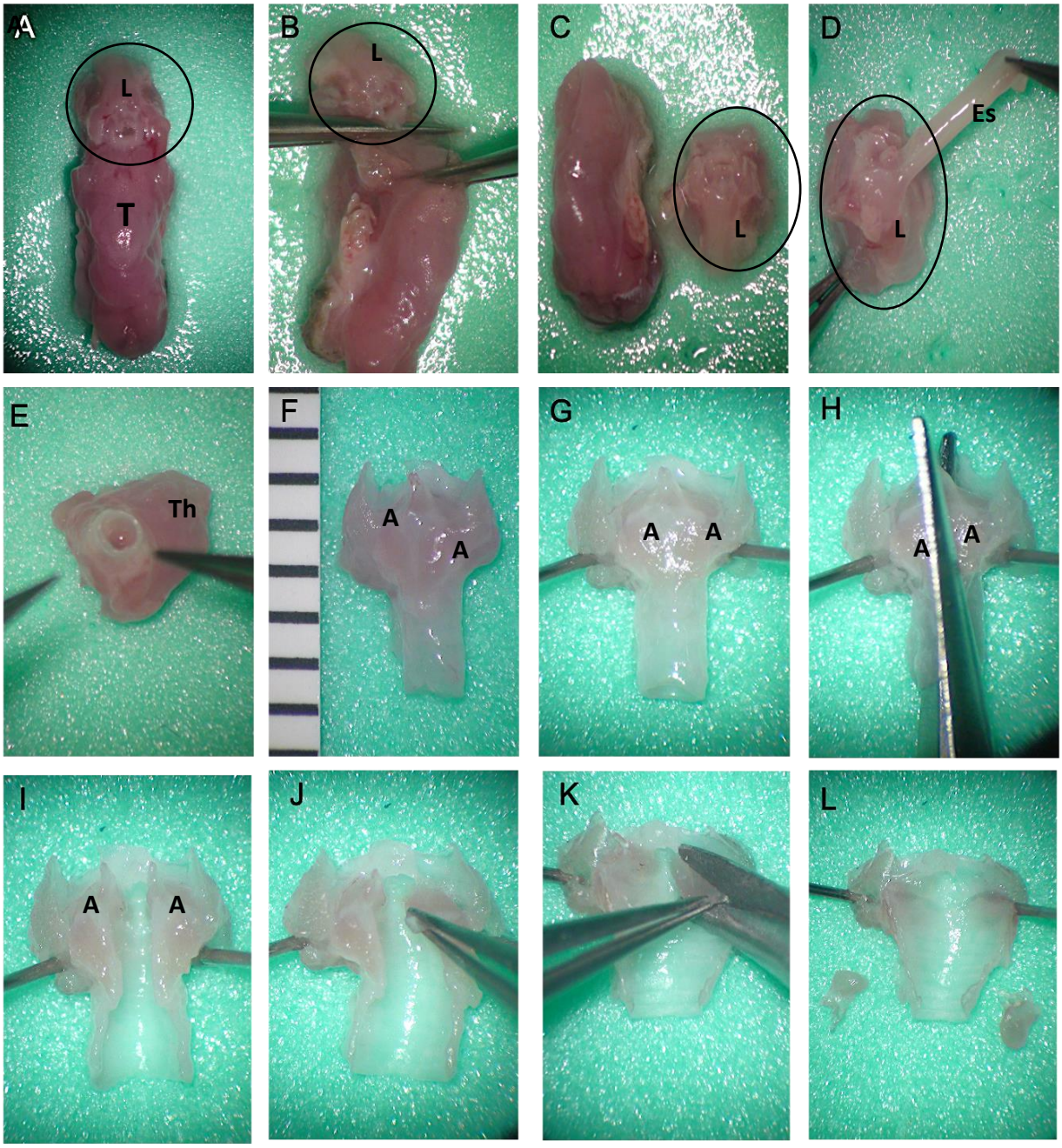

Figure 6: Adult vocal fold dissection protocol. (*A) Tissue Complex of Tongue (T)-Larynx (L)-Trachea-Esophagus, (B) Separation of the tongue from the larynx. (C) Separated larynx from the tongue, (D) Separation of the esophagus (Es) from the larynx (L), (E) Removal of the thyroid gland (Th), (F) Clean larynx – posterior view – Arytenoid cartilages (A), (G) Secured larynx on PE platform with needles, (H) Posterior Laryngotomy in between two Aryntenoid (A) cartilages, (I)Posteriorly opened larynx, (J-L) Dissection of right vocal fold with microscissors and forceps*.

Biologic Replicates

For single-cell dissociation and scRNAseq, eight larynges for E11.5, E13.4, E15.5, E18.5, and six newborn larynges were pooled together for one biological replicate regardless of their sex. For stages 4W, 12W, 1 year of age, and 1.5 years of age, 6 larynges (3 females and 3 males) were collected and their VFs were dissected out giving 6 pairs of VF tissue to make one biological replicate. For H&E, we used 3 biological replicates at any stage per staining.

Single-cell RNA Sequencing

Sample preparation

Isolated embryonic larynges or postnatal VFs were minced into 0.1 mm small pieces on a sterile petri dish with a razor blade. Three hundred uL of DMEM with minced tissue was transferred using wide-bore pipette tips into a 2ml tube. Seven hundred uL of enzyme mixture was added to the tube to dissociate the tissue into a single-cell suspension. The dissociation protocol by Sekiguchi & Hauser 2019 was used for the experiment and modified to optimize the enzyme composition & concentration and dissociation temperature and time . Specifically, three millilters of enzyme mixture contained 225 µl Accutase (Stem Cell Technologies, Cambridge, MA), 225 µl Accumax (Stem Cell Technologies, Cambridge, MA), 7 mg/ml Bacillus lichenformis protease (MilliporeSigma, Burlington, MA), 10mg/mL of Collagenase (Gibco, New York, NY) and 125 U/ml DNase I (MilliporeSigma, Burlington, MA) dissolved in sterile calcium/magnesium-free PBS (Gibco, New York, NY). Samples were gently triturated after 5 min using a wide-bore pipette tip during dissociation. Tissues were dissociated total of ten minutes in a cold room. Dissociation was performed for each biological replicate, separately. Undigested cartilage was removed from the 2ml tube; remaining enzyme mixture solution with

free-floating cells was transferred to a 15ml tube. Afterwards, 2 ml Ca/Mg-free PBS supplemented with 10% FBS to stop the enzymatic reaction and nourish the cells. The solution was then centrifuged at 300 g, for 8 mins, at 4°C to create a cell pellet at the bottom of the tube. The cell pellet was resuspended in 100 µl ACK lysing buffer (Lonza, Bend, OR) for 30 seconds to remove erythrocytes. The enzymatic reaction of ACK lysis buffer was neutralized by adding ice-cold 1ml of Ca/Mg-free PBS. The solution was then centrifuged at 300 g, for 8 min, at 4°C to create a cell pellet at the bottom of the tube. The cell pellet was resuspended in 1 ml of Ca/Mg-free PBS supplemented with 10% FBS. The single cell solution was filtered with a 40 µm cell strainer (MilliporeSigma, Burlington, MA), then centrifuged at 300 g, for 8 min, at 4°C. The supernatant was removed up to 200 uL. The cell were resuspended in the leftover 200uL of Ca/Mg-free PBS supplemented with 10% FBS and transferred on ice to Gene Expression Center at UW-Madison.

Droplet-based scRNA-seq

Libraries were prepared according to Chromium Single Cell 3' Reagent Kit v3.1. Single cell suspensions will be transported on ice to the University of Wisconsin Madison Biotechnology Center, where cell concentration and viability will be quantified on the Luna FX-7 (Logis Biosystems, Anyang, South Korea) with acridine orange/propidium iodide stain. The appropriate volume of cells was loaded onto the Single Cell Chip G required for yielding a cell recovery of six-thousand cells. Following the completion of the Chromium run the GEMs were transferred to emulsion safe strip tubes for GEM-RT using an Eppendorf MasterCycler Pro thermocycler (Eppendorf, Hamburg, Germany). Following RT, GEMs were broken, and the pooled single cell cDNA was amplified. Post-cDNA amplified product was purified using SPRIselect (Beckman Coulter, Brea, CA) and quantified on a Bioanalyzer 2100 (Agilent, Santa

Clara, CA) using the High Sensitivity DNA kit. A portion of the full-length cDNA was fragmented and used to generate cDNA libraries according to the standard 10X Genomics workflow. These libraries were sequenced on a NovaSeq with two S4 flow cells, 2x100bp sequencing. Data was processed with bcl2fastq.

ScRNA-seq Data Analysis

Data Quality Control

The quality control of sequenced samples was conducted utilizing MultiQC, a tool designed to aggregate and visualize multiple quality control outputs for bioinformatics analyses. We established predetermined quality thresholds, and only samples meeting these criteria were advanced for further analysis.

Read Alignment

Sequencing reads in FASTQ format were aligned to the human reference genome (GRCh38) using the CellRanger software suite (version 7.1.0). The alignment employed the default parameters, with modifications specified where deviation from default settings was necessitated by the specific experimental design.

Data Preprocessing

Distributions for metrics for each sample were visualized and carefully examined. Cells exhibiting a mitochondrial gene content exceeding 20% were excluded to avoid apoptotic or damaged cells. Additionally, cells were required to have a minimum of 500 total unique molecular identifiers (UMIs) and at least 250 detected genes to be retained for analysis. Genes

characteristic of hemoglobin was excluded to minimize bias from ambient blood contamination. DoubletFinder was used to detect and remove possible doublets.

Normalization

Raw gene expression counts were normalized to Counts Per Million (CPM) to account for differences in sequencing depth among cells. Subsequently, the normalized counts were log-transformed using the formula log (CPM + 1) to stabilize variance across genes.

Integration and Batch Correction

To integrate data across different samples and experimental conditions, we applied the Harmony algorithm, which is specifically optimized for batch correction in single-cell transcriptomics. This approach allows for the correction of systematic differences without obscuring biological variability.

Clustering and Sub Clustering

The Louvain algorithm implemented within Seurat (version 5.0.0) was employed for cellular clustering, with the resolution parameter set empirically at 1.4. This parameter was optimized through iterative testing to achieve the desired granularity in cell type resolution. Clusters of interest were further subjected to sub clustering to resolve finer cellular hierarchies. This process involved reapplying the analysis pipeline, with resolution parameters adjusted based on differential expression analysis to ensure meaningful biological interpretation.

Dimensionality Reduction

Variable gene selection, principal component analysis (PCA), and uniform manifold approximation and projection (UMAP) were conducted using Seurat. Selection of variable genes was implemented with the function FindVariableFeatures using the 'vst' method. The top 2,000 highly variable genes were centered and scaled with the ScaleData function. The first 30 corrected PCs were calculated via the RunHarmony function, after which the RunUMAP function was applied to generate UMAP embeddings for 2-dimensional visualization.

Differential Expression Analysis

Between-cluster differential expression analysis was conducted using the FindMarkers and FindAllMarkers functions in Seurat, employing a Wilcoxon rank sum test with a threshold of avg_logfc 0.25, adjusted p-value 0.05, and min.pct = 0.1. Between-stage differential expression analysis was conducted using the generalized linear model from Monocle3 (version 1.4.15) with default parameters. Significantly differentially expressed genes were identified based on a q-value threshold of 0.05. These genes were then grouped into modules using the find_gene_modules function to identify patterns of co-expression across different cell states.

Trajectory Analysis and Top 50 Genes across Timepoints

Pseudotime trajectories were inferred using Monocle3 for a selected subset of cells representing major cell types. This analysis facilitated the identification of genes whose expression changes significantly with pseudo time, providing insights into dynamic processes such as differentiation or response to stimulation. Specifically, previously derived dimension reduction results were used, interesting cell type combinations were chosen, and partitions were

manually added. The root node of the trajectory was selected based on the node closest to the earliest stage (E11.5). After obtaining the trajectory, genes that change significantly as a function of pseudo time were obtained using the graph_test function from Monocle3.

We also identified the top 50 genes displaying significant changes in expression over different stages by utilizing the fit_models() function from the Monocle3 library. Each gene was fitted with a generalized linear model to assess changes over time. Subsequently, genes were ranked based on the smallest q-values, and the top 50 were selected. These genes were then clustered and visualized in a heatmap.

Cell Annotation

Generated cell clusters were annotated based on top 20 differentially expressed genes using Cellkb.com and confirmed with established markers from the literature.

Hematoxylin and Eosin (H&E)

Embryonic and postnatal larynges were immediately fixed in 4% paraformaldehyde at 4°C overnight and remained in 70% ethanol until standard tissue processing procedures for paraffin sections. Paraffin-embedded sections were cut transversally into 5 µm sections and stored at 4°C until use. For H&E, paraffin-embedded slides were deparaffinized, rehydrated, and stained using a standard H&E protocol (Feldman and Wolfe 2014). Images were taken with a Nikon Eclipse Ti2 inverted microscope with a DS-Qi2 high-sensitivity monochrome camera (Nikon Instruments, Inc., Melville, NY) and adjusted for brightness using the NIS Elements software.

CHAPTER THREE: RESULTS

Identified Cell Populations

To investigate laryngeal and VF development at single-cell resolution, we established a protocol for single-cell dissociation of VF and laryngeal tissue which isolates all cell types including the epithelium, fibroblasts, and immune cells, at high quality. For each stage, we were able to recover 19, 004 (E11.5), 15, 536 (E13.5), 21, 368 (E15.5), 19, 184 (E18.5), 19, 275 (P0), 25, 588 (4W), 34, 529 (12W), 28, 745 (1Y), and 27, 578 (1.5Y) cells, respectively, covering laryngeal and VF development from early embryonic stages to elderly. All isolated single cells were used for scRNA-seq on a 10x Genomics platform. Cells from the nine time points were scaled for clustering and dimensional reduction using UMAP (Fig. 7). We identified 23 clusters which represent 23 unique cell populations found, in the larynx and VF, across lifespan. These cell populations consisted of 5 major groups - epithelial, mesenchymal, immune, endothelial and neuronal cells (Fig. 7) Within the epithelium cluster, we identified eight cell populations namely basement producing cell (BMPC), proliferating basal epithelial cell (PBEC), non-proliferating basal epithelial cell (NPBEC), suprabasal epithelial cell (SBEC), secretory cell (SEC), ciliated cell (CC), airway epithelial cell, and columnar cell. Mesenchyme included early proliferating mesenchymal progenitor (EPMP), stromal cell (STC), fibroblast (FB), muscle stem cell/satellite cell (MSC), skeletal muscle cell (SMC), smooth muscle cell (SMMC), and chondroblast (ChB). Within the immune cluster, we identified macrophage (MG), dendritic cell (DC), neutrophil and lymphocyte. Within endothelial cells, we identified blood vessel endothelial cell (BVEC) and lymphatic vessel endothelial cell (LVEC). Lastly, for the neuronal

population, we identified Schwann cell (SchC) and neuroendocrine cell (NEC). Individual cell populations were characterized using the top five differentially expressed genes (DEGs). These

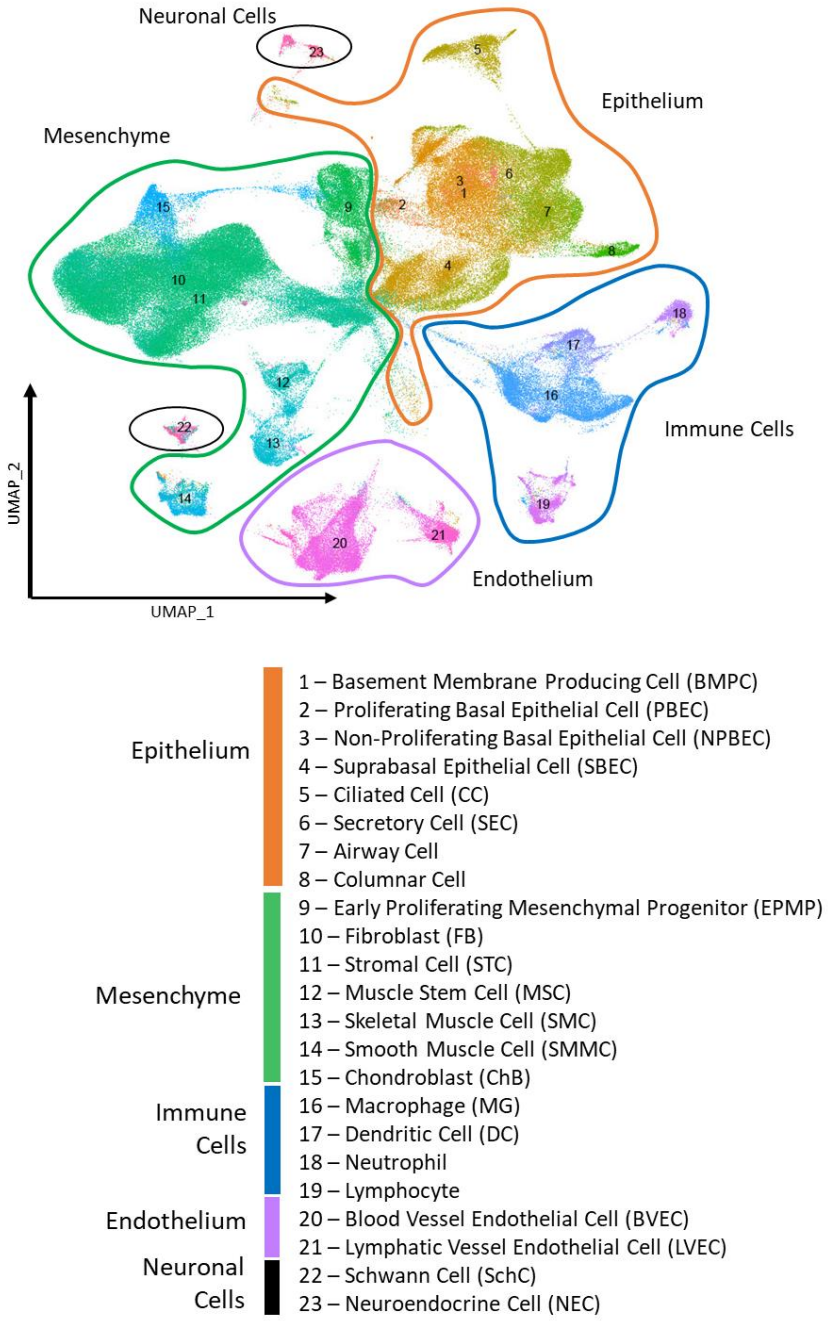

Figure 7: UMAP visualization of main cell types, in the developing larynx and vocal fols across the lifespan,. *Colors indicate major cell populations such as the epithelium (orange), mesenchyme (green)' immune cells (blue), endothelium (purple), and neuronal cells (black).*

identifications were further supported by specific markers from existing literature that align with their defining genes.

Definition of Laryngeal and Vocal Fold Major Cell Populations

Epithelial Cell Populations

The top 5 DEGs defining BMPC were *Cldn6, Shh, Foxa2,* and *Frem2* (Fig. 8). Frem2 belongs to a family of ECM proteins that constitutes components of the sublamina densa region of embryonic epithelial basement membrane. It has been also associated with epithelial-mesenchymal cohesion (Pavlakis et al., 2011). *Foxa2* and *Shh* point towards endodermal origin. These genes are expressed mostly in early embryonic stages. Moreover, this cluster expressed markers for mature basal cells such as *Trp63* and important genes linked to basement membrane production including *Lama2, Col4a6,* and *Col4a1* (Funk et al., 2018)

The PBEC population was defined by *Anln* and *Aspm*. *Anln* plays a vital role in epithelial cell proliferation, particularly in cytokinesis, and migration (Tuan & Lee, 2020). *Aspm* has been found in stem cells/progenitors of the oxyntic epithelium in the stomach serving as its marker (Bruland et al., 2015). Within this cluster, the top defining genes also encompassed *Mki67, Krt14, Krt5, Krt8, Kt17,* and *Hmgb2* (Fig. 8 and Supplementary Data 1). These genes play key roles in cell division (Mki67), stem cell differentiation (Hmgb2), and establishing the basal cell position within the epithelium *(Krt14, Krt5, Krt8, Krt17)* (Starkova et al., 2023; Sun & Kaufman, 2018).

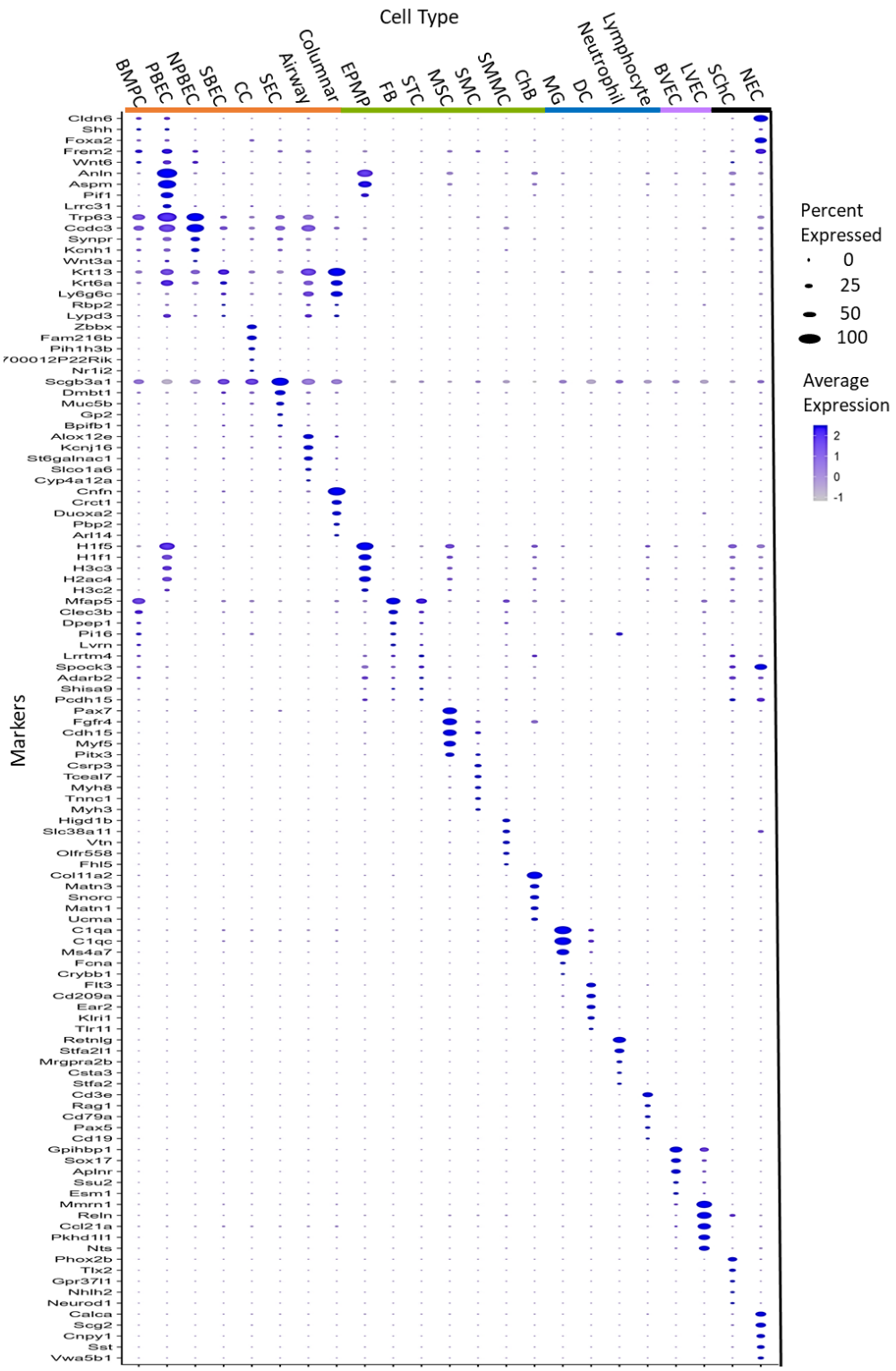

Figure 8: DOT-PLOT of top 5 differentially expressed genes that define major clusters. *Dot size corresponds to the ratio of cells expressing the gene, in the cell type. The color scale corresponds to the average expression levels.*

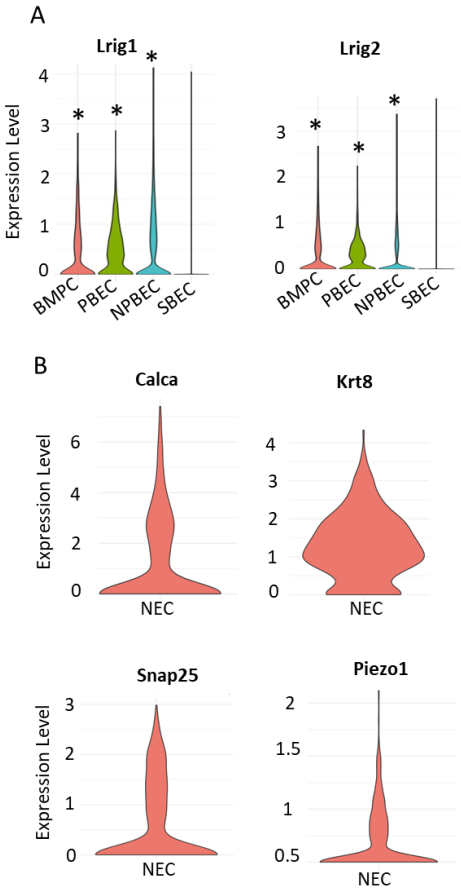

Figure 9: Gene expressions in populations of interest ***(A)*** *Violin plots displaying differentially expressed Lrig1 and Lrig2 genes for the basement membrane producing cell (BMPC), proliferating basal epithelial cell (PBEC), non-proliferating basal epithelial cells NPBEC and suprabasal epithelial cell (SBEC). (B) Violin plots displaying differentially expressed genes for the population of neuroendocrine cells.*

The NPBEC population was defined by high expression of *Trp63, Synpr, Ccdc3, Kcnh1,* and *Wnt3a* (Fig. 8). *Trp63* is a hallmark marker gene for basal cells in squamous and airway epithelium. (Zhou et al., 2022). SBEC, on the other hand, *expressed Krt6a, Krt13, Rbp2 and Lypd3* (Fig. 8). *Krt6a* and *Krt13* genes encode essential keratins found in VF stratified epithelium (Levendoski et al., 2014). Furthermore, SBEC expressed *Sfn* and *Calm3* (Supplementary Data 1). Both genes are responsible for epithelial stratification and are mainly found in the superficial layers of stratified squamous epithelium in the oral mucosa, playing a role in the differentiation of oral keratinocytes (Brooks et al., 2013).

All three epithelial cell populations, BMPC, PBEC and NPBEC, were also enriched in expression of stem cell markers namely *Lrig1* and *Lrig2* as compared to more specialized SBEC indicating that these cells were in less differentiating stage and, therefore, retain greater potential for self-renewal and differentiation. They can contribute to epithelial maintenance during both embryogenesis and adulthood (Fig. 9A).

The top 5 DEGs for the population of SEC included *Muc5b, Scgb3a1, Dmbt1, Gp2,* and *Bpif1* (Fig. 8). *Muc5b* is a primary gel-forming mucin in the respiratory tract and a member of the mucin family (Hancock et al., 2018). It is produced by secretory cells within the epithelium and submucosal glands. *Scgb3a1* is a member of the secretoglobulin family, commonly used as a marker for secretory cells in the luminal respiratory epithelium (Hewitt & Lloyd, 2021a). This gene is frequently co-expressed with *Scgb1a1*. The *Dmbt1* gene is associated with secretory antimicrobial functions (Hewitt & Lloyd, 2021a).

Other typical respiratory epithelial cell populations found in the larynx included CC, airway, and columnar cells (Fig. 8). The CC population was defined by *Zbbx, Fam216b, Pih1h3b,* and *Nr1i2*. These cells also expressed a canonical marker of CC, *Foxj1* (Plasschaert et al., 2018; You et al., 2004) along with key genes related to cilia movement, *Dynlrb2* and *Dnah12* (Greaney et al., 2020). The airway epithelial cell population exhibited *Kcnj16, Alox12e, St6galnac1, Slco1a5,* and *Cyp4a12a* among their top 5 DEGs. The specific type within the airway epithelium is unknown. Columnar cell population showed *Cnfn, Crct1, Duoxa2, Pbp2,* and *Arl14* in their top defining genes, consistent with literature describing columnar cells (Cellkb.com).

Mesenchymal Cell Populations

Exploring the mesenchymal cell population, EPMP displayed key proliferation markers *H1f1, H1f5, H3c3, H2ac4,* and *H3c2* in their top 5 DEGs (Fig. 8). Moreover, these cells expressed genes linked with mesenchymal development, *Gli1, Gli2,* and *Gli3,* which are downstream targets of Shh signaling pathway (Niewiadomski et al., 2019) along with other mesenchyme-related genes such as *Twist2* (Supplementary Data 1)(Chengxiao & Ze, 2015).

Other two mesenchymal cell populations, STC and FB, were defined by distinct sets of differentiated genes: *Pcdh15, Shisa9, Adarb2, Spock3,* and *Lrrtm4* in STC and *Clec3b, Dpep1, Mfap5, Pi16,* and *Lvrn* in FB (Fig. 8). The genes *Spock3* and *Pcdh15* expressed in STC are associated with neuronal development (*Spock3*) (Pascal et al., 2009) and mechanotransduction (*Pcdh15*) (Ivanchenko et al., 2023). As for the top DEGs in FB, they are involved in production of ECM including *Mfap5, Dcn* and *Eln* (Supplementary Data 1). These genes are considered as markers for FB cell type (Han et al., 2023; van Kuijk et al., 2023).

Other typical mesenchymal cell populations encompassed muscle cells and chondroblasts. In terms of muscle cells, the top 5 DEGs clearly distinguished between SMC defined by *Csrp3, Myh8,* and *Myh3,* canonical markers for skeletal muscles, MSC/satellite cells defined by *Pax7, Cdh15, Pitx3, Myf5, and Fgfr4*, these genes are highly abundant in muscle stem cells (Zammit et al., 2006) and SMMC defined by *Slc38a11, Vtn*. and *Higd1b* (Fig. 8). SMC population also expressed DEGs in their top defining genes (Walter et al., 2023), *Acta1* and *Myh3* that are important for muscle contraction (Supplementary Data 1). On the other hand, SMMC were enriched in expression of *Acta2* and *Myh11,* which are well-established markers for SMMC cell type (Muhl et al., 2022). In terms of the ChB, these cells highly expressed *Col11a2, Matn3, Snorc, Matn1,* and *Ucma* along with *Sox9* and *Col2a1* that are canonical markers for ChB cell population (Surmann-Schmitt et al., 2008) (Fig. 8, Supplementary Data 1). ChB expressed receptors for retinoic acid such as *Rxra* and *Rxrb* (Supplementary Data 1). In addition, ChB expressed *Hoxa5* and *Hoxa3* (Supplementary Data 1).

Immune Cells

Regarding immune cell populations, we focused on MG, DC, neutrophils and lymphocytes. The MG group expressed *Ms4a7, C1qc, C1qa, Fcna,* and *Crybb1* in their top 5 DEGs as compared to other immune cells (Fig. 8). *C1qc* and *C1qa* genes encode for complement chains that are present on MG membranes, serving as canonical markers for MG cell populations (Benoit et al., 2012; Horowitz et al., 2024). *Ms4a7* is plasma membrane molecule selectively expressed by MG-lineage cells (Mattiola et al., 2019). It is associated with activation of Syk-dependent signaling pathway, and the consequent production of cytokines and reactive oxygen species (Mattiola et al., 2019).

In their top 5 DEGs, DC showed expression of *Flt3*, *Cd209a*, *Ear2*, *Klri1*, and *Tlr11*. *Cd209a* (also known as DC-sign) plays a crucial role in the interaction between dendritic cells and T-cells (Ponichtera et al., 2014). Additionally, DC also expressed *H2-Ab1* and *H2-Eb* (Fig. 8) which are integral components of HLA type II, essential for antigen-presentation in DC and other antigen-presenting cells. (Khandelwal & Roche, 2010).

The top 5 DEGs for neutrophils were *Retnlg*, *Stfa2l1*, *Mrgpra2b*, *Csta3* and *Stfa2*. *Retnlg and Stfa2* are highly expressed neutrophiles in lung parenchyma (Zheng et al., 2022) and are associated with chemotaxis and innate immune cell infiltration (Ji & Fan, 2019) Neutrophils also expressed *S100a9* which is essential for neutrophil activation (Sprenkeler et al., 2022).

Lastly, the lymphocyte cell population was defined by *Cd3e* and *Rag1*. These cells also expressed *Trbc2, Skap1*, *Skap2*, and *Themis*. *Cd3e* serves as a universal marker for T-lymphocytes. *Trbc1* and *Trbc2* represent T-cell receptor B-chain constants, a major constituent of the T-cell receptor (Ferrari et al., 2024) (Fig. 8). *Skap1* encodes a T-cell adaptor protein (Ophir et al., 2013), while *Themis* plays a crucial role in T-cell development (Lesourne et al., 2009).

Endothelium

In our analysis of EC populations, we focused on those lining blood (BVEC) and lymphatic vessels (LVEC). The top 5 DEGs for BVEC included *Aplnr*, *Gpihbp1*, *Sox17*, *Esm1* and *Ssu2* (Fig. 8*). Sox17* is a crucial endothelial-specific transcription factor involved in arteriovenous differentiation and angiogenesis (Simmons Beck et al., 2023). BVEC additionally expressed *CD93* which is a canonical marker for EC (Galvagni et al., 2016) (Fig. 8). For LVEC, the top 5 DEGs included *Ccl21a, Mmrn1*, *Pkhd1l1*, *Reln,* and *Nts*. *Mmrn1* serves as a canonical marker for lymphatic EC (Li et al., 2021; Xiang et al., 2020) along with *Pdpn* (Breiteneder-Geleff et al., 1999) which was also found in top DEGs for this cell population.

Neuronal Cells

Neuronal cells included SchC and NEC. The SchC expressed *Neurod1*, *Nhlh2*, *Grp37l1*, *Txl2* and *Phox2b* in the top 5 DEG along with *Cryab*, *Mpz*, *Prph*, and *S100b* which are considered canonical markers for this population (Z. Liu et al., 2015; Wolbert et al., 2020) (Fig. 8, Supplemental Data 1). *Cryab* is an important regulator of myelination (Wolbert et al., 2020), while *Mpz* encodes for a peripheral nervous system myelin protein (Wolbert et al., 2020). The NEC was characterized by *Calca*, *Sst*, *Scg2, Vwa5b1*, and *Cnpy1* (Fig. 8, 9B). *Calca* serves as a canonical marker for NEC (Kuo et al., 2022). These cells also expressed *Snap25(chemoreceptor), Piezo1* (mechanoreceptor) (Foote & Thibeault, 2021) *Scg5*, *Krt8*, and *Chgb* (Fig. 9B). *Scg5* and *Chgb* are associated with peptidergic activity of these cells (Kuo et al., 2022), while *Krt8* links their location to the epithelium.

Cell Population Dynamics Throughout the Lifespan

Overall Population Dynamics Across Developmental Stages

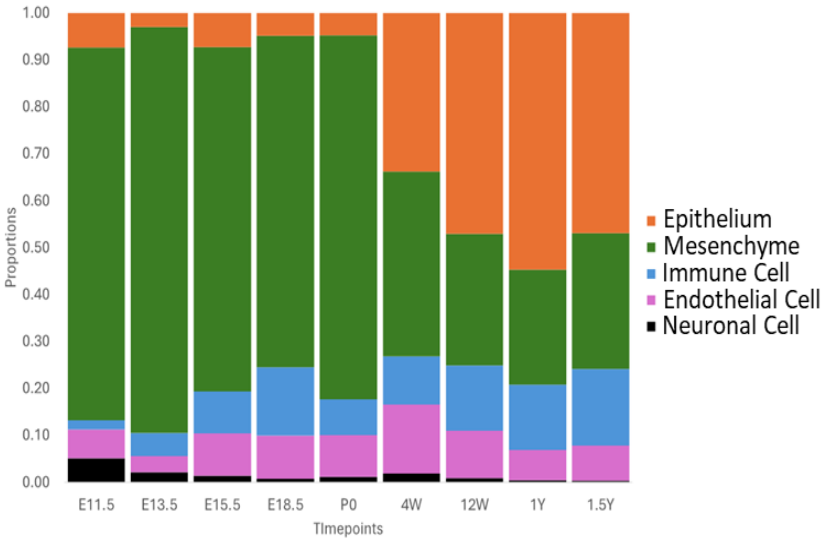

Figure 10: Proportion dynamics in major cell populations across developmental stages. *Colors indicate major cell populations –epithelium (orange), mesenchyme (green), immune cells (blue), endothelial cells (pink) and neuronal cells (black).*

Understanding the cellular dynamics across developmental stages offers valuable insights into tissue formation and maturation (Fig. 10). Our findings indicate that during embryonic and early postnatal stages up to 4W, mesenchymal cells were the dominant cell population, followed by epithelial cells. Interestingly, by 4W, proportions of mesenchyme and epithelium had become equivalent. Subsequently, from 12W until 1.5Y, epithelial cells became the dominant cell type.. Concurrently, the proportion of immune cells started to rise from 12W, reaching its peak at 1.5Y. Notably, neuronal tissue peaked at the E11.5 time point, consistent with existing literature (Wendt et al., 2022) (Fig. 10). These observations were further supported by UMAP analyses across developmental stages (Fig. 11). and validated by H&E staining which aligns well with prior research by Lungova et al 2020 (Fig. 12). H&E staining revealed a progressive differentiation of mesenchymal cells, which were not fully differentiated at E11.5, into laryngeal cartilages and muscles from E13.5 to P0, as well as the maturation of the epithelium and emergence of submucosal glands at E.18.5 through P0 with full development occurring by 4W of

age. Both processes, the prenatal formation of mesenchymal structures and the postnatal increase in epithelial cell types, likely contribute to the observed switch in cell populations throughout the lifespan (Figs. 11, 12). Furthermore, we also noted a gradual muscular atrophy accompanied by an accumulation of ECM and adipose tissue in laryngeal muscles at 1Y and 1.5Y of age.

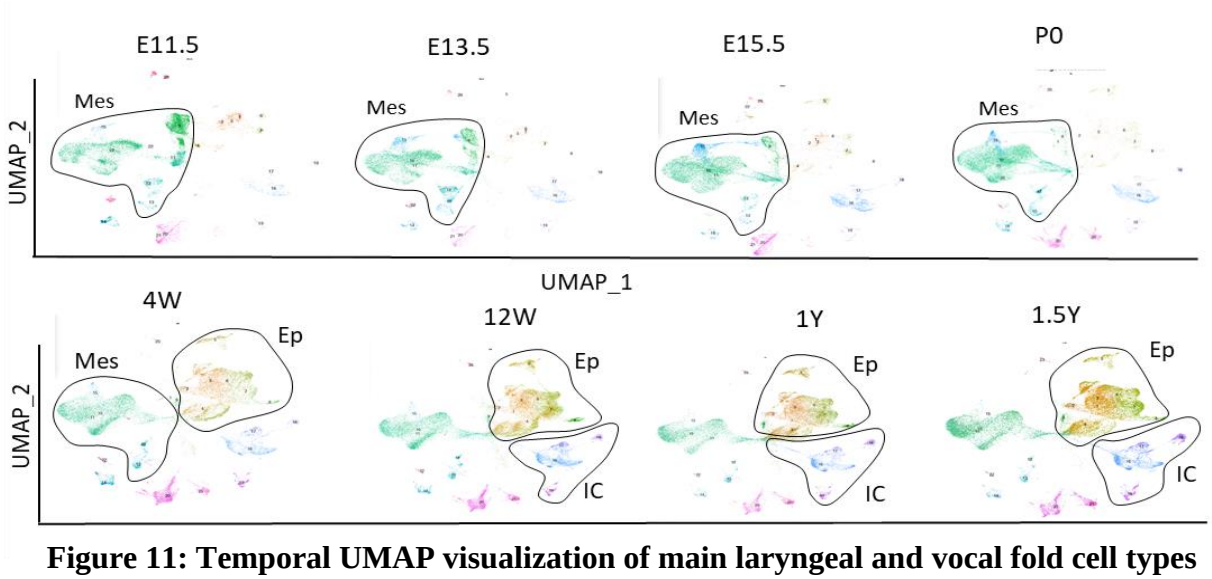

Figure 11: Temporal UMAP visualization of main laryngeal and vocal fold cell types across developmental stages. *Abbreviations: Ep, epithelium; IC, immune cells; Mes, mesenchyme.*

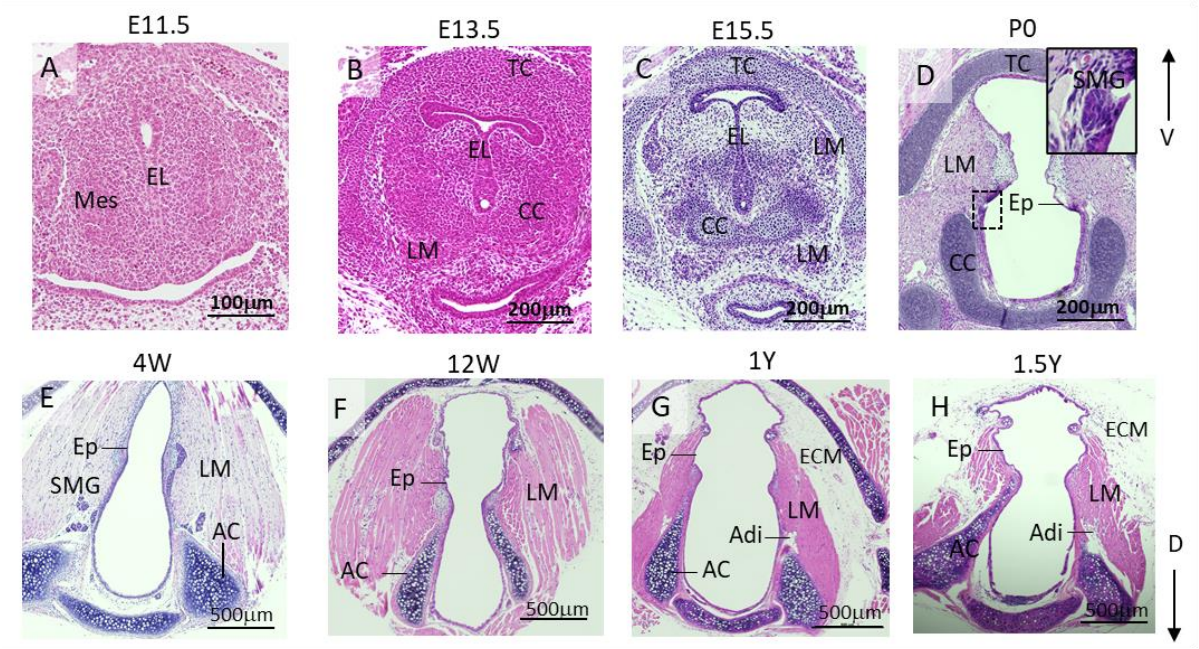

Figure 12: Morphology of the developing larynx and vocal folds across developmental stages. *(A) Morphology of the developing larynx at embryonic stage 11.5, that shows fused epithelium in the form of epithelial lamina and undifferentiated mesenchyme. (B, C) Morphology of developing larynx at embryonic stage E13.5 and 15.5, respectively. The epithelial lamina is still visible but initiates its recanalization. Mesenchymal structures start to differentiate into laryngeal cartilages and muscles. (D) Morphology of developing larynx at postnatal day P0. The epithelial lamina is completely recanalized and laryngeal cartilages and muscle are fully developed. The bracketed region indicates the location of the detailed image at the top right corner, which shows the developing submucosal glands. (E-H) Morphology of developing larynx at postnatal stages with the emergence of submucosal glands at 4W, muscular atrophy and depositions of extracellular matrix and adipose tissue at 1Y and 1.5Y of age. Abbreviations: AC, arytenoid cartilage; Adi, adipose tissue; CC, cricoid cartilage; ECM, extracellular matrix; EL, epithelial lamina; Ep, epithelium; LM, laryngeal muscles; SMG, submucosal glands.*

Epithelium

We next conducted a comprehensive analysis to delve deeper into the developmental dynamics of the individual cell populations. In the epithelium, development commenced with a high proportion of cells located at the basal cellular compartment such as BMPC, PBEC and NPBEC. As the embryonic development advanced, we observed a decline in BMPC and PBEC coupled with an increase in specialized cell populations such as SBEC, SEC and particularly CC

that first appeared at E15.5. Postnatally, both BMPC and PBEC continued to decrease, reaching minimal proportions. In contrast, NPBEC remained and reached its peak with aging (at 1.5Y). Among the specialized cell populations, SBEC and SEC were already present in the epithelium at E11.5, peaking at E18.5 and 4W, respectively, before gradually decreasing with age. A similar pattern was observed in CC that reached their peak before birth and declined thereafter (Fig. 13).

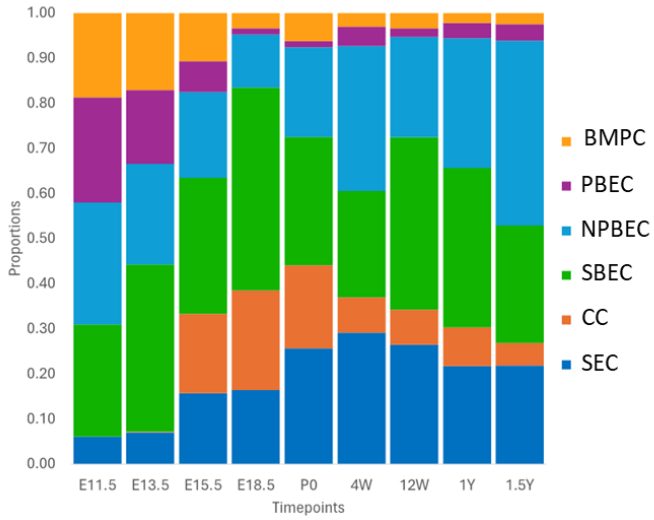

Figure 13: Dynamics of epithelial cell populations across lifespan. *Colors indicate major cell populations –within epithelium - BMPC (orange), PBEC (purple), NPBEC (green), CC (orange) and SEC (blue).*

Mesenchyme

In the mesenchymal cell population, at E11.5, EPMP cells were the predominant cell type in mesenchymal cells (Fig. 14). However, their proportion notably decreased as development advanced, although some cells retained the ability to proliferate into adulthood. Other cell types, such as FB and STC

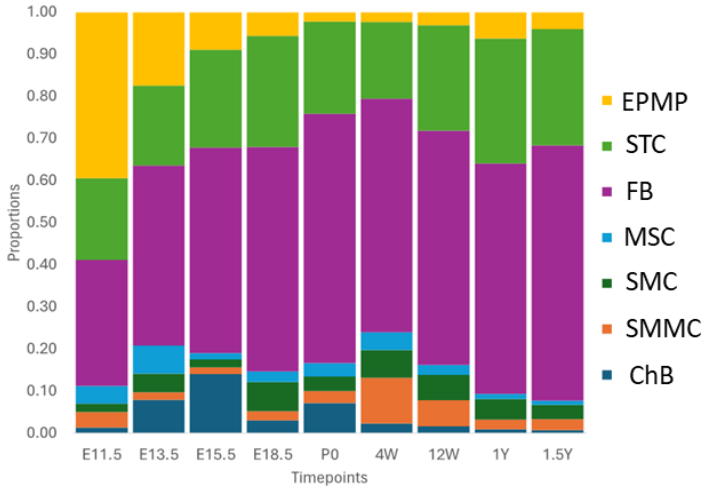

Figure 14: Dynamics of mesenchymal cell populations across lifespan. *Colors indicate major cell populations – within mesenchyme - EPMP (orange), STC (green), FB (purple), MSC (light blue), SMC (dark green), SMMC (orange), ChB (dark blue).*

were also present in the laryngeal region at E11.5. From E13.5 to 1.5Y, as the proportion of EPMP declined, FB became the dominant mesenchymal population, while STC maintained consistent proportions throughout development.

In terms of other mesenchymal cell populations, MCS reached their peak proportions at E13.5, which correlates with the onset of skeletal muscle development (Lungova et al., 2018a). Interestingly, MSC significantly decrease with age, which may impact skeletal muscle regeneration. The populations of SMC and SMMC peaked from E18.5 to 12W and from 4W to 12W, respectively, while ChB peaked between E13.5 and E15.5 which corelates with the establishment and differentiation of laryngeal muscles and cartilages (Lungova et al., 2018a).

Immune Cells

Lastly, we explored shifts in immune cell populations across the lifespan (Fig. 15).

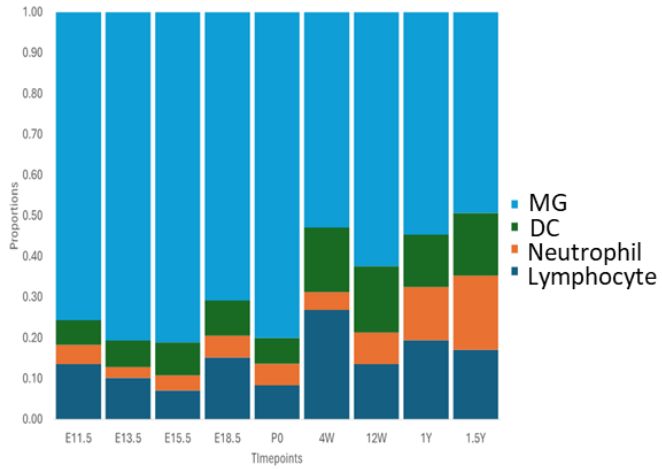

Figure 15: Dynamics of immune cell populations across lifespan. *Colors indicate major cell populations in immune cells – macrophages (light blue), dendritic cells (dark green), neutrophils (orange), lymphocyte (dark blue).*

Interestingly, all major types of immune cells were present in the larynx from early embryonic stages. The dominant cell population were the tissue-resident macrophages, which were notably abundant during embryonic stages but decreased in proportion, postnatally. In contrast, other immune cell types increased in proportion after birth**.** In aging mice, we observed a significant increase in neutrophils, suggesting increased immune cell infiltration.

Transcriptome Dynamics within VF Stratified Epithelium, Fibroblasts and Macrophages across Lifespan

To comprehensively examine transcriptional dynamics across our timepoints from E11.5 to 1.5Y, we identified the top 50 DEGs exhibiting the most significant changes over the lifespan. This analysis encompassed PBEC, NPBEC, SBEC, FB, and MG, yielding insightful data on the aging transcriptome changes of major cellular populations in VF mucosa.

Proliferating Basal Epithelial Cells (PBEC)

During early PBEC development, heightened expression of genes such as *H2az, H3f3b,* and *Hmgb2*, associated with cell division and epithelial-mesenchymal transition (EMT), was observed (Kelly et al., 2010). Concurrently, *Ptma*, linked to anti-apoptotic properties and proliferation, exhibited increased expression(Karetsou et al., 1998). However, as PBECs matured, a reduction in proliferative and EMT potential ensued, concomitant with elevated expression of keratins, indicative of enhanced epithelial incorporation and diminished migratory capacity into the mesenchyme (Supplementary Fig. 1)

Non-Proliferating Basal Epithelial Cells (NPBEC)

Early embryonic NPBECs demonstrated a notable potential for protein translation, evidenced by the expression of genes such as *Eef1a1* and *Tpt1*, which negatively regulate autophagy, alongside *Mecom,* crucial for hair cell differentiation from supporting cells in cochlea(Abbas et al., 2015; Chen et al., 2022). Subsequently, from 4W onwards, NPBECs expressed genes *like Krt17, Krt5, Krt15, Krt4, Krt14,* and *Aqp3*, suggestive of heightened epithelial incorporation, antimicrobial activity (*Bpif1*), and immunoregulatory properties

(*S100a11* and *S100a6*). Predominant expression of *Wnt4*, a gene for non-canonical Wnt ligand 4, in 1Y and 1.5Y, is associated with cell differentiation(Q. Zhang et al., 2021a) (Supplementary Fig 2).

Suprabasal Cells (SBEC)

SBECs initiated functional differentiation around 4W, reaching peak expression levels between 12W to 1Y. In detail, genes like *Sfn* and keratins exhibited early expression at 4W, peaking at 1Y, alongside antimicrobial (*Bpif1, Reg3g*) and chemotaxis-associated genes (*S100a11, S1006, Fth1*) expressed from P0 onwards(Hu et al., 2022; L. Zhang et al., 2021) (Supplementary Fig. 3).

Fibroblasts (FB)

Fibroblasts demonstrated diverse gene expression patterns across time points. Early stages were characterized by proliferation-related genes such as *H3f3b* and an anti-apoptotic phenotype mediated by *Ptma*. Notably, *Serpinh1*, a collagen-specific chaperone, crucial protein that recognizes collagenous repeats on triple helical procollagen and prevents local unfolding or aggregation of procollagen, commenced expression at E15.5(Ito & Nagata, 2017). Collagen-producing genes; *Col1a2*, *Col5a2*, *Col1a1*, *Col3a1*, *Eln (elastin)*, and *Vim (vimentin)* peaked between E18.5 to 4W, while old fibroblasts (1.5Y) exhibited expression of *Flt1*, *Fau*, and *Tmsb4x*. The first of which has been associated with fibrosis in pulmonary tissue. *Fau* gene is a tumor suppressor gene which regulates apoptosis (Pickard et al., 2011) (Supplementary Fig. 4).

Macrophages (MG)

Macrophages displayed increased proliferation over the lifespan, with heightened expression of histone-related genes such as *H3f3a* and *H3f3b*. Antimicrobial and phagocytic functions became evident starting at 4W. MG acquired signature genes like *C1qa, C1qb, C1qc,* and *Cyba*, essential for their phagocytic properties at E18.5 (Supplementary Fig. 5)(Z. Q. Liu et al., 2023).

Developmental Relationships among Cell Populations and their Differentiation Transcriptome Dynamics

Understanding the developmental relationships between individual cell types within major cell populations provides crucial insights into tissue formation, maturation, and function. This complex interplay typically starts with progenitor cells that differentiate into various specialized cell types as development advances. To elucidate these developmental relationships, we conducted pseudotime analysis, which allowed us to order cells along a developmental trajectory based on their gene expression profiles, thereby revealing the sequential differentiation events and potential lineage relationships within the individual cell populations.

Epithelium

In the epithelium, we examined the developmental relationships among PBEC, NPBEC and SBEC, as well as between PBEC, NPBEC and SEC and CC, respectively (Fig. 16). Our data show that PBEC represented the least differentiated cell population, transitioning into NPBEC, which subsequently gave rise to all specialized cells: SBEC, SEC, and CC.

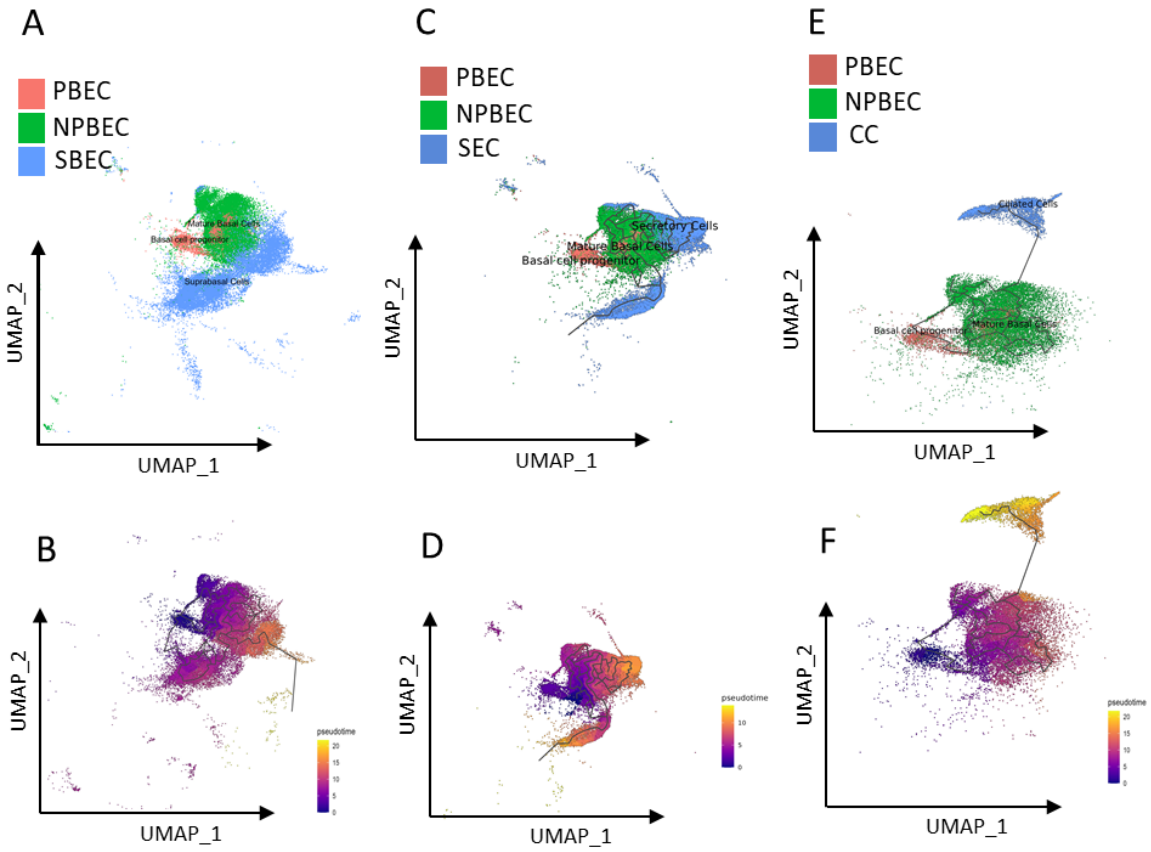

Figure 16: Developmental trajectories within epithelial cell populations. *(A, C, E) UMAPs showing epithelial cell populations included in the pseudotime analyses (A) proliferating basal epithelial cell in red, and non-proliferating basal epithelial cell, in green. The blue color denotes most differentiated cell types represented by suprabasal epithelial cell (A), secretory cell (C) and ciliated cell (E). (B, D and F) Developmental trajectories showing the transition between the most undifferentiated cell type represented by proliferating basal epithelial cell (dark blue) through non-proliferating basal epithelial cells (shades of purple and red) towards the most differentiated cell types represented by suprabasal epithelial cell (B), secretory cell (D) and ciliated cell (F) in shades of orange or yellow. Abbreviations: CC, ciliated cell; SC, secretory cell; NPBEC, non-proliferating basal epithelial cell; PBEC.*

To further elucidate the molecular mechanisms underlying epithelial differentiation, we performed DE analysis to identify top 50 DEGs whose expression significantly changed over pseudotime (Supplementary Figs. 6, 7). Among the top upregulated genes activated during the process of epithelial differentiation were genes associated with keratin deposition, including *Krt4, Krt19, Krt13, Krt7, Krt8* and *Krt23*. We also identified genes related to innate immunity and defense responses, such as *Bpifa1, Reg3g, Ltf, Ly6g6c, Ly6d*, and *Mal.* These genes likely play crucial roles in epithelial defense mechanisms and barrier functions. Furthermore, we found genes involved in various metabolic processes, including xenobiotic and carcinogen metabolism *(Gsto1),* glucose metabolism *(Cbr2),* and cytochrome activity *(Cyp2f2 and Cyp2a5*), which may be essential for maintaining cellular homeostasis and function during epithelial differentiation (Supplementary Fig. 6).

In contrast, the top DE downregulated genes were associated with cell proliferation, such as *Pard3* and *Stmn1,* and signaling regulatory pathways, including *Fgfr2, Wls*, *Efna5*, and *Egfr* (Supplementary Fig. 7). These findings suggest that as epithelial cells differentiate and transition into suprabasal layers, they become less responsive to mesenchymal growth signals, potentially resulting in a reduced ability to divide. Additionally, we identified a distinct set of downregulated DEGs involved in trans-synaptic signaling, namely *Synpr, Tenm2*, and *Tenm3,* suggesting a potential loss of signal transduction capability as the cells become more specialized and move into the suprabasal compartments.

Mesenchyme

In the mesenchymal cell populations, we conducted three developmental trajectory analyses to investigate the relationships between EPMP, STC, and FB. Subsequently, we

explored the connections between EPMP and muscle cells, followed by the relationship between EPMP and chondroblasts. Our pseudotime analyses supported the concept that EPMP gave rise to STC, which then differentiated into more specialized FB (Fig. 17A, B). Additionally, the EPMP cell population demonstrated the capacity to differentiate into MSCs, which subsequently followed two distinct paths: one leading to the development of SMC and the other to the differentiation of SMMC (Fig. 17C, D). Finally, EPMP also differentiated into chondroblasts (Fig. 17E, F).

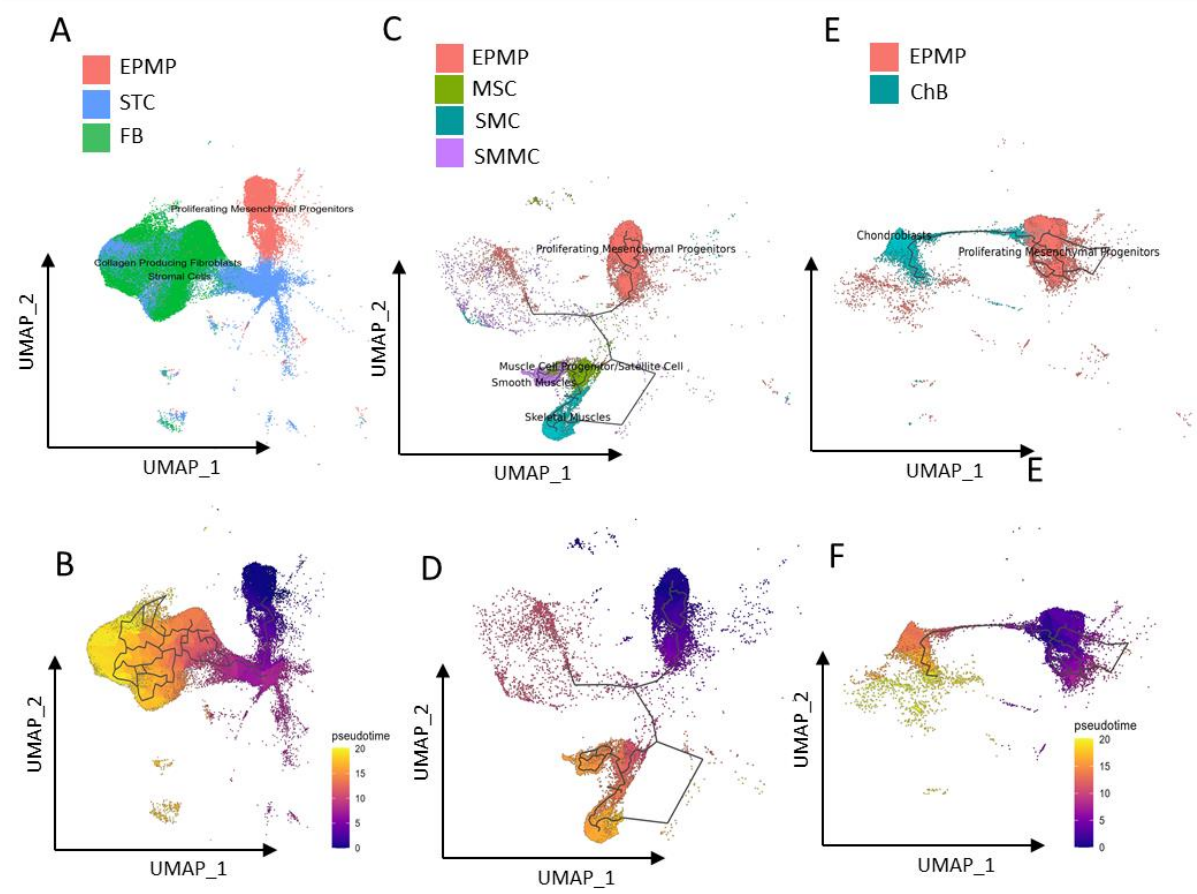

Figure 17: Developmental trajectories within mesenchymal cell populations. *(A, C, E) UMAPs showing mesenchymal cell populations included in the pseudotime analyses. (B, D and F) Developmental paths illustrate progression from the most undifferentiated cell type in dark blue, passing through intermediate cell populations in shades of purple or red, and culminating in the most specialized cell types in shades of orange or yellow. Abbreviation: EPMP, early proliferating mesenchymal progenitor; ChB, chondroblast; FB, fibroblast; MSC, muscle stem cell; SMC, skeletal muscle cell; SMMC, smooth muscle cell; STC, stromal cell.*

Similar to our analysis of epithelial cells, we identified the top 50 upregulated and downregulated DEGs that show significant changes during the maturation of mesenchymal structures (Supplementary Figs. 8, 9). Among the top upregulated genes activated during the process of mesenchymal differentiation were genes associated with extracellular matrix (ECM) deposition, such as *Col11a1, Col2a1, Col9a1, Col9a3, Col9a2, Col8a, Col11a2, Dcn,* and *Hapln1* which are typical ECM components produced by differentiated FB and ChB. Additionally, we pinpointed genes involved in musculoskeletal system development, such as *Tnn, Mkx, Thbs4,* and *Clip2*.

Among top 50 downregulating DEGs were, on the other hand, mostly genes regulating the cell cycle, namely *H2az1, Hmgb1, Hmgb2, Stmn1, Top2a*, and *H1f5* (Supplementary Fig. 9). This aligns with the characteristics of the initial EPMP cell population, which initially exhibits high proliferative potential that decreases as these cells mature and differentiate.

Sub-clustering Analysis

We conducted sub-clustering analysis to further deepen our understanding of the primary cell populations. This approach allowed us to identify smaller, more distinct subgroups based on unique gene expression profiles or functional characteristics. Our research specifically targeted key cell populations including BMPC, PBEC, NPBEC, SBEC, SEC, EPMP, FB, and MG.

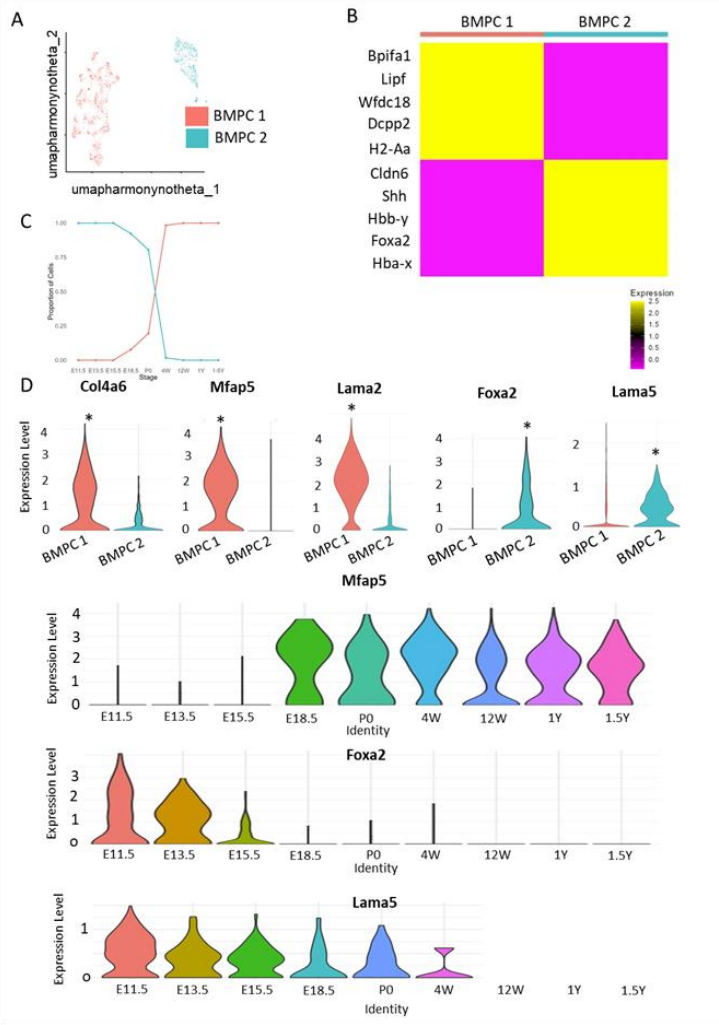

Figure 18: Sub-clustering analysis for population of basement membrane producing cells. *(A) UMAP visualization of subtypes identified in BMPC. (B) Heatmap displaying the top 5 differentially expressed genes for each subtype. (C) Cell proportion across subtypes and developmental stages. (D) Violin plots displaying differentially expressed genes for selected subtypes. (E-G) Expression profiles of genes of interest across timepoints. Asterixis signifies a significant Wilcoxon rank sum test with a threshold of avg_log fc 0.25, adjusted p-value < 0.05, and min.pct = 0.1.*

<u>Basement Membrane Producing Cell Subtypes</u>

We discovered two types of BMPC (Fig. 18A). The top 5 DEGs defining each subtype are shown in Fig. 18B. BMPC1 and BMPC2 were predominantly expressed in the E and postnatal stages, respectively (Fig. 18C). BMPC1 has been associated with more embryonic expression as such it expressed *Shh* and *Foxa2* at greater level. *Foxa2* expression levels decreased in the BMPC1 at E18.5. Interestingly, BMPC1 expressed

significantly ($p<0.05$) *Lama5* which is the most abundant embryonic laminin, pointing towards its function in establishment of embryonic basal lamina(Miner et al., 1998). *Lama5* expression decreased with increasing age reaching its lowest levels at 4W correlating with the disappearance of the BMPC1. BMPC2 had more mesenchymal phenotype expressing significantly ($p<0.05$) *Col4a6* and *Lama2*, major constituents to mature basal lamina (Maselli et al., 2012).

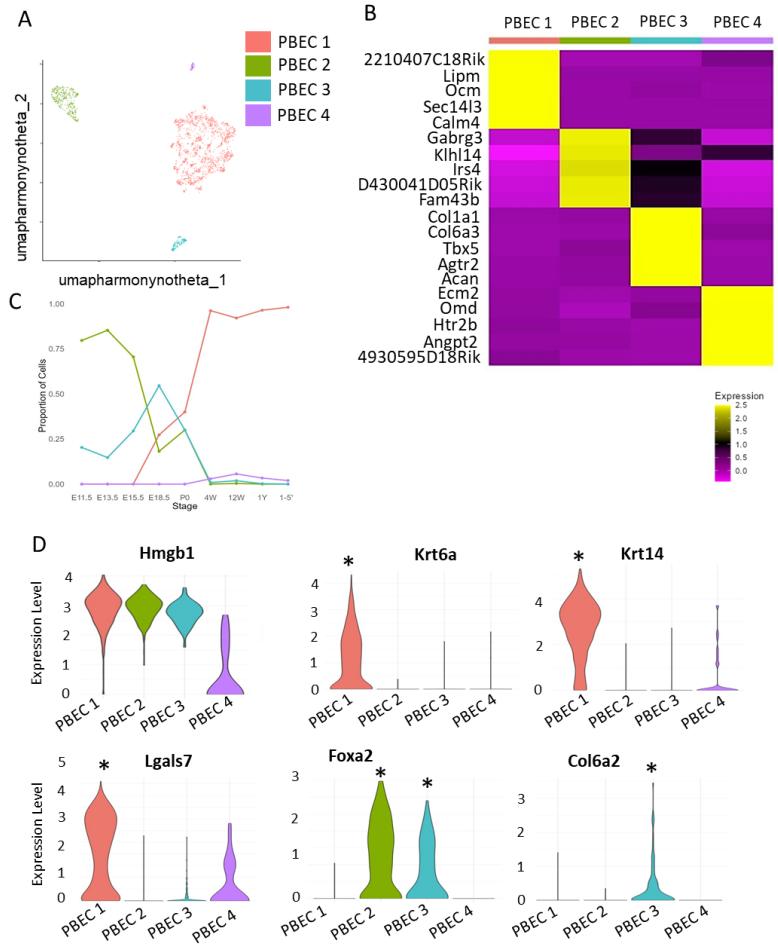

Figure 19: Sub-clustering analysis for proliferating basal epithelial cell population. *(A) UMAP visualization of subtypes identified in proliferating basal epithelial cells. (D) Heatmap displaying the top 5 differentially expressed genes for each subtype. (C) Cell proportion across subtypes and developmental stages. (D) Violin plots displaying differentially expressed genes for selected subtypes. Asterisks signifies a significant Wilcoxon rank sum test with a threshold of avg log fc 0.25, adjusted p-value < 0.05, and min.pct = 0.1.*

<u>Proliferating Basal Epithelial Cells Subtypes</u>

PBEC represent the most undifferentiated cell type with the epithelium that displays the high plasticity as showed by high expression levels of *Hmgb1* gene (Fig. 19D). We identified four subtypes of PBEC (Fig. 19A). The top 5 DEGs defining each subtype are shown in Fig. 19B. **PBEC1** exhibited significantly higher expression of *Krt6a, Krt14,* and *Lgals7* compared to the other subtypes ($p<0.05$) (Fig. 19D). Both *Krt6a* and *Krt14* are markers of

stratification, confirming the status of PBEC1 as a postnatal proliferating basal cell. **PBEC2** and **PBEC3** were predominantly present during the embryonic stages (Fig. 19C). They expressed markers of early embryonic endoderm, such as *Foxa2* (Fig. 19D). Additionally, PBEC3 expressed genes associated with ECM development, such as *Col1a1*, *Col6a3*, and *Col6a2* (Fig. 19B, D). **PBEC4** likely represents a postnatal subtype of PBEC and expressed *Mark3* and *Cit*, which are genes that inhibit the Hedgehog (HH) signaling pathway. This suggests a direction towards early differentiation rather than proliferation.

Non-Proliferating Basal Epithelial Cell Subtypes

We distinguished between three subtypes of non-proliferating basal epithelial cells (Fig. 20A, D). The top 5 DEGs defining each subtype are shown in Fig. 20B. **NPBEC1** is likely the most mature basal cell subtype compared to others, as its proportions increased during postnatal epithelial maturation (Fig. 20C) and it expressed significantly higher levels of keratins than the other subtypes ($p<0.05$) (Fig. 20D). Furthermore, *Clic3*, one of the top 5 DEGs in NPBEC1 (Fig. 19B) promotes cell migration (Dozynkiewicz et al., 2012). This indicates that NPBEC1 can detach from the basement membrane and migrate into the suprabasal compartment and

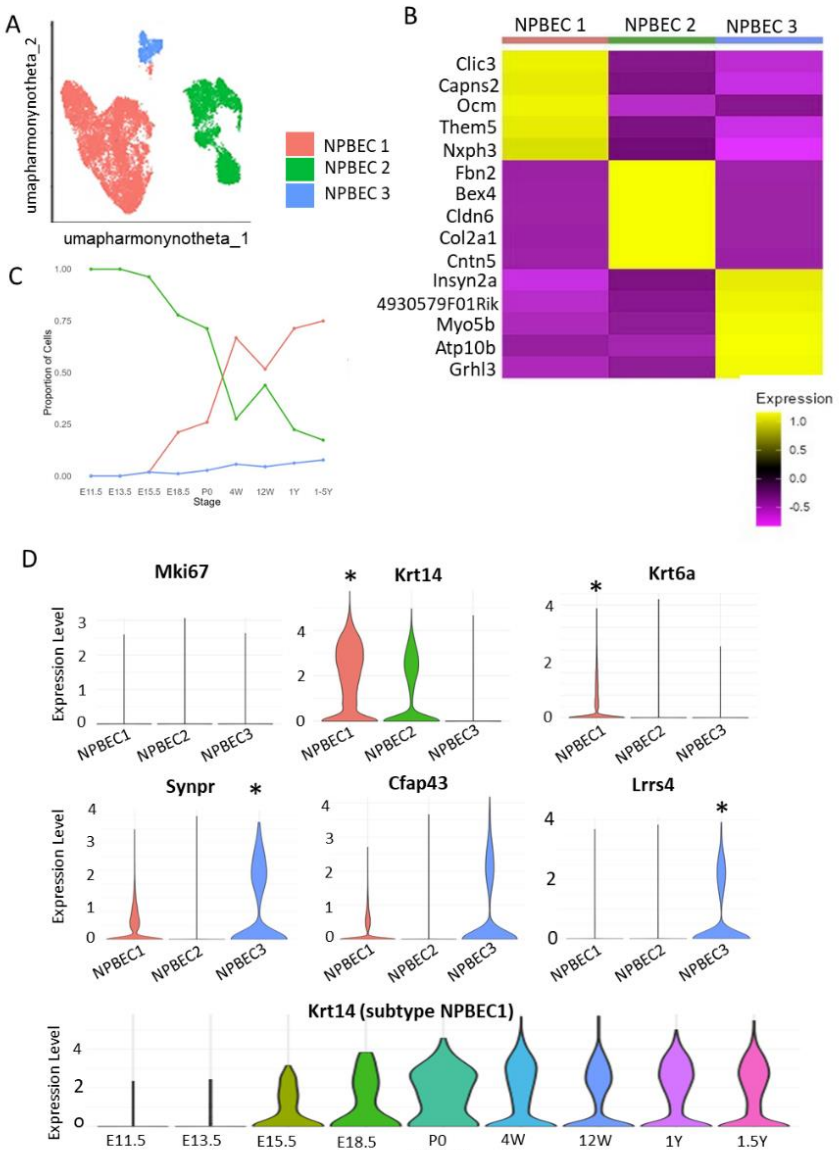

Figure 20: Sub-clustering analysis for non-proliferating basal epithelial cell population. *(A) UMAP visualization of subtypes identified in non-proliferating basal epithelial cells. (D) Heatmap displaying the top 5 differentially expressed genes for each subtype. (C) Cell proportion across subtypes and developmental stages. (D) Violin plots displaying differentially expressed genes for selected subtypes. Asterixis signifies a significant Wilcoxon rank sum test with a threshold of avg log fc 0.25, adjusted p-value < 0.05, and min.pct = 0.1.*

initiate the process of differentiation. **NPBEC2** expressed *Cldn6* in their top 5 DEGs supporting its early developmental origin. *Cldn6* belongs to the family of tight junctions and is predominantly found in fetal tissues. It plays an important role to establish skin and lung epithelial barrier (Qu et al., 2021). **NPBEC3** expressed *Synpr, Cfap43* and *Lrrs4* which point toward chemosensory cell development in the laryngeal epithelium (Fig. 20B and D)

Suprabasal Cells Subtypes

We characterized eight subtypes of suprabasal cells all of which expressed *Krt13*, a marker indicative of the suprabasal cell layer in stratified epithelium (Fig. 21A, D). The top 5 DEGs defining each subtype are shown in Fig. 21B. Besides *Krt13*, **SBEC1** further expressed *Krt6b, Krt6a,* and *Spink5* among their top defining genes, supporting a fully differentiated suprabasal cell phenotype (Fig. 21B, D). These cells are representative of postnatal cells (Fig. 21C). Additionally, SBEC1 exhibited *Cldn4* expression, a tight junction protein commonly found in differentiated stratified squamous cells (Fujiwara-Tani et al., 2023). Both, **SBEC2** and **SBEC3,** appeared during embryonic stages and persisted into the adulthood (Fig. 21C). SBEC2 displayed genes associated with cell cycle exit, like *Pngdh* and *Cdca7* (Fig. 21B), indicating location in parabasal cell layer. Meanwhile, **SBEC3** showed ECM production, including *Col1a1* (Fig. 21D)**. SBEC4, SBEC5** and **SBEC6** were found to be involved in immune system functions. SBEC4 expressed *Il1b* in its top 5 DEGs (Fig. 21B) as well as *C1qa* and *C1qb* that

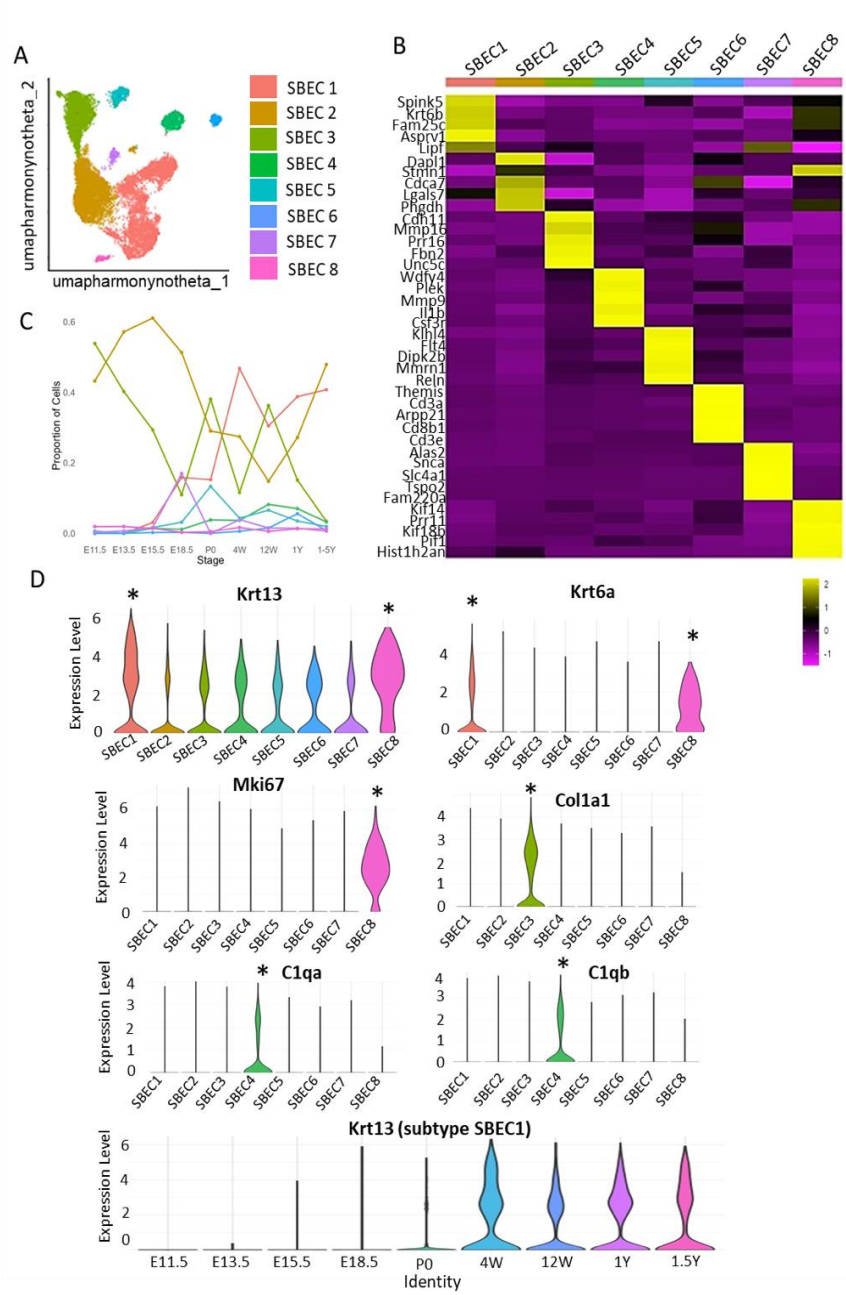

Figure 21: Sub-clustering analysis for suprabasal epithelial cell population. *(A) UMAP visualization of subtypes identified in suprabasal epithelial cells. (D) Heatmap displaying the top 5 differentially expressed genes for each subtype. (C) Cell proportion across subtypes and developmental stages. (D) Violin plots displaying differentially expressed genes for selected subtypes. Asterixis signifies a significant Wilcoxon rank sum test with a threshold of avg_log fc 0.25, adjusted p-value < 0.05, and min.pct = 0.1.*

play a role in regulating innate immune responses (Fig. 21D). SBEC5 and SBEC6 expressed markers supporting their role in regulating T-lymphocyte immune response such as *Themis* and *Cd3e* (Fig. 21B). SBEC6 was expressing genes involved in iron metabolism (Fig. 21B). Lastly, **SBEC7** maintained the proliferating properties such as *Hist1h2an* and *Mki67* together with markers of stratification suggesting its location in parabasal cell layer (Fig. 21B, D). The various subtypes of SBEC support the notion that the epithelium is not just a

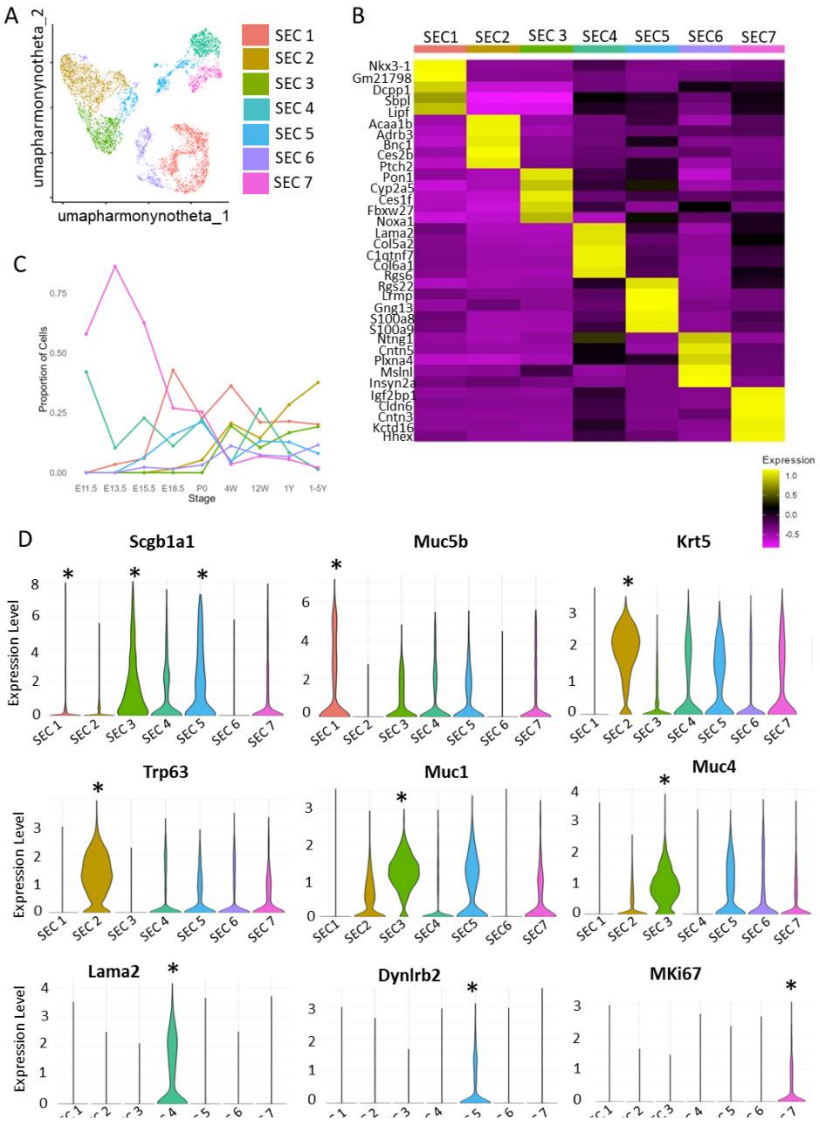

Figure 22: Sub-clustering analysis for secretory epithelial cell population. *(A) UMAP visualization of subtypes identified in secretory epithelial cells. (D) Heatmap displaying the top 5 differentially expressed genes for each subtype. (C) Cell proportion across subtypes and developmental stages. (D) Violin plots displaying differentially expressed genes for selected subtypes. Asterixis signifies a significant Wilcoxon rank sum test with a threshold of avg log fc 0.25, adjusted p-value < 0.05, and min.pct = 0.1.*

barrier between external environment but also interacts with cells of immune system and mesenchyme (Hewitt & Lloyd, 2021b).

<u>Secretory Cells Subtypes</u>

Seven subtypes of secretory cells were identified (Fig. 22A). The top 5 DEGs defining each subtype are shown in Fig. 22B. **SEC1** represented a population of mucus producing goblet cells due to its significantly ($p<0.05$) high production of *Muc5b*, the major mucin in airway epithelium (Fig. 22D). **SEC2** and **SEC3** were identified as two distinct

populations of club cells based on their expression profiles. Unlike goblet cells, club cells

express high levels of *Scgb3a2* and *Scgb1a1* and exhibit lower expression of *Muc5b*. SEC2 appeared to be a transitional club cell originating from basal cells, as it maintained gene expressions associated with basal cell phenotypes, such as *Trp63* and *Krt5* (Fig. 22D). In contrast, SEC3 lacked *Trp63* and *Krt5* expression and showed significantly higher expression of *Scgb1a1* and *Scgb3a2* ($p<0.05$) (Fig. 22D), indicating its status as a fully differentiated club cell. Additionally, SEC3 expressed *Muc1* and *Muc4* (Fig. 22D), membrane-bound mucins typically found in the *Scgb3a2*-high subtype of club cells (Zuo et al., 2020). **SEC4** appeared during embryonic stages (Fig. 22C), these cells exclusively produced *Lama2*, *Col5a2* and *Col6a1*, indicating its role in contributing to ECM and basement membrane formation in VF. This observation aligns with similar secretory cells found in lung parenchyma, which also play a role in ECM deposition. (Zuo et al., 2020). **SEC5** represents a population of Tuft cells, as it expressed *Gng13* among its top 5 DEGs (Fig. 22D). These cells are involved in immune and neuronal response of the airway to external environment (Hewitt & Lloyd, 2021b). The last subtype includes **SEC7** represented proliferating secretory cell as it expressed genes associated with proliferation such as *Mki67*, *Top2a*, and *Hist1h2ap.* This subpopulation was the dominant subtype during the embryonic stages (Fig. 22C).

Early Proliferating Mesenchymal Progenitors Subtypes

We characterized five subtypes of EPMP (Fig. 23A). The top 5 DEGs defining each subtype are shown in Fig. 23B. While most of these progenitors were identified during prenatal development, EPMP2 showed an increase during postnatal stages (Fig. 23C). All EPMP apart from EPMP2 expressed *Gli2* (Fig. 23D), downstream targets of the *Shh* pathway, which are crucial for the development of the lamina propria and surrounding mesenchyme, as well as for

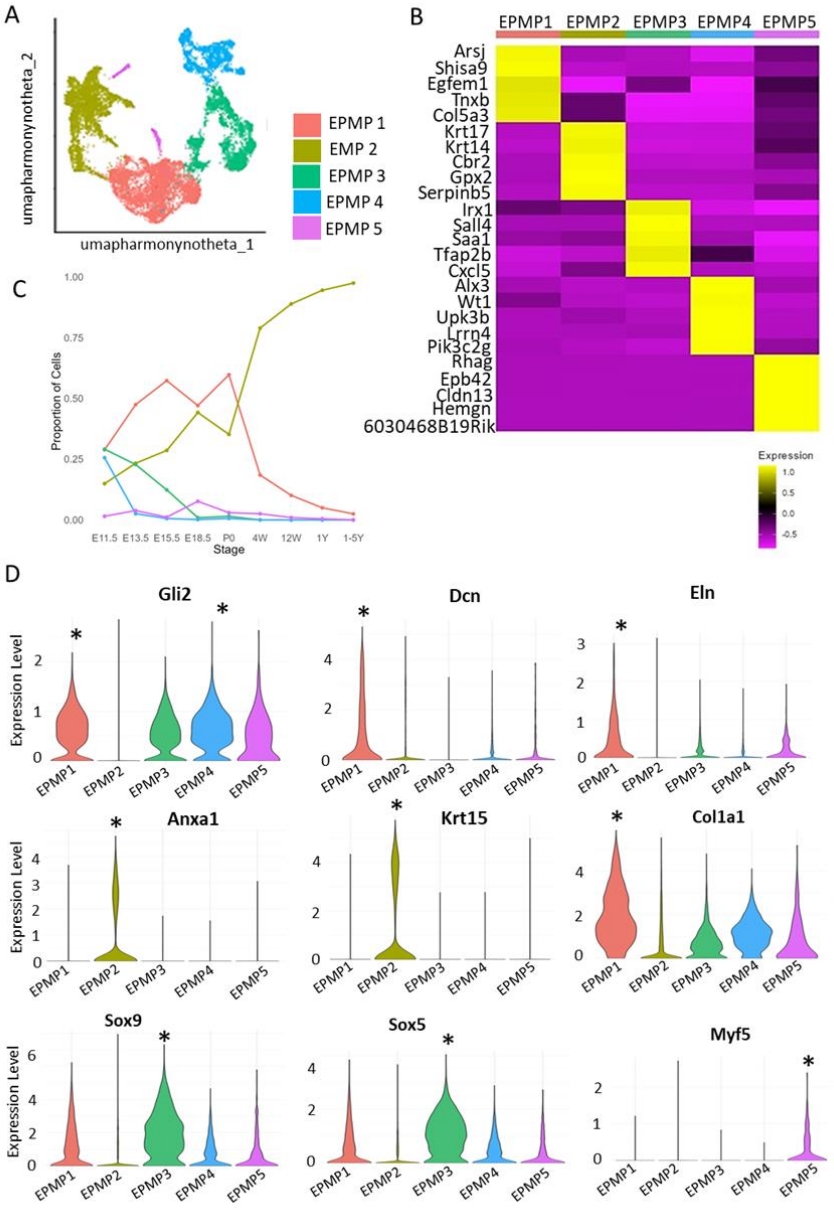

Figure 23: Sub-clustering analysis for early proliferating mesenchymal progenitor population. *(A) UMAP visualization of subtypes identified in early proliferating mesenchymal progenitors. (D) Heatmap displaying the top 5 differentially expressed genes for each subtype. (C) Cell proportion across subtypes and developmental stages. (D) Violin plots displaying differentially expressed genes for selected subtypes. Asterixis signifies a significant Wilcoxon rank sum test with a threshold of avg log fc 0.25, adjusted p-value < 0.05, and min.pct = 0.1.*

regulating the integration of neural crest cells (NCC) into the mesenchyme. **EPMP1** exhibited the most mature signs of differentiation based on the expression of *Dcn, Eln,* and *Col1a1*, suggesting a potential development pathway towards fibroblasts. **EPMP2** expressed genes typically associated with epithelial cells, including *Krt15*, *Krt14*, and *Anxa1*. *Anxa1* has been linked to epithelial-mesenchymal transition, a process that allows cells to adopt a more migratory phenotype. **EPMP3** gene expression profile

indicated involvement in cartilage development, as evidenced by its significantly high expression of *Sox9* and *Sox5* ($p<0.05$) (Smits et al., 2001). This subtype also expressed *Tfap2b* gene that has been associated with cranial NCCs, making EPMP3 a potential progenitor for thyroid cartilage due to its NCC origin (Nguyen et al., 2024). **EPMP4** also had an NCC origin, expressing *Alx3* among its top 5 DEGs, which is enriched in the frontobasal population of NCCs (Nguyen et al., 2024). Lastly, **EPMP5** expression profile suggested it could serve as a mesenchymal progenitor for muscle stem cells, as it expressed genes associated with muscle development, such as *Myf5* and *Myod1*, a fundamental regulator of skeletal muscle lineage determination in embryos (Yamamoto et al., 2018). EPMP5 also exhibited *Isl1* gene which supports its origin from cranial mesoderm.

Fibroblast Subtypes

We identified six subtypes of fibroblasts across the lifespan (Fig. 24A). The top 5 DEGs defining each subtype are shown in Fig. 24B. All these subtypes emerged during embryonic development and persists after birth (Fig. 24C). **FB1** expressed *Coch* among its top 5 DEGs. The *Coch* gene is associated with mechano-sensation and is found in the inner ear and eye to sense intraocular pressure. This finding supports the hypothesis that fibroblasts can sense VF vibration (Carreon et al., 2017; Foote et al., 2019; Foote & Thibeault, 2021). **FB2** expressed various types of collagens, *Vim* (Vimentin) and *Dcn* similar to Col14a1+ matrix lung fibroblasts. FB2 also expressed significantly *Col14a1*, *Pi16*, *Cygb* ($p<0.05$). **FB3** expression profile indicated

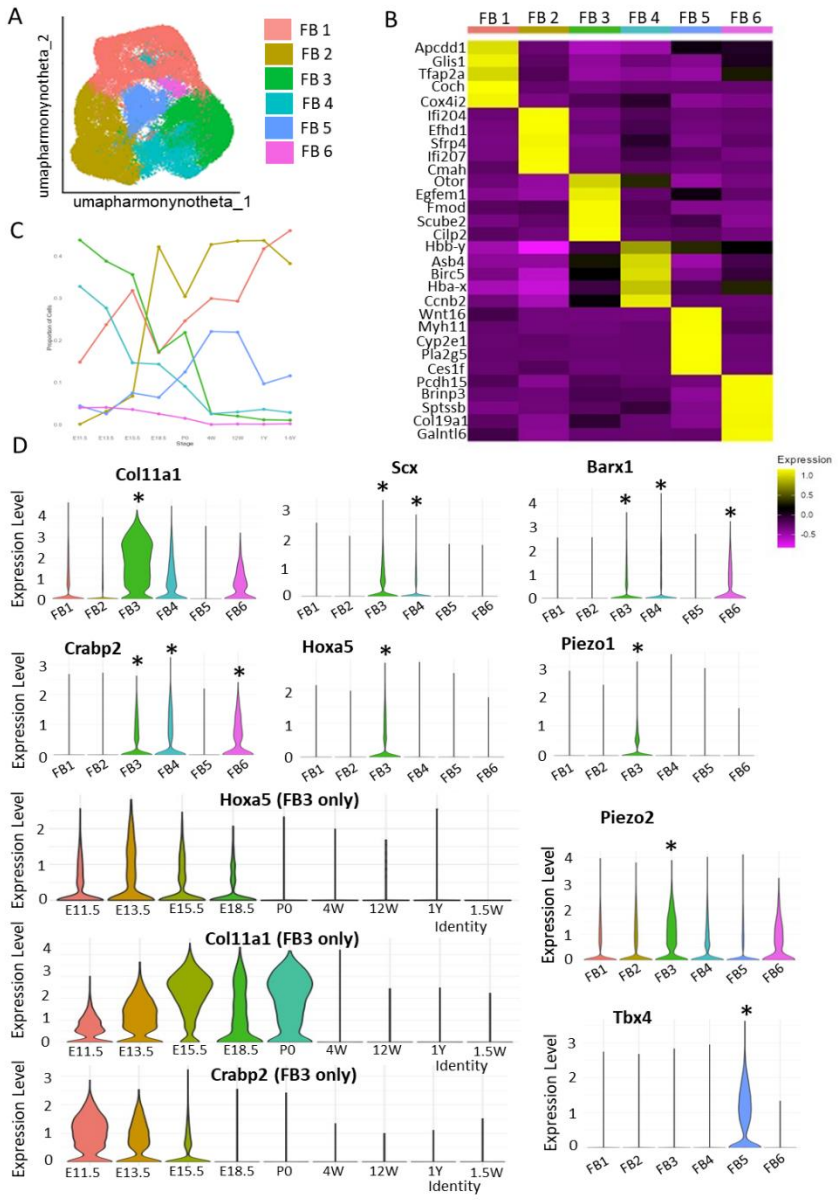

Figure 24: Sub-clustering analysis for population of fibroblasts. *(A) UMAP visualization of subtypes identified in fibroblasts. (D) Heatmap displaying the top 5 differentially expressed genes for each subtype. (C) Cell proportion across subtypes and developmental stages. (D) Violin plots displaying differentially expressed genes for selected subtypes and across the life span. Asterixis signifies a significant Wilcoxon rank sum test with a threshold of avg_log fc 0.25, adjusted p-value < 0.05, and min.pct = 0.1.*

involvement in musculoskeletal development, specifically cartilage, as evidenced by the expression of *Col11a1*, *Scx*, and *Hoxa5*. FB3 may be associated with the perichondrium, a fibrous tissue surrounding cartilage that promotes development, healing, and regeneration (Gvaramia et al., 2022) Additionally, FB3 expresses mechanoreceptors *Piezo1* and *Piezo 2* (Fig. 24D) suggesting that these FB are mechanically active or they sense mechanical changes. We also performed temporal analysis of expression of *Hoxa5*, *Crabp2* and

Col11a1 specifically for FB3 subtype showing that all these genes are preferentially expressed in the embryonic stages correlating with cartilage development (Lungova et al., 2018a). **FB4** was implicated in cartilage development, expressing *Barx1* and *Crabp2* among its top genes, although it appeared less differentiated than FB3. *Barx1* is associated with condensed mesenchyme in pharyngeal arches, supporting cartilage development (Sperber & Dawid, 2008), while *Crabp2* suggests a response to retinoic acid. **FB5** represents a population of myofibroblasts, expressing *Tbx4* and mainly *Myh11* among its top 5 DEGs, indicating contractile properties (Xie et al., 2018). Lastly, **FB6** expressed *Col19a1* and *Brinp3* among its top 5 DEGs. *Col19a1* regulates cardiac muscle ECM structure and ventricular function (Sadri et al., 2022), while *Brinp3* suggests retinoic acid influence.

Macrophages Subtypes

We discovered 6 subtypes of macrophages (Fig. 25A). The top 5 DEGs defining each subtype are shown in Fig. 25B. All MG subtypes originate during embryonic development and continue to exist into adulthood. MG1 increases proportionally with aging (Fig. 25C). Upon further investigation into MG function, two macrophage subtypes, **MG1** and **MG4**, were found to be associated with a pro-inflammatory phenotype. MG1 expressed *Ube2l6* among its top 5 DEGs which promotes pro-inflammatory macrophage polarization through activation of STAT1 pathway (Gao et al., 2021) (Fig. 25B). Among the top 5 DEGs in MG4 were genes associated with proliferation such as *H2ac4* and *H3c2* (histone-related genes) (Fig. 25B) (Karetsou et al., 1998). MG1 and MG4 both expressed *Aif1* which is calcium-binding protein that participates in

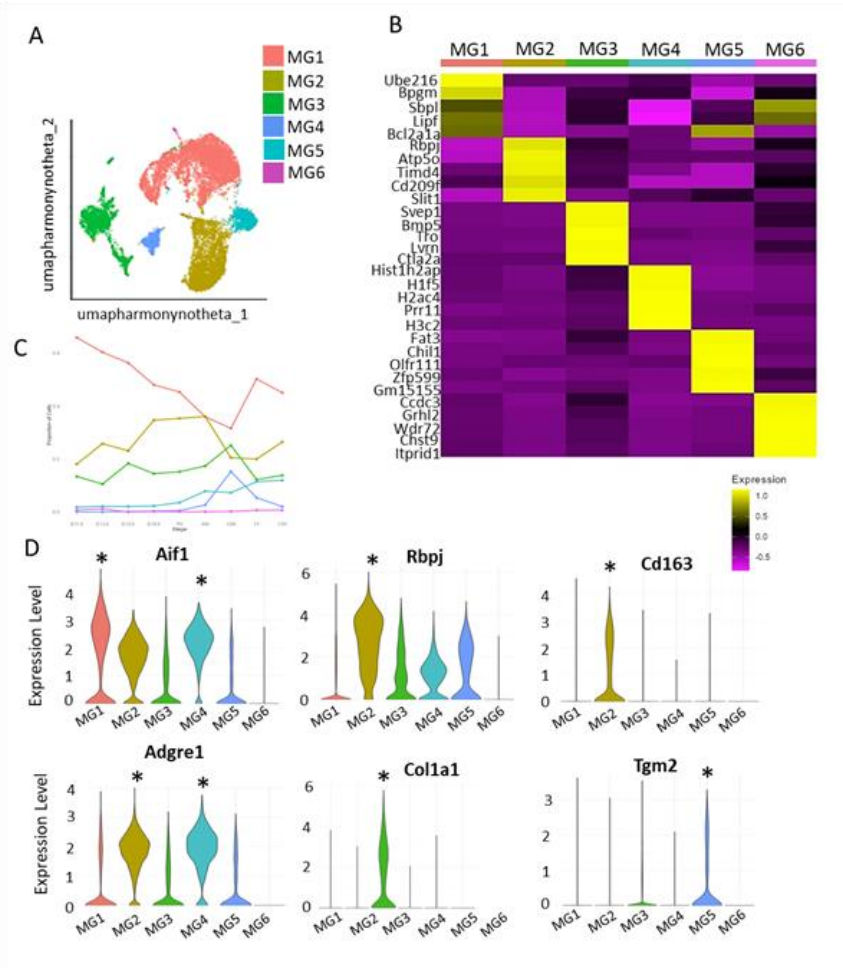

Figure 25: Sub-clustering analysis for population of macrophages. *(A) UMAP visualization of subtypes identified in macrophages. (B) Heatmap displaying the top 5 differentially expressed genes for each subtype. (C) Cell proportion across subtypes and developmental stages. (D) Violin plots displaying differentially expressed genes for selected subtypes. Asterixis signifies a significant Wilcoxon rank sum test with a threshold of avg_log fc 0.25, adjusted p-value < 0.05, and min.pct = 0.1.*

phagocytosis (Fig. 25D) (De Leon-Oliva et al., 2023). This gene has been linked with activation of a pro-inflammatory phenotype. Relating to their origin, MG1 and MG4 expressed *Adgre1* (F4/80) which points towards yolk-sac origin which are independent of bone marrow and *Myb* signalling pathway (Schulz et al., 2012). We also discovered three macrophages; **MG2, MG3** and **MG5** that expressed genes which promote anti-inflammatory phenotype. MG2 expressed *Rbpj* among its top 5 DEGs (Fig. 25B). *Rbpj* integrates signals from multiple pathways including Notch pathway, and is critically involved in polarization of macrophages into anti-inflammatory phenotype (Foldi et al., 2016). MG2, 3 and 5 also expressed other markers associated with anti-inflammatory phenotype such as *Cd163* and *Tgm2* (Fig. 25D)(Martinez et al., 2013). MG3 had

enriched GO processes for ECM establishment and expressed *Col1a1* supporting its anti-inflammatory function. **MG6** expressed *Grhl2* among its top5 DEGs (Fig. 25D) which is essential for epithelial development and mesenchyme-epithelial translocation.

CHAPTER FOUR: DISCUSSION

Using time-series single-cell transcriptomics, we have developed a detailed cellular atlas that includes epithelial, mesenchymal, immune, endothelial, and neuronal cells across the stages of laryngeal and VF development, and postnatal maturation. These findings are in line with recent scRNA -seq publication in our field that identified similar cell types in adult anterior VFs with major cell populations sharing similar markers. Our study however explores the cell populations in deeper level such as collecting embryonic, newborn and aged VF tissue. In addition, our study uncovered new temporal interactions among these cell types and quantified their proportions as well as proportion of major subpopulations throughout the lifespan. Employing advanced analytical techniques, we explored the developmental trajectories among these cell types and identified top upregulated and downregulated DEGs that change during the process of differentiation as a function of pseudotime and process of aging across our timepoints, thus identified new elements in the laryngeal development. Notably, we discovered previously unrecognized populations of basement membrane-producing cells and neuroendocrine cells, enriching the complexity of laryngeal cellular framework.

Our findings substantiated our hypotheses that early embryonic stages are marked by epithelial and mesenchymal progenitors, particularly evident at E11.5. Trajectory analysis demonstrated that these progenitors differentiate into mature and specialized cell populations over time. As age advances, major cell populations achieve functional and structural maturity, peaking at 12W. During aging, the epithelium experiences a shift where NPBEC become the predominant cell type, at the expense of more specialized SBEC and CC. Additionally, we confirmed immune cell infiltration in the VF tissue during aging, specifically neutrophils,

accompanied by proinflammatory changes in resident MG, potentially contributing to VF tissue degeneration.

Unique Cell Populations Identified in the Dataset

Basement membrane-producing cells were defined by high expression of embryonic genes such *Clnd6, Shh* and *Foxa2* indicating that these cells are epithelial cells originally derived from the anterior foregut endoderm. Remarkably, upon re-clustering, this cell population clearly split into two sub populations, one demonstrating active embryonic traits and distinct epithelial characteristics, while the other emerged postnatally. This latter subtype was marked by the expression of typical mesenchymal genes associated with basement membrane production. This transition between populations suggests a potential relationship, where the embryonic population may give rise to the postnatal one. Moreover, the embryonic cell population is enriched in expression of *Frem2* which is associated production of embryonic basement membrane and epithelo-mesenchymal transformation. These findings are consistent with previous research, which demonstrated in genetically labeled *Shh-Cre-TdTom* mice that some TdTom red-labeled cells persisted within the epithelium, contributing to the development of laryngeal and VF epithelium, while others delaminated from the epithelium, migrated into the adjacent mesenchyme, and integrated into the lamina propria and other mesenchymal structures (Lungova et al., 2018b).

In our dataset, we identified a novel cell population: neuroendocrine cell (NEC), characterized by the expression of genes such as *Calca* and *Scg2*. Neuroendocrine cells are predominantly found in the respiratory system and are referred to as pulmonary neuroendocrine cells. They are dispersed throughout the airway epithelium and tend to cluster at bronchial

branchpoints, acting as vigilant monitors of airway condition. Pulmonary neuroendocrine cells exhibit a diverse repertoire of peptidergic genes, with each cell expressing a unique combination of up to 18 peptidergic genes, along with various receptors for mechanical, thermal, acidic, and chemical stimuli. These signals can target numerous cell types in the lung, including sensory neurons, and potentially influence distant body tissues via circulation. Within the NEC population identified in our data set, the expression of *Piezo1*, involved in mechano-sensation, was observed. Given the VF are highly biomechanically active, the expression of Piezo 1 in these cells suggests their potential role in detecting and responding to mechanical stimuli within the dynamic environment of the VF (Foote et al., 2019).

Furthermore, due to their complex role in maintaining airway balance, tone, and diameter, as well as their responsiveness to various stimuli, pulmonary NEC are often linked to pathological conditions such as asthma, sudden infant death syndrome (SIDS), and bronchopulmonary dysplasia. In the context of the larynx, inducible laryngeal obstruction (ILO), which is frequently misdiagnosed as asthma, may also involve these cells. We found NEC present specifically between 4W to 1Y correlating to human young adolescent to middle-aged adult which coincides with the highest prevalence of ILO occurs(Fujiki et al., 2024; Lunga et al., 2022). Exploring the role of NEC in laryngeal conditions like ILO could provide valuable insights into their broader physiological and pathological significance.

Heterogeneity and Developmental Dynamics of Major Populations

This study provides the first comprehensive insight into delineating the entire cellular composition of larynx and VF and their dynamic changes during cell differentiation and over time. Despite being a relatively small organ, laryngeal and VF cell populations are remarkably diverse. While these cell populations have been studied independently in the larynx previously,

none of the previous research has focused on their progression, over the lifespan. Our findings reveal that the early stages of VF development are dominated by mesenchymal populations. Among these, mesenchymal progenitors emerge as the most prevalent cell type, exhibiting high proliferative potential and plasticity. This proliferative capacity not only plays a crucial role in generating sufficient cells for the establishment of mesenchymal structures but also contributes to the juxtaposition of the lateral wall and the formation of the epithelial lamina at E11.5 (Lungova et al., 2015). The population of EPMP peaks at E11. 5 and declines thereafter with correlates with the decline in cell proliferation (Griffin et al., 2021a). This decline coincides with the emergence of more specialized cell populations, notably STC and particularly FB.

In mice, fibroblasts (FBs) mature between E18.5 and 4W of age, characterized by robust ECM production, including the deposition of elastin and collagen. However, as FBs age, their capacity to produce collagen and elastin decreases. Instead, they produce decorin and likely undergo transdifferentiation into myofibroblasts, as evidenced by increased expression of *Myl6* in aged FBs. This shift in FB behavior and ECM production may account for the impaired ability to repair ECM damage following VF injuries or trauma in older patients(De Araújo et al., 2019).

Our results suggest the presence of diverse fibroblast subtypes, each fulfilling specific roles within the intricate architecture of the larynx and VFs. Notably, we have delineated a cohort of fibroblasts involved in maintenance of the ECM surrounding muscular fibers. This specialized subset is implicated in the formation and sustenance of muscle perimysium, endomysium, and tendon structures (Chapman et al., 2016). Moreover, our investigation has identified two distinct FB subpopulations involved in cartilage maintenance, presumably localized within the perichondral niche. The perichondrium, characterized by a dense fibroblast presence, serves as a pivotal hub for supporting cartilage homeostasis, growth, and regenerative

processes (Duynstee et al., 2002) however, their specific function within larynx and VF needs further investigation. FB1 and FB2 may be responsible for producing and maintaining the ECM within the LP due to increased expression of collagen, elastin, and fibronectin. These ECM proteins provide structural support and elasticity to the VF, allowing them to withstand mechanical stresses during voicing and swallowing. Our data sets revealed unique subset of FB, specifically FB1 and FB3 involved in mechanosensation, as they express *Coch* and contain mechanoreceptors such as *Piezo1* and *Piezo2*. *Cochlin* is known to be involved in mechanosensation in the inner ear, where it plays a role in detecting mechanical vibrations and facilitating hearing(Goel et al., 2012). Given that VF FBs also experience mechanical stress and strain during vocalization, it is plausible that *Cochlin* expression in these cells could contribute to their mechanosensitive properties. It is also possible that cochlin-expressing VF FBs share mechanosensitive mechanisms similar to the inner ear, allowing the FBs to respond to mechanical stimuli, in a similar manner. This could involve shared signaling pathways or mechanotransduction mechanisms that enable both the VF FBs and the inner ear cells to detect and respond to mechanical forces. Further investigations into the role of *cochlin* in mechanosensation in VF FBs will be beneficial for the field by providing a deeper understanding of the molecular mechanisms underlying VF physiology and pathology in relation to mechanical forces. *Piezo 1* and *2* are members of the Piezo family of mechanosensitive ion channels, which play a crucial role in sensing mechanical stimuli such as touch, stretch, and shear stress. These channels are large, transmembrane proteins that can open in response to mechanical forces, allowing ions to flow across the cell membrane and generate electrical signals. Both genes have been mainly studies in relation with epithelial cells (Foote et al., 2022). The fact that Piezo1 and 2 are also detected in the VF FB is a novel finding that is worth further exploration.

The epithelial population represents the second largest identified group in our datasets, and its prominence increases postnatally. This postnatal expansion is likely attributed to the maturation of the epithelium starting 4W of age. Given the heterogeneity observed within this sizeable cell population, we categorized it into major cell types using multiple criteria to capture its complexity comprehensively. First, we differentiated the cells based on their location, specifically distinguishing between basal and suprabasal cells. Subsequently, we further categorized the cells according to their proliferation versus differentiation status to identify less differentiated and more specialized cell types. The developmental relationships between the main cell types were further validated through a developmental trajectory analysis. The PBEC population was identified as the most undifferentiated cell type within the epithelium. This cell type gives rise to transitional NPBEC, which further differentiate into specialized SBEC, SEC and CC. The PBEC population reaches its peak at E11.5, some cells retain their proliferative capacity into adulthood, contributing to postnatal VF epithelial maintenance. PBEC has high plasticity and mobility expressing *Hmgb1* similar to BMPC and also express *Lrig1* and *2* suggesting its role in VF epithelial maintenance. During the lifespan, in PBEC genes involved in intense proliferation become downregulated while genes that encode mature epithelial markers become upregulated which may contribute to reduced regeneration and repair capacity of the VF epithelium after injury or phonotrauma (Watson et al. 2020). In our data set we identified 4 subtypes. Notably, PBEC1 was enriched in *Krt6a*, *Krt14*, and *Lgals7* suggesting of more mature nonproliferating basal cell phenotype. Interestingly, embryonic subtype PBEC3 was enriched for collagen production potentially contributing to the establishment of VF LP. NPBEC represent a transitional cell population that gradually exits the cell cycle. This cell population matures at 4W of age, when it exhibits a distinct expression pattern consistent with mature basal epithelial cells.

Importantly, this population possesses the capability to differentiate into specialized cell types, including SBEC, SEC, or CC.

SBEC population posses physical barrier, immunoregulatory and antimicrobial functions which is supported by our data where SBEC subtypes have distinct functions. Across lifespan genes associated with physical barrier function such as keratins, immunoregulatory and antimicrobial functions are established at 4W of age, peaking later in life at 12W-1Y of age. . Hence the immature VF epithelium after birth can contribute to susceptibility to either phonotrauma or infection. The former may result in VF nodules in young children and adolescents which are considered the most common etiology for voice disorders in this age group (Karalı et al., 2022; Lee et al., 2022). Also, the low antimicrobial and immunoregulatory function could be associated with children being prone to HPV infection and respiratory papillomatosis. This infection leads to recurring VF papillomas which can cause severe laryngeal obstruction and dyspnea (Kurita et al., 2019).

The functional immaturity of the VF epithelium correlates with cell composition immaturity. The epithelium in embryonic stages is more primitive compared to postnatal stages, as not all cell populations within the epithelium have fully differentiated yet. As the embryonic development progresses, secretory and ciliated cells become increasingly evident in the VF epithelium. By 12 weeks, SBEC constitute the largest proportion of all epithelial cell populations, followed by SEC. SEC express a variety of antimicrobial genes and serve as a primary defense against pathogens. However, in later postnatal stages, the VF epithelium begins to simplify once more. The proportion of SEC, CC, and SBEC decreases, while NPBEC become the most abundant cell type. The pattern of cellular composition highlights two vulnerable periods in VF development. The first vulnerable period occurs between newborn and 4W of age,

characterized by functional immaturity. The second vulnerable period occurs between 1Y and 1.5Y of age, during which there is a loss of the suprabasal protective layer and the secretory cells that produce antimicrobial genes. This loss may render the epithelium susceptible to invasion by pathogens and phonotrauma, potentially compromising VF health and function.

We identified four immune cell populations within the larynx and VFs such as dendritic cells, macrophages, lymphocytes and neutrophils. All immune cell populations were found already in embryonic stages. In our work we mostly focused on macrophages because they are important players in the innate immune system. They serve as frontline defenders against invading pathogens. They are also key players in tissue homeostasis, regeneration, and repair. In our data set we identified 6 subtypes. The anti-inflammatory M2 phenotypes were observed predominantly in embryonic stages thus they likely contribute to the establishment of ECM and stimulate mesenchymal populations to produce collagen and other constituents of ECM. On the other hand, pro-inflammatory phenotypes were prominent in postnatal stages suggesting that aging in VF may be associated with pro-inflammatory environment that stimulates macrophages into M1 phenotype. Similar phenomenon of predominance of M1 macrophages has been observed in aged skin however further research is warranted what causes pro-inflammatory environment in VF with aging(Gather et al., 2022). In addition, we observed increased proportions of neutrophiles in 1.5y timepoint that promote the pro-inflammatory environment and can accelerate VF aging and their degeneration.

Signaling Pathways

Our findings confirmed the significant roles of the *Shh/Gli*, *Wnt*, *Hox* genes and retinoic acid *(RA)* signaling pathways in the early stages of laryngeal embryogenesis, likely governing

the proliferation and differentiation of epithelial and mesenchymal cells. Specifically, *Shh* signaling is prominently active in the developing larynx at E11.5 but decreases thereafter, aligning with reduced cell proliferation in the epithelium and lamina propria (Griffin et al., 2021b) In our datasets, the Shh-expressing cell populations BMPC, PBEC, and NEC were identified. These epithelial cell populations originate from the anterior foregut and co-express *Foxa2*.

Mesenchymal structures originate from the cranial mesoderm (myogenic progenitors), somitic mesoderm and migrating neural crest cell (NCCs) populations, that give rise to intrinsic laryngeal muscles, cartilages and the lamina propria (Frisdal & Trainor, 2014; Tabler et al., 2017) Multiple signaling pathways regulate migration and integration of NCC and myoblasts into the larynx, such as Shh pathway via Gli proteins. Our findings demonstrated elevated expression of Gli2 and Gli3 particularly in the EPMP cell populations. Further sub- clustering of EPMP revealed that this group comprise both NCC descendants, namely EPMP3 and EPMP4, as validated by Tfap2b and Alx3, respectively, and EPMP5 migratory myogenic progenitors from cranial mesoderm as confirmed by Islt1, Myod, Myh5 expression, Gli genes, especially Gli2 and Gli3, were also identified in residing more mature EPMP1 subpopulation that also expressed Eln, Col1a1. These cells likely facilitate the incorporation of migratory cells into the larynx. Our findings correlate with results published in the literature that have shown the importance of Gli genes for proper development of laryngeal mesenchymal structures. Gli3 deletion in Gli3−/− mutant mice leads to abnormal NCC accumulation in the ventral glottic compartment, disrupting vocal ligament and muscle attachment, thus affecting vocalization, as reported by Tabler et al. 2017. These mice may also display a more severe Pallister-Hall syndrome-like phenotype with a

range of developmental anomalies, such as the absence of the epiglottis and laryngeal clefts, leading to improper larynx-esophagus connections (Böse et al., 2002).

Additional enriched pathways identified in our study that play a role in NCC and myoblast development and migration include retinoic acid (RA) signaling and Hox genes. RA plays a vital role in the segmentation and formation of the 3rd to 6th pharyngeal arches (Vermot et al., 2003) Vitamin A deficiencies result in malformations of laryngeal and tracheal cartilages and incomplete glottic separation in rat embryos (Tateya et al., 2007). Likewise, mutations in the *Raldh2* gene, which converts vitamin A into RA, result in similar pharyngeal arch and laryngeal cartilage defects (Niederreither et al., 2003; Vermot et al., 2003). Consistent with existing literature, our study revealed increased expression of RA-related genes, in cell populations associated with cartilage development. Specifically, elevated expression of *Crabp2* was observed in EPMP3 and EPMP4, while both *Crabp2* and *Brinp2* were upregulated in FB3 and FB4. Additionally, increased expression of *Rxra* and *Rxrb* was identified in the ChB.

In addition, RA is a well-known regulator of *Hox* gene activity via the presence of RA response elements in the promoter region of many Hox ((Marshall et al., 1996) Consistent with this, we observed significantly elevated levels of *Hoxa3* and *Hoxa5* in FB3 and ChB during the early stages of laryngeal embryogenesis, underscoring their involvement in laryngeal cartilage formation. These findings align with previous studies demonstrating that the deletion of *Hoxa3* in the caudal pharyngeal endoderm leads to multiple skeletal defects, including dysmorphogenesis of the cricoid and thyroid cartilage (Manley & Capecchi, 1997). Likewise, loss-of-function mutations in the *Hoxa5* gene in the mesenchyme surrounding the respiratory diverticulum result in a hyperplastic cricoid, disorganization of the tracheal rings, and hypoplasia of the pulmonary tree (Aubin et al., 1997).

Signaling molecule identified in our dataset that has been significantly upregulated in adulthood and aging was *Wnt4.* This ligand plays a crucial role in the development and differentiation of various cell types during both embryonic development and adult tissue homeostasis, as they stimulate myofibroblast differentiation (La et al., 2018; Q. Zhang et al., 2021b) Increased levels of *Wnt4* in the senile lungs, leads to enhanced myofibroblast-like differentiation. These findings align with our observations showing upregulation of *Wnt4* in the epithelium that correlates with elevated *Myl6* expression in adjacent FB in aged mice. *Myl6* supports myofibroblast differentiation.

Together, these findings suggest that upregulation of Wnt4 and Wnt5a may contribute to age-related alterations in VF tissue structure and function, potentially leading to age-related changes in biomechanical properties of the lamina propria, and age-associated diseases and conditions. Further investigation is required to fully understand the specific roles and mechanisms of *Wnt4* and *Wnt5a* in aging and adult during the early stages of laryngeal embryogenesis VF tissue homeostasis.

Limitations

In our scRNA-seq analysis, we employed two distinct sampling approaches: isolating single cells from whole larynges at embryonic stages ranging from E11.5 to P0 and using solely VF tissue from 4W to 1.5Y postnatal. This difference in sampling strategies may influence the representation of specific cell populations, such as chondroblasts and other mesenchymal populations, previously associated with cartilage development. Notably, the only cartilage tissue extracted during postnatal stages was from the arytenoid cartilages, although cartilage populations were not the primary focus of this study. In addition, sample differences can influence the proportion dynamics of other cell populations within mesenchyme for embryonic

and P0 stages. Additionally, the conclusions drawn from our bioinformatics methods, including trajectory analysis, necessitate further validation through experimental and functional investigations, such as in-situ hybridization or RNA in-situ hybridization (RNAish). A significant limitation of our study lies in the absence of spatial information regarding individual cell populations and subtypes within the VF tissue. To address this limitation in future research, the employment of either in-situ hybridization techniques or spatial transcriptomics will be crucial to visualize these cell populations and their subtypes within the VF tissue more comprehensively.

CHAPTER FIVE: CONCLUSION

Our time-series single-cell transcriptomics analysis has generated a comprehensive cellular atlas encompassing epithelial, mesenchymal, immune, endothelial, and neuronal cells across laryngeal and VF development stages and postnatal maturation. This study elucidated trajectory interactions among these cell types, quantified their proportions and major subpopulations throughout lifespan, and delineated their change in transcriptome across lifespan. Advanced analytical techniques enabled the identification of top upregulated and downregulated differentially expressed genes (DEGs) during differentiation and aging processes, unveiling new insights into laryngeal development. This material will serve as a benchmark for improving tissue engineering strategies, cross-species comparison with human tissue and translational research focused on age-, gene-, and population-specific treatment options.

APPENDICES

Supplemental Data

Supplemental data are available upon request. Please contact principal investigator Dr. Susan Thibeault.

Supplemental Figures

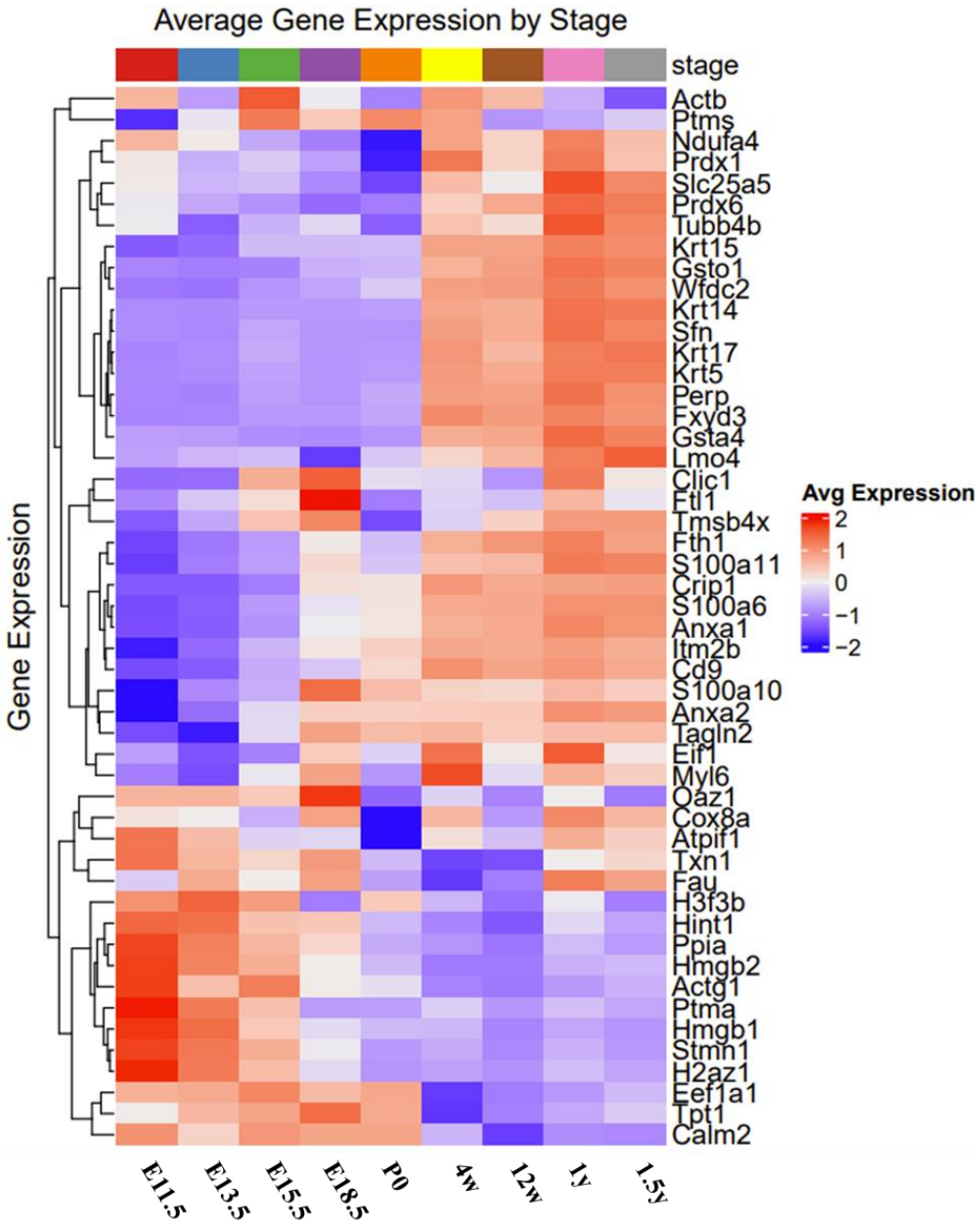

Supplemental Figure 1: *Heatmap displaying the top 50 differentially expressed genes in proliferating basal epithelial cells that are expressed at all timepoints from E11.5 to 1.5y. Red color signifies upregulated, dark blue signifies downregulated genes.*

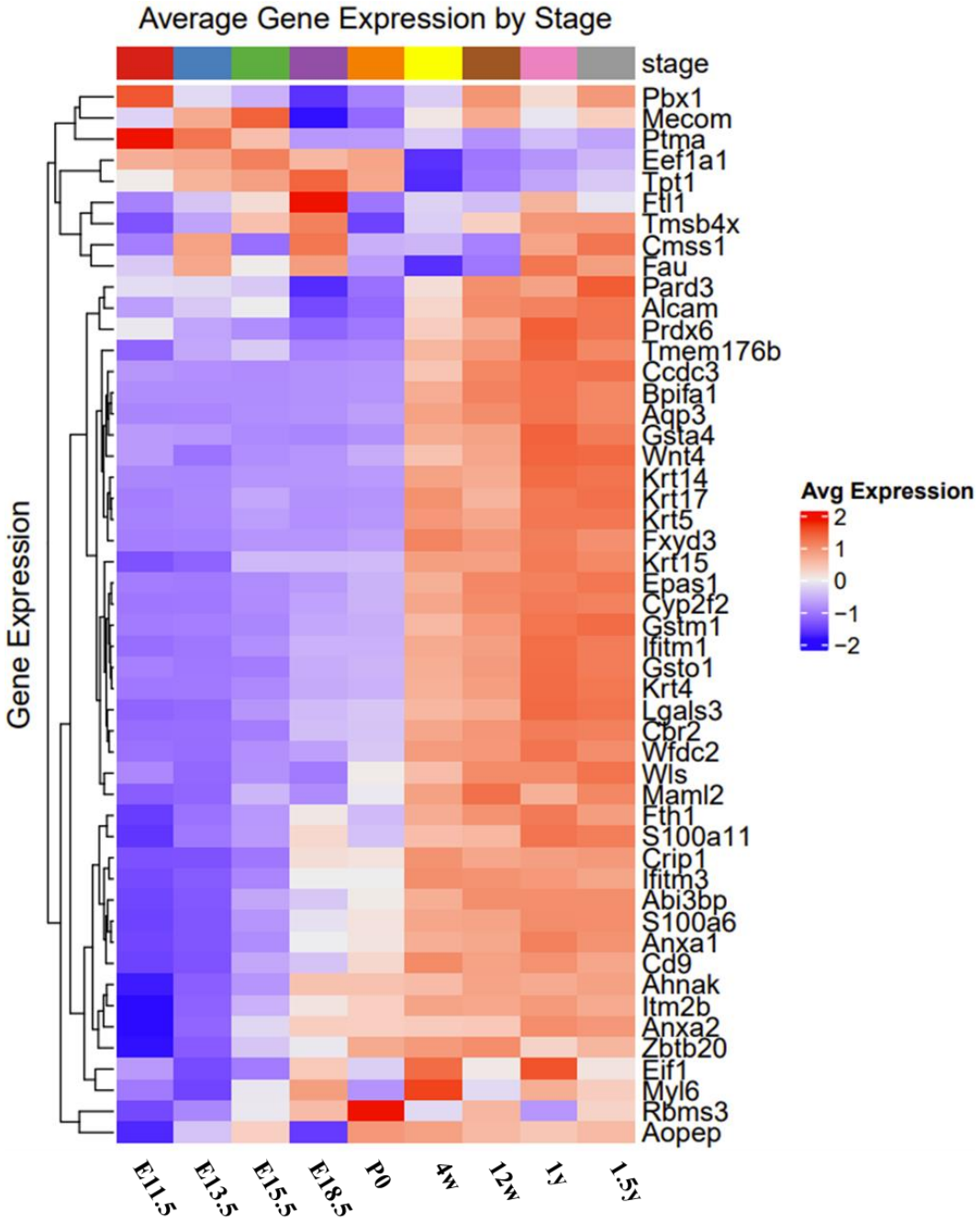

Supplemental Figure 2: *Heatmap displaying the top 50 differentially expressed genes in non-proliferating basal epithelial cells that are expressed at all timepoints from E11.5 to 1.5y. Red color signifies upregulated, dark blue signifies downregulated genes*.

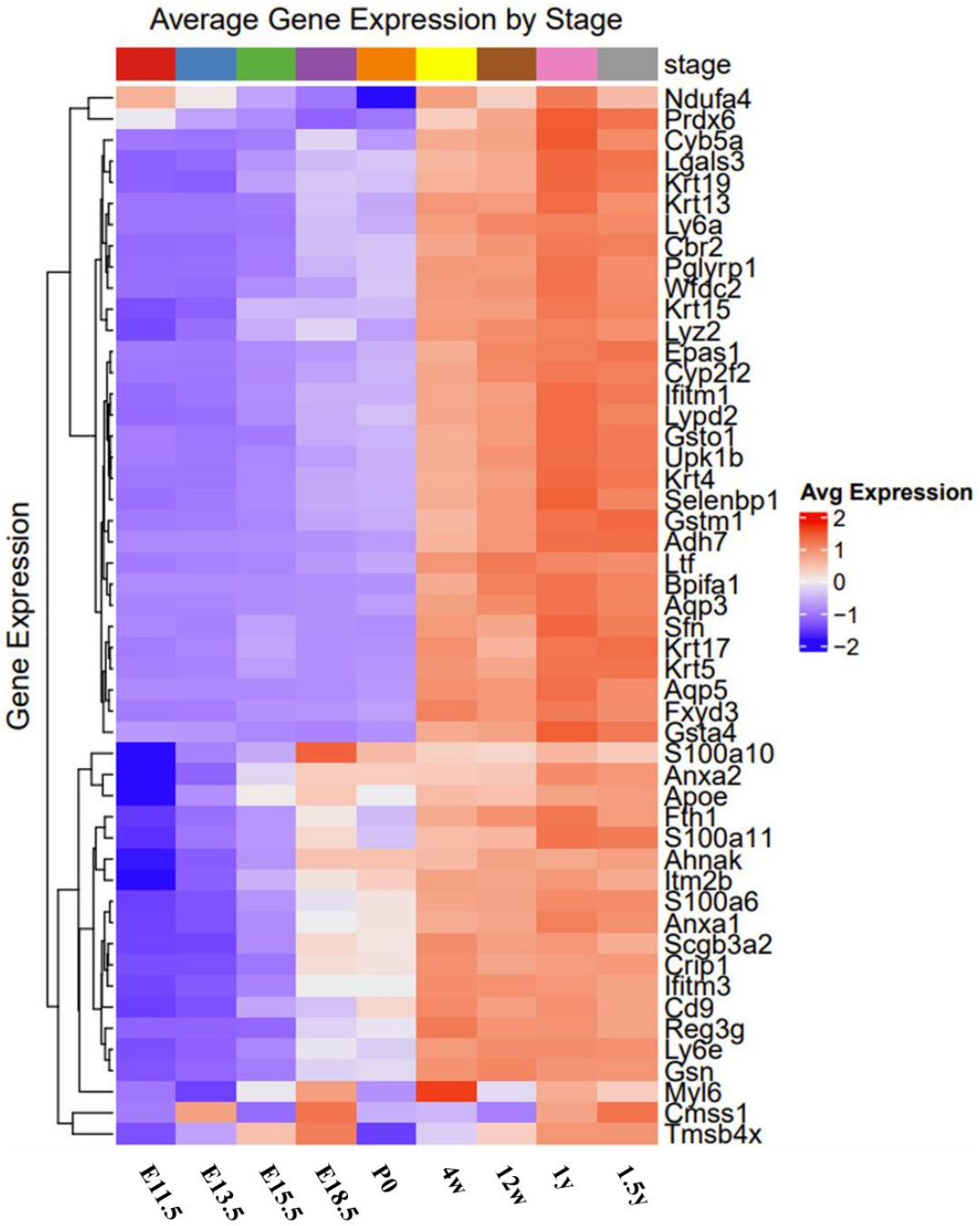

Supplemental Figure 3: *Heatmap displaying the top 50 differentially expressed genes in suprabasal cells that are expressed at all timepoints from E11.5 to 1.5y. Red color signifies upregulated, dark blue signifies downregulated genes.*

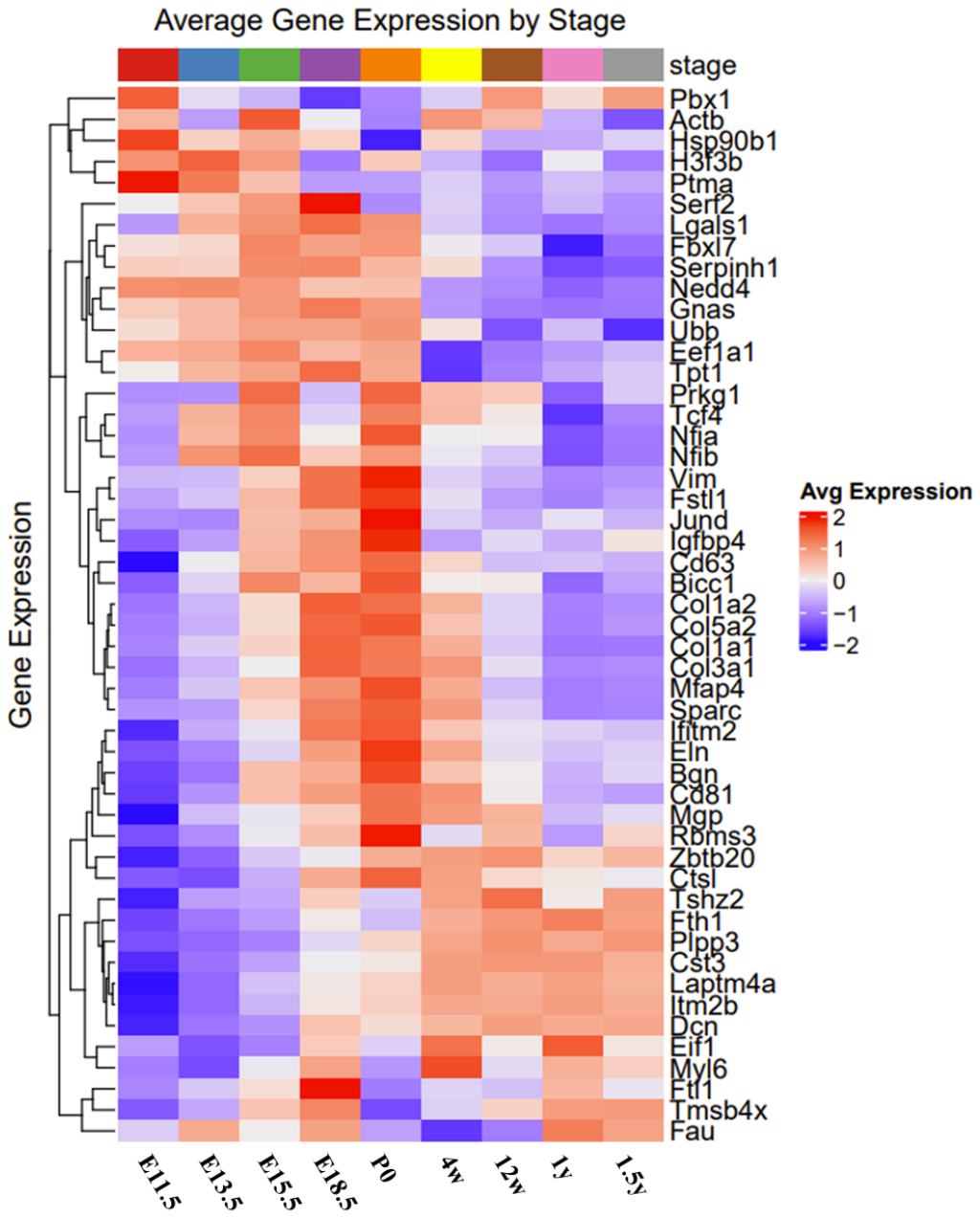

Supplemental Figure 4: *Heatmap displaying the top 50 differentially expressed genes in **fibroblasts** that are expressed at all timepoints from E11.5 to 1.5y. Red color signifies upregulated, dark blue signifies downregulated genes.*

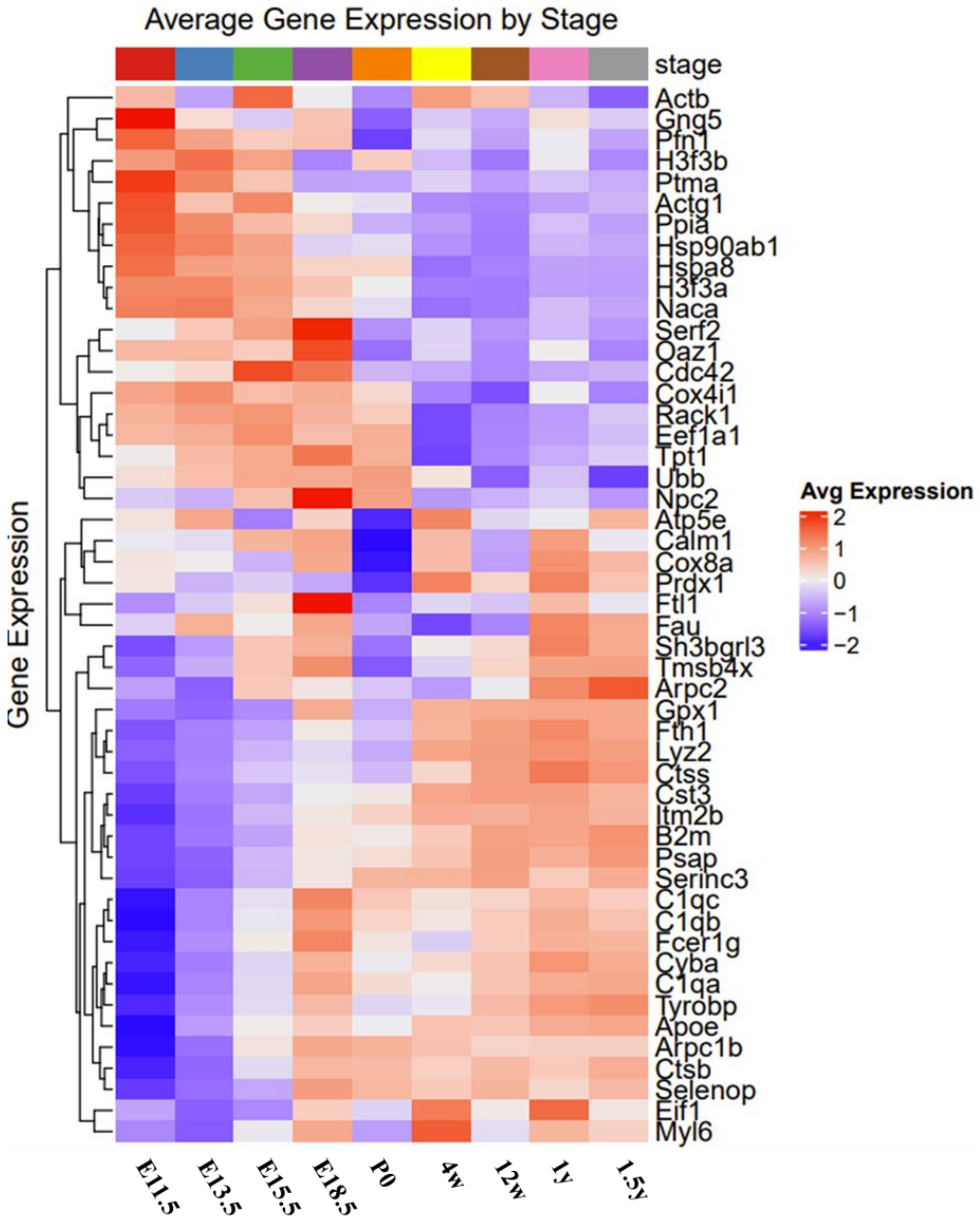

Supplemental Figure 5: *Heatmap displaying the top 50 differentially expressed genes in* ***macrophages*** *that are expressed at all timepoints from E11.5 to 1.5y. Red color signifies upregulated, dark blue signifies downregulated genes*.

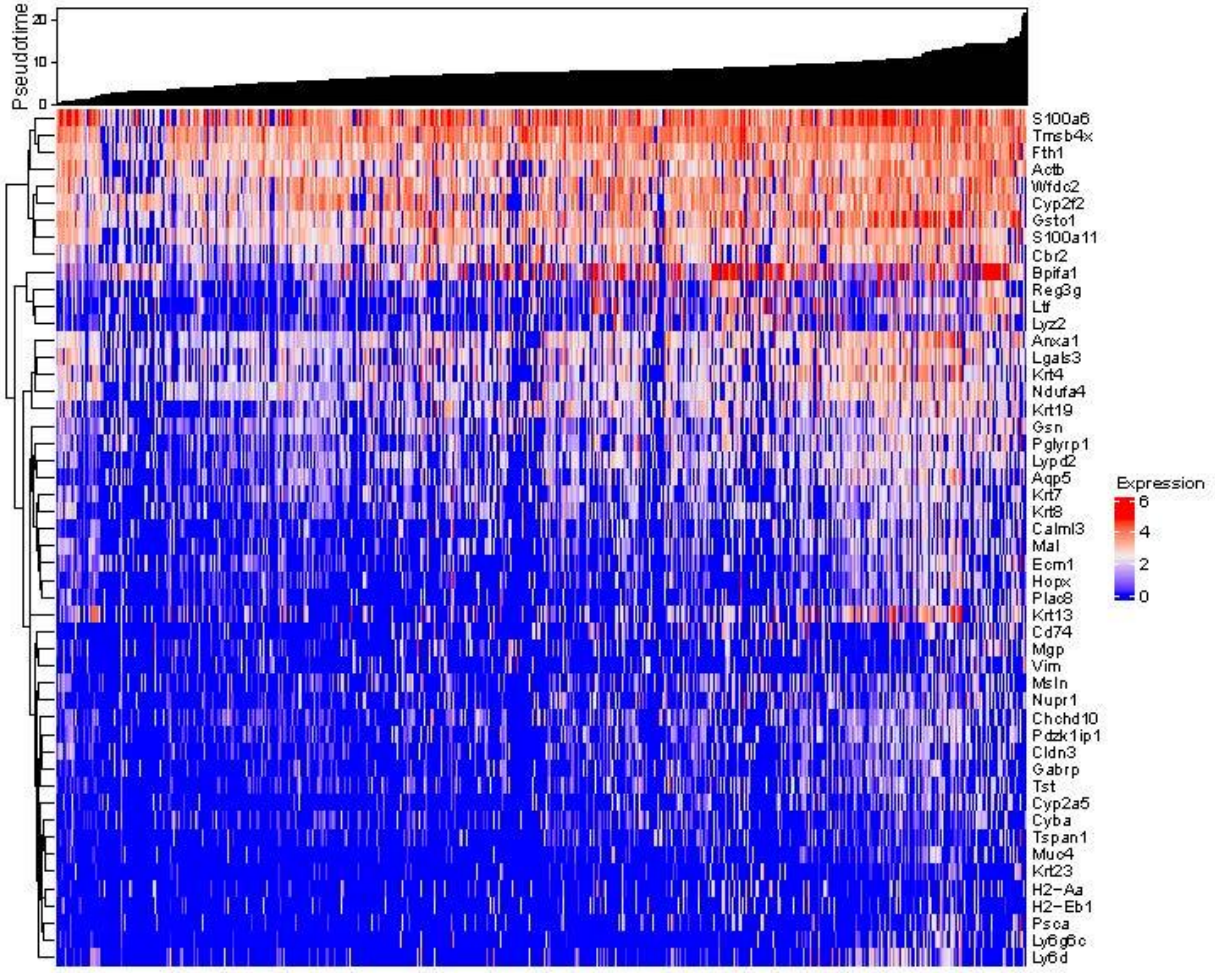

Supplemental Figure 6: *Heatmap displaying the top 50 differentially expressed genes that are* ***upregulated*** *in the VF stratified epithelium during the process of differentiation from proliferating basal epithelial cells, nonproliferating basal epithelial cell to suprabasal epithelial cell.*

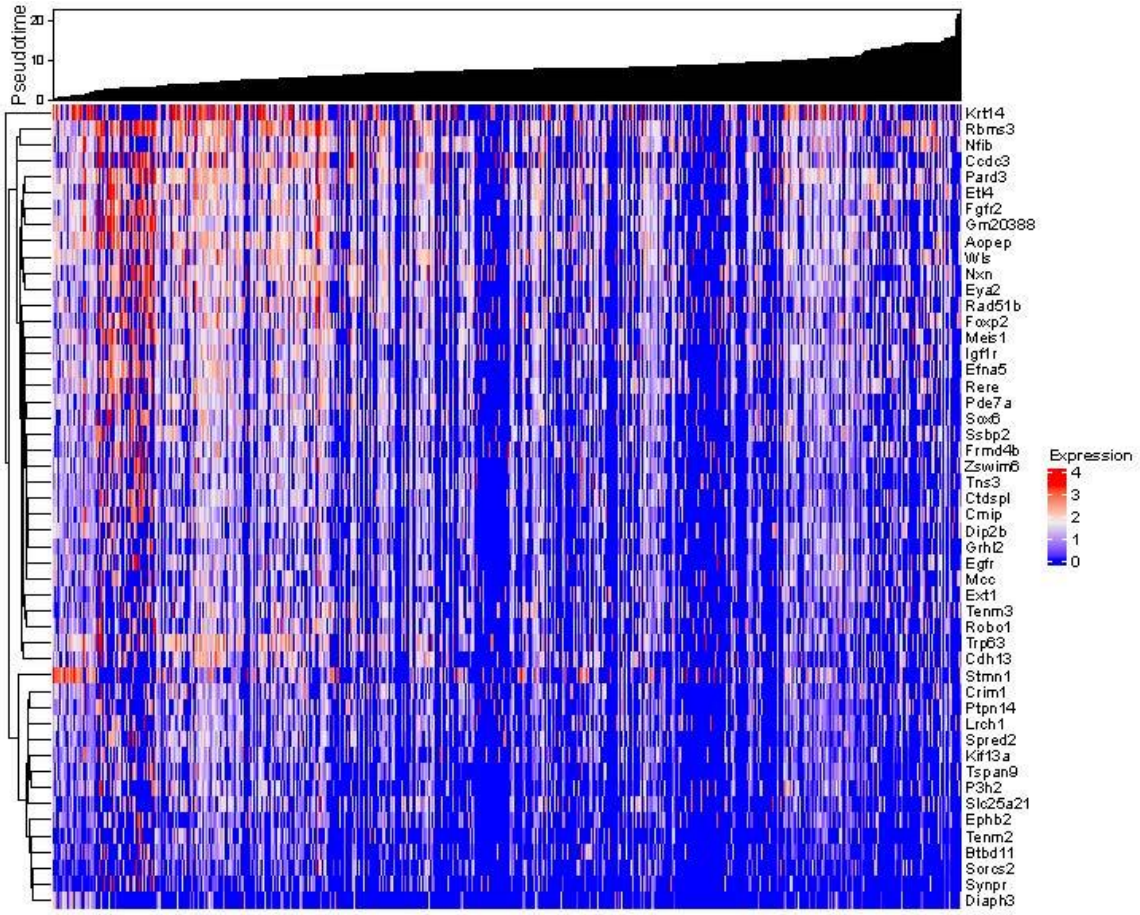

Supplemental Figure 7: *Heatmap displaying the top 50 differentially expressed genes that were* ***downregulated*** *in the epithelium during the process of differentiation of proliferating basal epithelial cells, nonproliferating basal epithelial cell to suprabasal epithelial cell.*

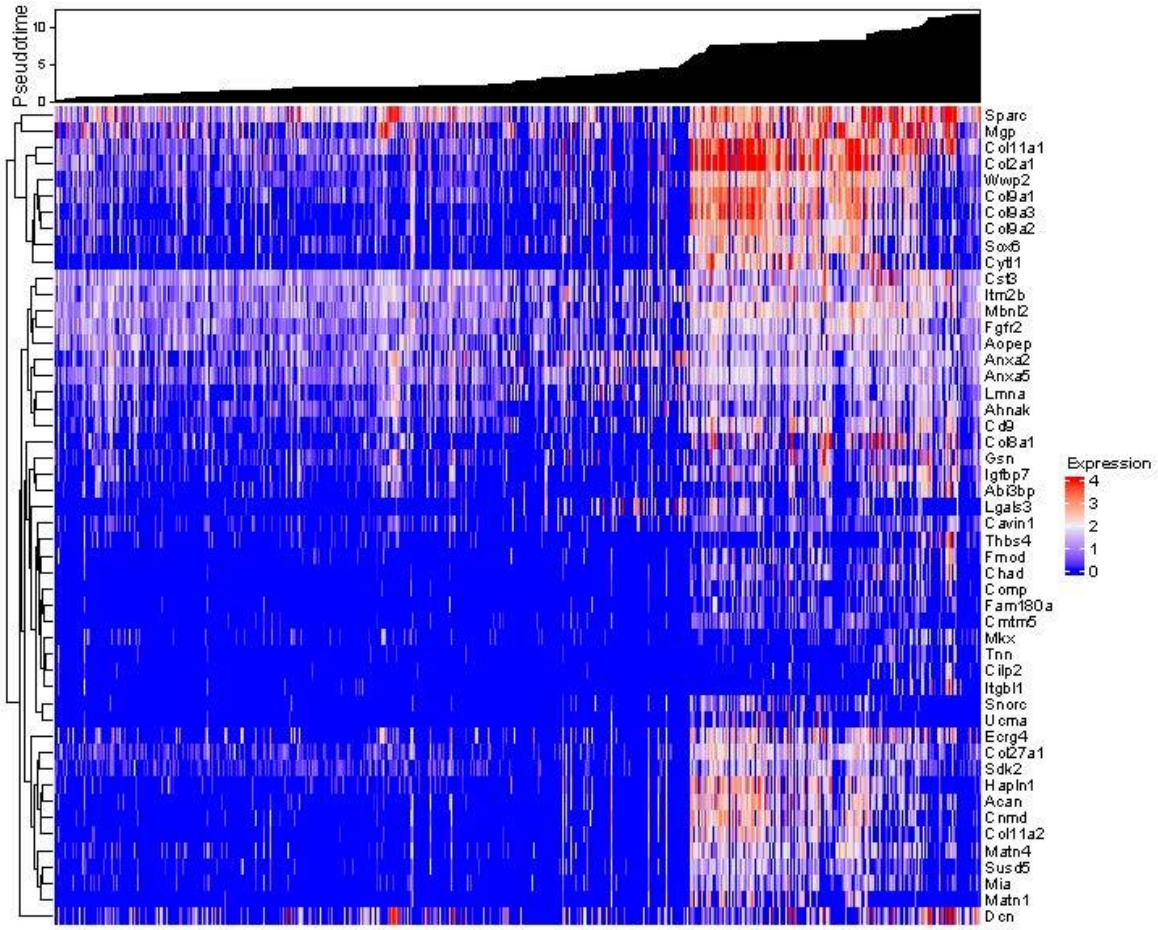

Supplemental Figure 8: *Heatmap displaying the top 50 differentially expressed genes that are* ***upregulated*** *in the mesenchyme during the process of differentiation of proliferating mesenchymal progenitors, stromal cells and fibroblasts.*

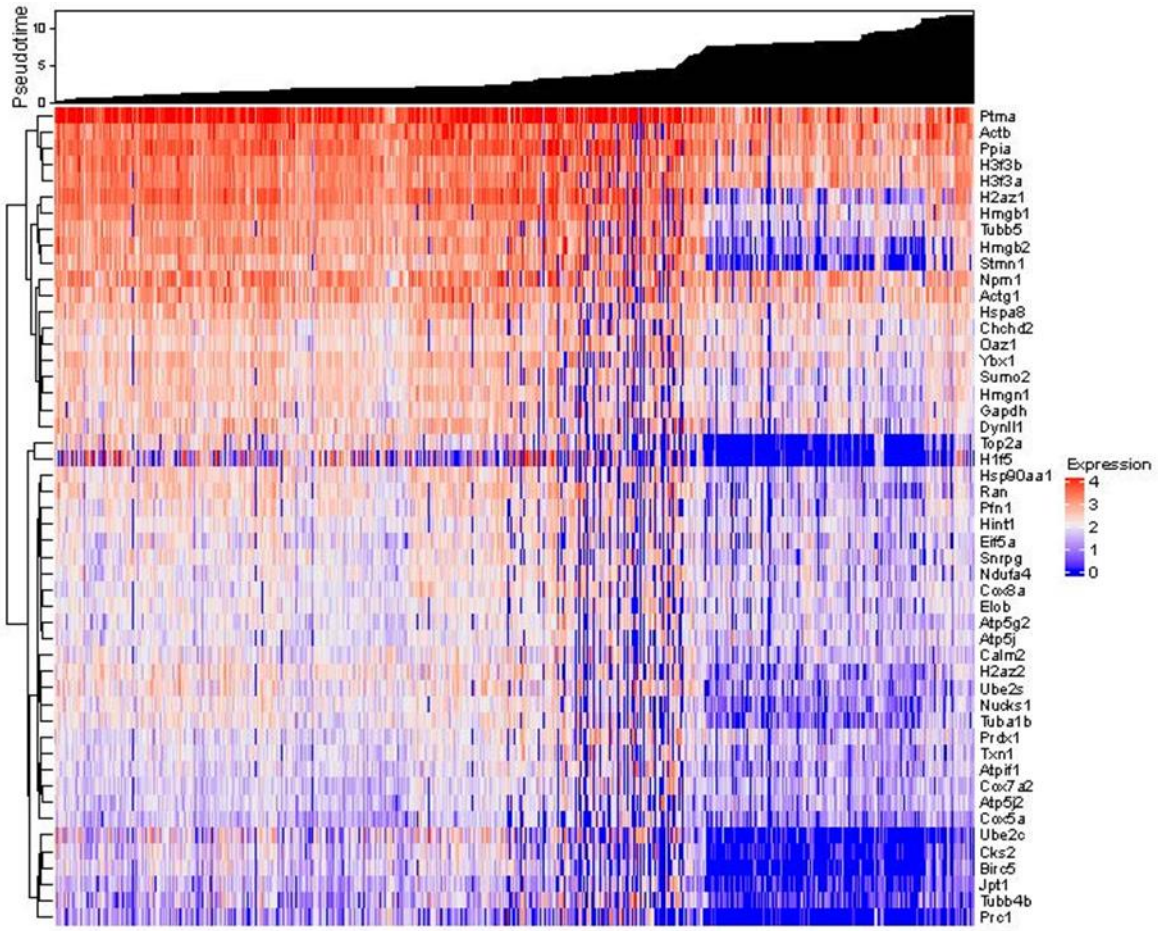

Supplemental Figure 9: *Heatmap displaying the top 50 differentially expressed genes that are* ***downregulated*** *in the mesenchyme during the process of differentiation of proliferating mesenchymal progenitors, stromal cells and fibroblasts.*

REFERENCES

Abdelkafy, Wael M., Johnathon Q. Smith, Oswaldo A. Henriquez, Justin S. Golub, Jianguo Xu, Mauricio Rojas, Kenneth L. Brigham, and Michael M. Johns. 2007. "Age-Related Changes in the Murine Larynx: Initial Validation of a Mouse Model." *Annals of Otology, Rhinology and Laryngology* 116 (8): 618–22. https://doi.org/10.1177/000348940711600810.

Apelo, Sebastian I.Arriola, Cassidy P. Pumper, Emma L. Baar, Nicole E. Cummings, and Dudley W. Lamming. 2016. "Intermittent Administration of Rapamycin Extends the Life Span of Female C57BL/6J Mice." *The Journals of Gerontology. Series A, Biological Sciences and Medical Sciences* 71 (7): 876–81. https://doi.org/10.1093/GERONA/GLW064.

Asp, Michaela, Stefania Giacomello, Ludvig Larsson, Chenglin Wu, Daniel Fürth, Xiaoyan Qian, Eva Wärdell, et al. 2019. "A Spatiotemporal Organ-Wide Gene Expression and Cell Atlas of the Developing Human Heart." *Cell* 179 (7): 1647-1660.e19. https://doi.org/10.1016/J.CELL.2019.11.025.

Bailly, Lucie, Thibaud Cochereau, Laurent Orgéas, Nathalie Henrich Bernardoni, Sabine Rolland du Roscoat, Anne McLeer-Florin, Yohann Robert, et al. 2018. "3D Multiscale Imaging of Human Vocal Folds Using Synchrotron X-Ray Microtomography in Phase Retrieval Mode." *Scientific Reports 2018 8:1* 8 (1): 1–20. https://doi.org/10.1038/s41598-018-31849-w.

Bainbridge, Kathleen E., Nelson Roy, Katalin G. Losonczy, Howard J. Hoffman, and Seth M. Cohen. 2017. "Voice Disorders and Associated Risk Markers Among Young Adults in the United States." *The Laryngoscope* 127 (9): 2093. https://doi.org/10.1002/LARY.26465.

Beatriz, Anna, Paiva Gomes, Marcia Simões-Zenari, and Kátia Nemr. n.d. "Brief Communication Comunicações Breves Aged Voice: Does Advancing Age Generate

Different Impacts? Voz Do Idoso: O Avanço Da Idade Gera Diferentes Impactos?" https://doi.org/10.1590/2317-1782/20202020126.

Bennett, Richard D., Mark R. Pittelkow, and Emanuel E. Strehler. 2013. "Immunolocalization of the Tumor-Sensitive Calmodulin-Like Protein CALML3 in Normal Human Skin and Hyperproliferative Skin Disorders." *PLOS ONE* 8 (4): e62347. https://doi.org/10.1371/JOURNAL.PONE.0062347.

Benoit, Marie E., Elizabeth V. Clarke, Pedro Morgado, Deborah A. Fraser, and Andrea J. Tenner. 2012. "Complement Protein C1q Directs Macrophage Polarization and Limits Inflammasome Activity during the Uptake of Apoptotic Cells." *Journal of Immunology (Baltimore, Md. : 1950)* 188 (11): 5682. https://doi.org/10.4049/JIMMUNOL.1103760.

Boudoux, Caroline, Shelby C. Leuin, Wang Yuhl Oh, Melissa J. Suter, Adrien E. Desjardins, Benjamin J. Vakoc, Brett E. Bouma, Christopher J. Hartnick, and Guillermo J. Tearney. 2009. "Optical Microscopy of the Pediatric Vocal Fold." *Archives of Otolaryngology–Head & Neck Surgery* 135 (1): 53–64. https://doi.org/10.1001/ARCHOTO.2008.518.

Breiteneder-Geleff, Silvana, Afschin Soleiman, Heinrich Kowalski, Reinhard Horvat, Gabriele Amann, Ernst Kriehuber, Katja Diem, et al. 1999. "Angiosarcomas Express Mixed Endothelial Phenotypes of Blood and Lymphatic Capillaries: Podoplanin as a Specific Marker for Lymphatic Endothelium." *American Journal of Pathology* 154 (2): 385–94. https://doi.org/10.1016/S0002-9440(10)65285-6.

Cajal, SR y. 1911. *Histologie Du Système Nerveux de l'homme & Des Vertébrés: Cervelet, Cerveau Moyen, Rétine, Couche Optique, Corps Strié, Écorce Cérébrale Générale &*. https://books.google.com/books?hl=en&lr=&id=qx86AQAAMAAJ&oi=fnd&pg=PA61&dq=Histologie+du+système+nerveux+de+l%27homme+des+vertébrés&ots=f-

BaHpKtt4&sig=TxoJ6eyy_ufzqVghoKO-h7dZ0KE.

Chen, Dongsheng, Jian Sun, Jiacheng Zhu, Xiangning Ding, Tianming Lan, Xiran Wang, Weiying Wu, et al. 2021. “Single Cell Atlas for 11 Non-Model Mammals, Reptiles and Birds.” *Nature Communications 2021 12:1* 12 (1): 1–17. https://doi.org/10.1038/s41467-021-27162-2.

Chengxiao, Zhao, and Yang Ze. 2015. “Biological Function and Molecular Mechanism of Twist2.” *Yi Chuan = Hereditas / Zhongguo Yi Chuan Xue Hui Bian Ji* 37 (1): 17–24. https://doi.org/10.16288/J.YCZZ.2015.01.003.

Delobel, Pauline, Benjamin Ginter, Eliane Rubio, Karl Balabanian, and Gwendal Lazennec. 2022. “CXCR2 Intrinsically Drives the Maturation and Function of Neutrophils in Mice.” *Frontiers in Immunology* 13 (October). https://doi.org/10.3389/FIMMU.2022.1005551/FULL.

Enge, Martin, H. Efsun Arda, Marco Mignardi, John Beausang, Rita Bottino, Seung K. Kim, and Stephen R. Quake. 2017. “Single-Cell Analysis of Human Pancreas Reveals Transcriptional Signatures of Aging and Somatic Mutation Patterns.” *Cell* 171 (2): 321-330.e14. https://doi.org/10.1016/j.cell.2017.09.004.

Fawcett, DW. 1966. “Atlas of Fine Structure.” https://agris.fao.org/agris-search/search.do?recordID=US201300594888.

Fawkner-Corbett, David, Agne Antanaviciute, Kaushal Parikh, Marta Jagielowicz, Ana Sousa Gerós, Tarun Gupta, Neil Ashley, et al. 2021. “Spatiotemporal Analysis of Human Intestinal Development at Single-Cell Resolution.” *Cell* 184 (3): 810-826.e23. https://doi.org/10.1016/J.CELL.2020.12.016.

Fayoux, Pierre, Bruno Marciniak, Louise Devisme, and Laurent Storme. 2008. “Prenatal and

Early Postnatal Morphogenesis and Growth of Human Laryngotracheal Structures." *Journal of Anatomy* 213 (2): 86. https://doi.org/10.1111/J.1469-7580.2008.00935.X.

Feldman, Ada T., and Delia Wolfe. 2014. "Tissue Processing and Hematoxylin and Eosin Staining." *Methods in Molecular Biology (Clifton, N.J.)* 1180: 31–43. https://doi.org/10.1007/978-1-4939-1050-2_3.

Ferrari, Mathieu, Matteo Righi, Vania Baldan, Patrycja Wawrzyniecka, Anna Bulek, Alexander Kinna, Biao Ma, et al. 2024. "Structure-Guided Engineering of Immunotherapies Targeting TRBC1 and TRBC2 in T Cell Malignancies." *Nature Communications 2024 15:1* 15 (1): 1–16. https://doi.org/10.1038/s41467-024-45854-3.

Foote, Alexander G., Ziyue Wang, Christina Kendziorski, and Susan L. Thibeault. 2019. "Tissue Specific Human Fibroblast Differential Expression Based on RNAsequencing Analysis." *BMC Genomics 2019 20:1* 20 (1): 1–19. https://doi.org/10.1186/S12864-019-5682-5.

Fried, M. P., J. H. Kelly, and M. Strome. 1982. "Comparison of the Adult and Infant Larynx." *Journal of Family Practice* 15 (3): 557–58, 561.

Funk, Steven D., Raymond H. Bayer, Andrew F. Malone, Karen K. McKee, Peter D. Yurchenco, and Jeffrey H. Miner. 2018. "Pathogenicity of a Human Laminin B2 Mutation Revealed in Models of Alport Syndrome." *Journal of the American Society of Nephrology* 29 (3): 949–60. https://doi.org/10.1681/ASN.2017090997/-/DCSUPPLEMENTAL.

Galvagni, Federico, Federica Nardi, Marco Maida, Giulia Bernardini, Silvia Vannuccini, Felice Petraglia, Annalisa Santucci, and Maurizio Orlandini. 2016. "CD93 and Dystroglycan Cooperation in Human Endothelial Cell Adhesion and Migration Adhesion and Migration." *Oncotarget* 7 (9): 10090–103. https://doi.org/10.18632/ONCOTARGET.7136.

Gardner, L. E., J. D. White, M. J. Eimerbrink, G. W. Boehm, and M. J. Chumley. 2016.

"Imatinib Methanesulfonate Reduces Hyperphosphorylation of Tau Following Repeated Peripheral Exposure to Lipopolysaccharide." *Neuroscience* 331 (September): 72–77. https://doi.org/10.1016/J.NEUROSCIENCE.2016.06.007.

Gatti, William M., Eileen MacDonald, and Emilio Orfei. 1987. "Congenital Laryngeal Atresia." *The Laryngoscope* 97 (8): 966–69. https://doi.org/10.1288/00005537-198708000-00015.

Gilfillan, Margaret, and Vineet Bhandari. 2020. "Immune Modulators for the Therapy of BPD." *Tantalizing Therapeutics in Bronchopulmonary Dysplasia*, January, 207–31. https://doi.org/10.1016/B978-0-12-818987-0.00011-4.

Gill, G. A., A. Buda, M. Moorghen, P. W. Dettmar, and M. Pignatelli. 2005. "Characterisation of Adherens and Tight Junctional Molecules in Normal Animal Larynx; Determining a Suitable Model for Studying Molecular Abnormalities in Human Laryngopharyngeal Reflux." *Journal of Clinical Pathology* 58 (12): 1265–70. https://doi.org/10.1136/JCP.2004.016972.

Graber, Ted G., Jong Hee Kim, Robert W. Grange, Linda K. McLoon, and La Dora V. Thompson. 2015. "C57BL/6 Life Span Study: Age-Related Declines in Muscle Power Production and Contractile Velocity." *Age* 37 (3). https://doi.org/10.1007/S11357-015-9773-1.

Gray, Steven D., Fariborz Alipour, Ingo R. Titze, and Thomas Hale Hammond. 2000a. "Biomechanical and Histologic Observations of Vocal Fold Fibrous Proteins." *Annals of Otology, Rhinology and Laryngology* 109 (1): 77–85. https://doi.org/10.1177/000348940010900115.

———. 2000b. "Biomechanical and Histologic Observations of Vocal Fold Fibrous Proteins." *The Annals of Otology, Rhinology, and Laryngology* 109 (1): 77–85.

https://doi.org/10.1177/000348940010900115.

———. 2000c. “Biomechanical and Histologic Observations of Vocal Fold Fibrous Proteins.” *Annals of Otology, Rhinology and Laryngology* 109 (1): 77–85. https://doi.org/10.1177/000348940010900115.

Greaney, Allison M., Taylor S. Adams, Micha Sam Brickman Raredon, Elise Gubbins, Jonas C. Schupp, Alexander J. Engler, Mahboobe Ghaedi, Yifan Yuan, Naftali Kaminski, and Laura E. Niklason. 2020. “Platform Effects on Regeneration by Pulmonary Basal Cells as Evaluated by Single-Cell RNA Sequencing.” *Cell Reports* 30 (12): 4250. https://doi.org/10.1016/J.CELREP.2020.03.004.

Griffin, Kate, Hailey Pedersen, Kari Stauss, Vlasta Lungova, and Susan L. Thibeault. 2021. “Characterization of Intrauterine Growth, Proliferation and Biomechanical Properties of the Murine Larynx.” *PLOS ONE* 16 (1): e0245073. https://doi.org/10.1371/JOURNAL.PONE.0245073.

Gunter, Heather E. 2004. “Modeling Mechanical Stresses as a Factor in the Etiology of Benign Vocal Fold Lesions.” *Journal of Biomechanics* 37 (7): 1119–24. https://doi.org/10.1016/J.JBIOMECH.2003.11.007.

Hammond, Nigel L., Denis J. Headon, and Michael J. Dixon. 2012. “The Cell Cycle Regulator Protein 14-3-3σ Is Essential for Hair Follicle Integrity and Epidermal Homeostasis.” *Journal of Investigative Dermatology* 132 (6): 1543–53. https://doi.org/10.1038/JID.2012.27.

Han, Chen, Trevor R. Leonardo, Bruna Romana-Souza, Junhe Shi, Shalyn Keiser, Heidi Yuan, Mohamad Altakriti, et al. 2023. “Microfibril-Associated Protein 5 and the Regulation of Skin Scar Formation.” *Scientific Reports 2023 13:1* 13 (1): 1–15.

https://doi.org/10.1038/s41598-023-35558-x.

Han, Lu, Praneet Chaturvedi, Keishi Kishimoto, Hiroyuki Koike, Talia Nasr, Kentaro Iwasawa, Kirsten Giesbrecht, et al. 2020. "Single Cell Transcriptomics Identifies a Signaling Network Coordinating Endoderm and Mesoderm Diversification during Foregut Organogenesis." *Nature Communications 2020 11:1* 11 (1): 1–16. https://doi.org/10.1038/s41467-020-17968-x.

Hancock, Laura A., Corinne E. Hennessy, George M. Solomon, Evgenia Dobrinskikh, Alani Estrella, Naoko Hara, David B. Hill, et al. 2018. "Muc5b Overexpression Causes Mucociliary Dysfunction and Enhances Lung Fibrosis in Mice." *Nature Communications 2018 9:1* 9 (1): 1–10. https://doi.org/10.1038/s41467-018-07768-9.

Hanson, Summer E., Jaehyup Kim, Beatriz H. Quinchia Johnson, Bridget Bradley, Melissa J. Breunig, Peiman Hematti, and Susan L. Thibeault. 2010. "Characterization of Mesenchymal Stem Cells from Human Vocal Fold Fibroblasts." *The Laryngoscope* 120 (3): 546–51. https://doi.org/10.1002/LARY.20797.

Hartnick, Christopher J, Reza Rehbar, and Vinay Prasad. 2005. "Development and Maturation of the Pediatric Human Vocal Fold Lamina Propria." https://doi.org/10.1097/01.mlg.0000150685.54893.e9.

Hauser, Belinda R., Marit H. Aure, Michael C. Kelly, Matthew P. Hoffman, and Alejandro M. Chibly. 2020. "Generation of a Single-Cell RNAseq Atlas of Murine Salivary Gland Development." *IScience* 23 (12): 101838. https://doi.org/10.1016/J.ISCI.2020.101838.

Henick, D. H. 1993. "Three-Dimensional Analysis of Murine Laryngeal Development." *Annals of Otology, Rhinology and Laryngology* 102 (3 II SUPPL. 159): 3–24. https://doi.org/10.1177/00034894931020S301.

Herriges, Michael, and Edward E. Morrisey. 2014. “Lung Development: Orchestrating the Generation and Regeneration of a Complex Organ.” *Development (Cambridge)* 141 (3): 502–13. https://doi.org/10.1242/dev.098186.

Hewitt, Richard J., and Clare M. Lloyd. 2021. “Regulation of Immune Responses by the Airway Epithelial Cell Landscape.” *Nature Reviews. Immunology* 21 (6): 347. https://doi.org/10.1038/S41577-020-00477-9.

Hill, Mark Anthony. 2007. “Early Human Development.” *Clinical Obstetrics and Gynecology* 50 (1): 2–9. https://doi.org/10.1097/GRF.0b013e31802f119d.

Hirano, Minoru. 1974. “Morphological Structure of the Vocal Cord as a Vibrator and Its Variations.” *Folia Phoniatrica et Logopaedica* 26 (2): 89–94. https://doi.org/10.1159/000263771.

Hirano, Minoru, Shigejiro Kurita, and Shinji Sakaguchi. 2009. “Ageing of the Vibratory Tissue of Human Vocal Folds.” *Http://Dx.Doi.Org/10.3109/00016488909127535* 107 (5–6): 428–33. https://doi.org/10.3109/00016488909127535.

Hlrano, Mlnoru, and Kiminori Sato. 1999. “ELECTRON MICROSCOPIC AND IMMUNOHISTOCHEMICAL INVESTIGATION OF REINKE’S EDEMA.” *Ann Olol Rhinol Laryngol* 108.

Horowitz, Amir, Haocheng Yu, Sonalisa Pandey, Bud Mishra, Debashis Sahoo, and Jennifer Lipschultz. 2024. “C1QA Is an Invariant Biomarker for Tissue Macrophages.” *BioRxiv*, January, 2024.01.26.577475. https://doi.org/10.1101/2024.01.26.577475.

Hwang, Byungjin, Ji Hyun Lee, and Duhee Bang. 2018. “Single-Cell RNA Sequencing Technologies and Bioinformatics Pipelines.” *Experimental & Molecular Medicine 2018 50:8* 50 (8): 1–14. https://doi.org/10.1038/s12276-018-0071-8.

Infusino, Scott A., Shilpa Ojha, Rie Maurer, Peter M. Sadow, William C. Faquin, and Christopher J. Hartnick. 2013. “The Utility of Histopathology in Identifying Structural Differences among Layers of the Lamina Propria.” *International Journal of Pediatric Otorhinolaryngology* 77 (10): 1651–54. https://doi.org/10.1016/J.IJPORL.2013.07.018.

Innos, Jürgen, Kati Koido, Mari Anne Philips, and Eero Vasar. 2013. “Limbic System-Associated Membrane Protein as a Potential Target for Neuropsychiatric Disorders.” *Frontiers in Pharmacology* 4 MAR (March): 42968. https://doi.org/10.3389/FPHAR.2013.00032/BIBTEX.

Ira, H. 1974. “Morphological Structure of the Vocal Cord as a Vibrator and Its Variations M in o Ru” 26: 89–94.

Ishii, Kosuke, Masumi Akita, Kotaro Yamashita, and Hajime Hlrose. 2000. “AGE-RELATED DEVELOPMENT OF THE ARRANGEMENT OF CONNECTIVE TISSUE FIBERS IN THE LAMINA PROPRIA OF THE HUMAN VOCAL FOLD.” *Ann Owl Rhinol Laryngol* 109.

Jetté, Marie E., Matthew S. Clary, Jeremy D. Prager, and Thomas E. Finger. 2020. “Chemical Receptors of the Arytenoid: A Comparison of Human and Mouse.” *The Laryngoscope* 130 (2): 423–30. https://doi.org/10.1002/LARY.27931.

Joanisse, Sophie, Joshua P. Nederveen, Jeff M. Baker, Tim Snijders, Carlo Iacono, and Gianni Parise. 2016. “Exercise Conditioning in Old Mice Improves Skeletal Muscle Regeneration.” *FASEB Journal : Official Publication of the Federation of American Societies for Experimental Biology* 30 (9): 3256–68. https://doi.org/10.1096/FJ.201600143RR.

Kahane, Joel C. 1978. “A Morphological Study of the Human Prepubertal and Pubertal Larynx.”

Kakodkar, Kedar A., James W. Schroeder, and Lauren D. Holinger. 2012. “Laryngeal

Development and Anatomy." In *Pediatric Airway Surgery*, 73:1–11. https://doi.org/10.1159/000334108.

Karlsson, Max, Cheng Zhang, Loren Méar, Wen Zhong, Andreas Digre, Borbala Katona, Evelina Sjöstedt, et al. 2021. "A Single–Cell Type Transcriptomics Map of Human Tissues." *Science Advances* 7 (31). https://doi.org/10.1126/SCIADV.ABH2169/SUPPL_FILE/SCIADV.ABH2169_SM.PDF.

Keener, Amanda B. 2019. "Single-Cell Sequencing Edges into Clinical Trials." *Nature Medicine* 25 (9): 1322–26. https://doi.org/10.1038/D41591-019-00017-6.

Khandelwal, Sanjay, and Paul A. Roche. 2010. "Distinct MHC Class II Molecules Are Associated on the Dendritic Cell Surface in Cholesterol-Dependent Membrane Microdomains." *Journal of Biological Chemistry* 285 (46): 35303–10. https://doi.org/10.1074/JBC.M110.147793.

King, Suzanne N, Fei Chen, Marie E Jetté, and Susan L Thibeault. 2012. "Vocal Fold Fibroblasts Immunoregulate Activated Macrophage Phenotype q,Qq." https://doi.org/10.1016/j.cyto.2012.09.023.

Kishimoto, Ayami Ohno, Yo Kishimoto, Xudong Shi, Elizabeth B. Hutchinson, Hua Zhang, Yatao Shi, Gisele Oliveira, Lingjun Li, Nathan V. Welham, and Ian J. Rowland. 2021. "High-Resolution Magnetic Resonance and Mass Spectrometry Imaging of the Human Larynx." *Journal of Anatomy* 239 (3): 545–56. https://doi.org/10.1111/JOA.13451.

Kishimoto, Yo, Ayami Ohno Kishimoto, Shuyun Ye, Christina Kendziorski, and Nathan V. Welham. 2016a. "Modeling Fibrosis Using Fibroblasts Isolated from Scarred Rat Vocal Folds." *Laboratory Investigation 2016 96:7* 96 (7): 807–16. https://doi.org/10.1038/labinvest.2016.43.

———. 2016b. “Modeling Fibrosis Using Fibroblasts Isolated from Scarred Rat Vocal Folds.” *Laboratory Investigation 2016 96:7* 96 (7): 807–16. https://doi.org/10.1038/labinvest.2016.43.

Knight, Darryl A., and Stephen T. Holgate. 2003. “The Airway Epithelium: Structural and Functional Properties in Health and Disease.” *Respirology* 8 (4): 432–46. https://doi.org/10.1046/J.1440-1843.2003.00493.X.

Kuhn, Maggie A. 2014a. “Histological Changes in Vocal Fold Growth and Aging.” *Current Opinion in Otolaryngology and Head and Neck Surgery* 22 (6): 460–65. https://doi.org/10.1097/MOO.0000000000000108.

———. 2014b. “Histological Changes in Vocal Fold Growth and Aging.” *Current Opinion in Otolaryngology and Head and Neck Surgery* 22 (6): 460–65. https://doi.org/10.1097/MOO.0000000000000108.

Kuijk, Kim van, Ian R. McCracken, Renée J.H.A. Tillie, Sebastiaan E.J. Asselberghs, Dlzar A. Kheder, Stan Muitjens, Han Jin, et al. 2023. “Human and Murine Fibroblast Single-Cell Transcriptomics Reveals Fibroblast Clusters Are Differentially Affected by Ageing and Serum Cholesterol.” *Cardiovascular Research* 119 (7): 1509–23. https://doi.org/10.1093/CVR/CVAD016.

Kuleshov, Maxim V., Matthew R. Jones, Andrew D. Rouillard, Nicolas F. Fernandez, Qiaonan Duan, Zichen Wang, Simon Koplev, et al. 2016. “Enrichr: A Comprehensive Gene Set Enrichment Analysis Web Server 2016 Update.” *Nucleic Acids Research* 44 (1): W90–97. https://doi.org/10.1093/NAR/GKW377.

Kuo, Christin S., Spyros Darmanis, Alex Diaz de Arce, Yin Liu, Nicole Almanzar, Timothy Ting Hsuan Wu, Stephen R. Quake, and Mark A. Krasnow. 2022. “Neuroendocrinology of the

Lung Revealed by Single-Cell RNA Sequencing." *ELife* 11. https://doi.org/10.7554/ELIFE.78216.

Kutta, Hannes, Philipp Steven, Guido Kohla, Bernhard Tillmann, and Friedrich Paulsen. 2002. "The Human False Vocal Folds – an Analysis of Antimicrobial Defense Mechanisms." *Anatomy and Embryology 2002 205:4* 205 (4): 315–23. https://doi.org/10.1007/S00429-002-0255-8.

Lesourne, Renaud, Shoji Uehara, Jan Lee, Ki Duk Song, Li Qi Li, Julia Pinkhasov, Yongqing Zhang, et al. 2009. "THEMIS, a New T Cell Specific Protein Important for Late Thymocyte Development." *Nature Immunology* 10 (8): 840. https://doi.org/10.1038/NI.1768.

Levendoski, Elizabeth Erickson, Ciara Leydon, and Susan L. Thibeault. 2014a. "Vocal Fold Epithelial Barrier in Health and Injury: A Research Review." *Journal of Speech, Language, and Hearing Research* 57 (5): 1679–91. https://doi.org/10.1044/2014_JSLHR-S-13-0283.

———. 2014b. "Vocal Fold Epithelial Barrier in Health and Injury: A Research Review." *Journal of Speech, Language, and Hearing Research* 57 (5): 1679–91. https://doi.org/10.1044/2014_JSLHR-S-13-0283.

Li, Jin, Erwei Li, Rafael S Czepielewski, Paul Cohen, Linus Tsai, and Evan D Rosen Correspondence. 2021. "Neurotensin Is an Anti-Thermogenic Peptide Produced by Lymphatic Endothelial Cells." *Cell Metabolism* 33: 1449-1465.e6. https://doi.org/10.1016/j.cmet.2021.04.019.

Li, Linqing, Jeanna M. Stiadle, Hang K. Lau, Aidan B. Zerdoum, Xinqiao Jia, Susan L. Thibeault, and Kristi L. Kiick. 2016. "Tissue Engineering-Based Therapeutic Strategies for Vocal Fold Repair and Regeneration." *Biomaterials* 108 (November): 91–110. https://doi.org/10.1016/J.BIOMATERIALS.2016.08.054.

Li, Lvyuan, Fang Xiong, Yumin Wang, Shanshan Zhang, Zhaojian Gong, Xiayu Li, Yi He, et al. 2021. “What Are the Applications of Single-Cell RNA Sequencing in Cancer Research: A Systematic Review.” *Journal of Experimental & Clinical Cancer Research 2021 40:1* 40 (1): 1–12. https://doi.org/10.1186/S13046-021-01955-1.

Li, Xinmin, and Cun Yu Wang. 2021. “From Bulk, Single-Cell to Spatial RNA Sequencing.” *International Journal of Oral Science 2021 13:1* 13 (1): 1–6. https://doi.org/10.1038/s41368-021-00146-0.

Li, Yan, Li Zhang, Francesca Polverino, Feng Guo, Yuan Hao, Taotao Lao, Shuang Xu, et al. 2021. “Hedgehog Interacting Protein (HHIP) Represses Airway Remodeling and Metabolic Reprogramming in COPD-Derived Airway Smooth Muscle Cells.” *Scientific Reports 2021 11:1* 11 (1): 1–12. https://doi.org/10.1038/s41598-021-88434-x.

Lindeboom, Rik G.H., Aviv Regev, and Sarah A. Teichmann. 2021. “Towards a Human Cell Atlas: Taking Notes from the Past.” *Trends in Genetics* 37 (7): 625–30. https://doi.org/10.1016/J.TIG.2021.03.007.

Liu, Zhangyin, Yu Qing Jin, Lulu Chen, Yang Wang, Xiaonan Yang, Jia Cheng, Wei Wu, Zuoliang Qi, and Zunli Shen. 2015. “Specific Marker Expression and Cell State of Schwann Cells during Culture In Vitro.” *PLoS ONE* 10 (4). https://doi.org/10.1371/JOURNAL.PONE.0123278.

Lungova, Vlasta, Kate V. Griffin, Tadeas Lunga, and Susan L. Thibeault. 2020. “Drainage of Amniotic Fluid Delays Vocal Fold Separation and Induces Load-Related Vocal Fold Mucosa Remodeling.” *Developmental Biology* 466 (1–2): 47–58. https://doi.org/10.1016/j.ydbio.2020.08.003.

Lungova, Vlasta, and Susan L. Thibeault. 2020. “Mechanisms of Larynx and Vocal Fold

Development and Pathogenesis." *Cellular and Molecular Life Sciences 2020 77:19* 77 (19): 3781–95. https://doi.org/10.1007/S00018-020-03506-X.

Lungova, Vlasta, Jamie M. Verheyden, John Herriges, Xin Sun, and Susan L. Thibeault. 2015a. "Ontogeny of the Mouse Vocal Fold Epithelium." *Developmental Biology* 399 (2): 263–82. https://doi.org/10.1016/j.ydbio.2014.12.037.

———. 2015b. "Ontogeny of the Mouse Vocal Fold Epithelium." *Dev Biol* 399 (2): 2. https://doi.org/10.1016/j.ydbio.2014.12.037.

Lungova, Vlasta, Jamie M. Verheyden, Xin Sun, and Susan L. Thibeault. 2018. "β-Catenin Signaling Is Essential for Mammalian Larynx Recanalization and the Establishment of Vocal Fold Progenitor Cells." *Dev (Cambridge)* 145 (4): 4. https://doi.org/10.1242/dev.157677.

Martins, Regina Helena Garcia, Henrique Abrantes do Amaral, Elaine Lara Mendes Tavares, Maira Garcia Martins, Tatiana Maria Gonçalves, and Norimar Hernandes Dias. 2016. "Voice Disorders: Etiology and Diagnosis." *Journal of Voice* 30 (6): 761.e1-761.e9. https://doi.org/10.1016/J.JVOICE.2015.09.017.

Mattiola, Irene, Federica Tomay, Maria De Pizzol, Rita Silva-Gomes, Benedetta Savino, Tamara Gulic, Andrea Doni, et al. 2019. "The Macrophage Tetraspan MS4A4A Enhances Dectin-1-Dependent NK Cell–Mediated Resistance to Metastasis." *Nature Immunology* 20 (8): 1012–22. https://doi.org/10.1038/S41590-019-0417-Y.

Mcclintock, Timothy S, Chad E Glasser, Soma C Bose, Daniel A Bergman, Mcclintock Ts, Glasser Ce, Bose Sc, and Bergman Da. 2008. "Tissue Expression Patterns Identify Mouse Cilia Genes." *Physiol Geno-Mics* 32: 198–206. https://doi.org/10.1152/physiolgenomics.00128.2007.-In.

Mereu, Elisabetta, Atefeh Lafzi, Catia Moutinho, Christoph Ziegenhain, Davis J. McCarthy, Adrián Álvarez-Varela, Eduard Batlle, et al. 2020. “Benchmarking Single-Cell RNA-Sequencing Protocols for Cell Atlas Projects.” *Nature Biotechnology 2020 38:6* 38 (6): 747–55. https://doi.org/10.1038/s41587-020-0469-4.

Merrill, Ray M., Allison E. Anderson, and Arielle Sloan. 2011. “Quality of Life Indicators According to Voice Disorders and Voice-Related Conditions.” *The Laryngoscope* 121 (9): 2004–10. https://doi.org/10.1002/LARY.21895.

Miklaszewska, Danuta, Aleksandra Gawlikowska-Sroka, Florian Czerwiński, Edyta Dzieciołowska-Baran, and Ewa Adamiec. 2010. “A Morphometric Study of Prenatal Development of the Human Larynx.” *Annales Academiae Medicae Stetinensis* 56 (3): 103–6. https://europepmc.org/article/med/22053632.

Mižíková, Ivana, Flore Lesage, Chanele Cyr-Depauw, David P. Cook, Maria Hurskainen, Satu M. Hänninen, Arul Vadivel, et al. 2022. “Single-Cell RNA Sequencing-Based Characterization of Resident Lung Mesenchymal Stromal Cells in Bronchopulmonary Dysplasia.” *Stem Cells* 40 (5): 479–92. https://doi.org/10.1093/STMCLS/SXAB023.

Mohad, Vidisha, Vlasta Lungova, Jamie Verheyden, and Susan L. Thibeault. 2021. “Inactivation of Lats1 and Lats2 Highlights the Role of Hippo Pathway Effector YAP in Larynx and Vocal Fold Epithelium Morphogenesis.” *Developmental Biology* 473 (May): 33–49. https://doi.org/10.1016/J.YDBIO.2021.01.012.

Moore, Jaime, and Susan Thibeault. 2012. “Insights into the Role of Elastin in Vocal Fold Health and Disease.” *Journal of Voice*. https://doi.org/10.1016/j.jvoice.2011.05.003.

Mosser, David M., and Justin P. Edwards. 2008. “Exploring the Full Spectrum of Macrophage Activation.” *Nature Reviews Immunology 2008 8:12* 8 (12): 958–69.

https://doi.org/10.1038/nri2448.

Muhl, Lars, Giuseppe Mocci, Riikka Pietilä, Jianping Liu, Liqun He, Guillem Genové, Stefanos Leptidis, et al. 2022. “A Single-Cell Transcriptomic Inventory of Murine Smooth Muscle Cells.” *Developmental Cell* 57 (20): 2426-2443.e6. https://doi.org/10.1016/J.DEVCEL.2022.09.015.

Murry, Thomas, and Clark A. Rosen. 2000. “OUTCOME MEASUREMENTS AND QUALITY OF LIFE IN VOICE DISORDERS.” *Otolaryngologic Clinics of North America* 33 (4): 905–16. https://doi.org/10.1016/S0030-6665(05)70251-6.

Nakamura, Ryosuke, Renjie Bing, Gary J. Gartling, and Ryan C. Branski. 2022. “Macrophages Alter Inflammatory and Fibrotic Gene Expression in Human Vocal Fold Fibroblasts.” *Experimental Cell Research* 419 (1): 113301. https://doi.org/10.1016/J.YEXCR.2022.113301.

Niewiadomski, Paweł, Sylwia M. Niedziółka, Łukasz Markiewicz, Tomasz Uśpieński, Brygida Baran, and Katarzyna Chojnowska. 2019. “Gli Proteins: Regulation in Development and Cancer.” *Cells* 8 (2). https://doi.org/10.3390/CELLS8020147.

Ophir, Michael J., Beiyun C. Liu, and Stephen C. Bunnell. 2013. “The N Terminus of SKAP55 Enables T Cell Adhesion to TCR and Integrin Ligands via Distinct Mechanisms.” *The Journal of Cell Biology* 203 (6): 1021–41. https://doi.org/10.1083/JCB.201305088.

Panina, Yulia, Peter Karagiannis, Andreas Kurtz, Glyn N. Stacey, and Wataru Fujibuchi. 2020. “Human Cell Atlas and Cell-Type Authentication for Regenerative Medicine.” *Experimental & Molecular Medicine 2020 52:9* 52 (9): 1443–51. https://doi.org/10.1038/s12276-020-0421-1.

Plasschaert, Lindsey W., Rapolas Žilionis, Rayman Choo-Wing, Virginia Savova, Judith Knehr,

Guglielmo Roma, Allon M. Klein, and Aron B. Jaffe. 2018. “A Single Cell Atlas of the Tracheal Epithelium Reveals the CFTR-Rich Pulmonary Ionocyte.” *Nature* 560 (7718): 377. https://doi.org/10.1038/S41586-018-0394-6.

Ponichtera, Holly E., Mara G. Shainheit, Beiyun C. Liu, Raktima Raychowdhury, Bridget M. Larkin, Joanne M. Russo, D. Brenda Salantes, et al. 2014. “CD209a Expression on Dendritic Cells Is Critical for the Development of Pathogenic Th17 Cell Responses in Murine Schistosomiasis.” *Journal of Immunology (Baltimore, Md. : 1950)* 192 (10): 4655. https://doi.org/10.4049/JIMMUNOL.1400121.

Premoli, Marika, Maurizio Memo, and Sara Bonini. 2021. “Ultrasonic Vocalizations in Mice: Relevance for Ethologic and Neurodevelopmental Disorders Studies.” *Neural Regeneration Research* 16 (6): 1158. https://doi.org/10.4103/1673-5374.300340.

Quake, Stephen R. 2022. “A Decade of Molecular Cell Atlases.” *Trends in Genetics* 38 (8): 805–10. https://doi.org/10.1016/J.TIG.2022.01.004.

Rapoport, Sarah K., Jayme Meiner, and Nazaneen Grant. 2018. “Voice Changes in the Elderly.” *Otolaryngologic Clinics of North America* 51 (4): 759–68. https://doi.org/10.1016/J.OTC.2018.03.012.

Regev, Aviv, Sarah A. Teichmann, Eric S. Lander, Ido Amit, Christophe Benoist, Ewan Birney, Bernd Bodenmiller, et al. 2017. “The Human Cell Atlas.” *ELife* 6 (December). https://doi.org/10.7554/ELIFE.27041.

Riede, Tobias, Heather L. Borgard, and Bret Pasch. 2017. “Laryngeal Airway Reconstruction Indicates That Rodent Ultrasonic Vocalizations Are Produced by an Edge-Tone Mechanism.” *Royal Society Open Science* 4 (11). https://doi.org/10.1098/RSOS.170976.

Rinn, John L., Chanda Bondre, Hayes B. Gladstone, Patrick O. Brown, and Howard Y. Chang.

2006. “Anatomic Demarcation by Positional Variation in Fibroblast Gene Expression Programs.” *PLOS Genetics* 2 (7): e119. https://doi.org/10.1371/JOURNAL.PGEN.0020119.

Roberts, T., R. Morton, and Saad Al-Ali. 2011. “Microstructure of the Vocal Fold in Elderly Humans.” *Clinical Anatomy* 24 (5): 544–51. https://doi.org/10.1002/CA.21114.

Rosow, David E., and Debbie R. Pan. 2019. “Presbyphonia and Minimal Glottic Insufficiency.” *Otolaryngologic Clinics of North America* 52 (4): 617–25. https://doi.org/10.1016/J.OTC.2019.03.005.

Rubin, John S. (John Stephen), Robert Thayer Sataloff, and Gwen S. Korovin. n.d. “Diagnosis and Treatment of Voice Disorders,” 1019. Accessed November 1, 2022. https://books.google.com/books/about/Diagnosis_and_Treatment_of_Voice_Disorde.html?id=CZQ1BwAAQBAJ.

Sañudo, J R, and J M Domenech-Mateu. 1990. “The Laryngeal Primordium and Epithelial Lamina. A New Interpretation.” *Journal of Anatomy* 171 (August): 207. /pmc/articles/PMC1257142/?report=abstract.

Sapienza, Christine, and Bari Hoffman. 2020. *Voice Disorders*. Plural Publishing.

Sapienza, Christine M., Bari Hoffman Ruddy, and Susan Baker. 2004. “Laryngeal Structure and Function in the Pediatric Larynx.” *Language, Speech, and Hearing Services in Schools* 35 (4): 299–307. https://doi.org/10.1044/0161-1461(2004/029).

Sato, Kiminori. 2018. “Pericytes in the Human Vocal Fold Mucosa.” *Advances in Experimental Medicine and Biology* 1109: 79–93. https://doi.org/10.1007/978-3-030-02601-1_7/FIGURES/15.

Schweinfurth, John M., and Susan L. Thibeault. 2008. “Does Hyaluronic Acid Distribution in the Larynx Relate to the Newborn’s Capacity for Crying?” *The Laryngoscope* 118 (9): 1692–

99. https://doi.org/10.1097/MLG.0B013E3181782754.

Sebastian, Aimy, Jillian L. McCool, Nicholas R. Hum, Deepa K. Murugesh, Stephen P. Wilson, Blaine A. Christiansen, and Gabriela G. Loots. 2021. "Single-Cell RNA-Seq Reveals Transcriptomic Heterogeneity and Post-Traumatic Osteoarthritis-Associated Early Molecular Changes in Mouse Articular Chondrocytes." *Cells* 10 (6). https://doi.org/10.3390/CELLS10061462/S1.

Seino, Yutomo, and Jacqui E. Allen. 2014. "Treatment of Aging Vocal Folds: Surgical Approaches." *Current Opinion in Otolaryngology and Head and Neck Surgery* 22 (6): 466–71. https://doi.org/10.1097/MOO.0000000000000099.

Shoji, Hirotaka, Keizo Takao, Satoko Hattori, and Tsuyoshi Miyakawa. 2016. "Age-Related Changes in Behavior in C57BL/6J Mice from Young Adulthood to Middle Age." *Molecular Brain* 9 (1). https://doi.org/10.1186/S13041-016-0191-9.

Simmons Beck, Robert, Olin D. Liang, and James R. Klinger. 2023. "Light at the ENDothelium-Role of Sox17 and Runx1 in Endothelial Dysfunction and Pulmonary Arterial Hypertension." *Frontiers in Cardiovascular Medicine* 10. https://doi.org/10.3389/FCVM.2023.1274033.

Sprenkeler, Evelien G.G., Judith Zandstra, Nadine D. van Kleef, Ines Goetschalckx, Bibian Verstegen, Cathelijn E.M. Aarts, Hans Janssen, et al. 2022. "S100A8/A9 Is a Marker for the Release of Neutrophil Extracellular Traps and Induces Neutrophil Activation." *Cells* 11 (2). https://doi.org/10.3390/CELLS11020236.

Squier, CA, MJ Kremer - JNCI Monographs, and undefined 2001. n.d. "Biology of Oral Mucosa and Esophagus." *Academic.Oup.Com*. Accessed September 5, 2022. https://academic.oup.com/jncimono/article-abstract/2001/29/7/911372.

Starkova, Tatiana, Alexander Polyanichko, Alexey N. Tomilin, and Elena Chikhirzhina. 2023. "Structure and Functions of HMGB2 Protein." *International Journal of Molecular Sciences* 24 (9). https://doi.org/10.3390/IJMS24098334.

Sun, Xiaoming, and Paul D. Kaufman. 2018. "Ki-67: More than a Proliferation Marker." *Chromosoma* 127 (2): 175. https://doi.org/10.1007/S00412-018-0659-8.

Surmann-Schmitt, Cordula, Uwe Dietz, Trayana Kireva, Nadia Adam, Jung Park, Andreas Tagariello, Patrik Önnerfjord, et al. 2008. "Ucma, a Novel Secreted Cartilage-Specific Protein with Implications in Osteogenesis." *Journal of Biological Chemistry* 283 (11): 7082–93. https://doi.org/10.1074/JBC.M702792200.

Tabler, Jacqueline M., Maggie M. Rigney, Gordon J. Berman, Swetha Gopalakrishnan, Eglantine Heude, Hadeel Adel Al-Lami, Basil Z. Yannakoudiadkis, et al. 2017. "Cilia-Mediated Hedgehog Signaling Controls Form and Function in the Mammalian Larynx." *ELife* 6 (February): 1–26. https://doi.org/10.7554/elife.19153.

Takano, Shingo, Miwako Kimura, Takaharu Nito, Hiroshi Imagawa, Ken Ichi Sakakibara, and Niro Tayama. 2010. "Clinical Analysis of Presbylarynx—Vocal Fold Atrophy in Elderly Individuals." *Auris Nasus Larynx* 37 (4): 461–64. https://doi.org/10.1016/J.ANL.2009.11.013.

Tang, Xiaoning, Yongmei Huang, Jinli Lei, Hui Luo, and Xiao Zhu. 2019. "The Single-Cell Sequencing: New Developments and Medical Applications." *Cell and Bioscience* 9 (1). https://doi.org/10.1186/S13578-019-0314-Y.

Thomas, Lisa B., Joseph C. Stemple, Richard D. Andreatta, and Francisco H. Andrade. 2009. "Establishing a New Animal Model for the Study of Laryngeal Biology and Disease: An Anatomic Study of the Mouse Larynx." *J Speech Lang Hear Res* 52 (3): 802–11.

https://doi.org/10.1044/1092-4388(2008/08-0087).

Travaglini, Kyle J., Ahmad N. Nabhan, Lolita Penland, Rahul Sinha, Astrid Gillich, Rene V. Sit, Stephen Chang, et al. 2020. "A Molecular Cell Atlas of the Human Lung from Single-Cell RNA Sequencing." *Nature 2020 587:7835* 587 (7835): 619–25. https://doi.org/10.1038/s41586-020-2922-4.

Walter, Lauren D., Jessica L. Orton, Ern Hwei Hannah Fong, Viviana I. Maymi, Brian D. Rudd, Jennifer H. Elisseeff, and Benjamin D. Cosgrove. 2023. "Single-Cell Transcriptomic Analysis of Skeletal Muscle Regeneration across Mouse Lifespan Identifies Altered Stem Cell States Associated with Senescence." *BioRxiv*. https://doi.org/10.1101/2023.05.25.542370.

Wang, Zhao, Jun Chen, Shengjie Wang, Zelong Sun, Zhe Lei, Hong Tao Zhang, and Jie Huang. 2022. "RGS6 Suppresses TGF-β-Induced Epithelial-Mesenchymal Transition in Non-Small Cell Lung Cancers via a Novel Mechanism Dependent on Its Interaction with SMAD4." *Cell Death & Disease* 13 (7). https://doi.org/10.1038/S41419-022-05093-0.

Ward, P. Daniel, Susan L. Thibeault, and Steven D. Gray. 2002. "Hyaluronic Acid: Its Role in Voice." *Journal of Voice : Official Journal of the Voice Foundation* 16 (3): 303–9. https://doi.org/10.1016/S0892-1997(02)00101-7.

Wendt, Kristy D., Jared Brown, Vlasta Lungova, Vidisha Mohad, Christina Kendziorski, and Susan L. Thibeault. 2022. "Transcriptome Dynamics in the Developing Larynx, Trachea, and Esophagus." *Frontiers in Cell and Developmental Biology* 0 (July): 1319. https://doi.org/10.3389/FCELL.2022.942622.

Wilbrey-Clark, Anna, Kenny Roberts, and Sarah A. Teichmann. 2020. "Cell Atlas Technologies and Insights into Tissue Architecture." *Biochemical Journal* 477 (8): 1427–42.

https://doi.org/10.1042/BCJ20190341.

Wolbert, Jolien, Xiaolin Li, Michael Heming, Anne K. Mausberg, Dagmar Akkermann, Clara Frydrychowicz, Robert Fledrich, et al. 2020. "Redefining the Heterogeneity of Peripheral Nerve Cells in Health and Autoimmunity." *Proceedings of the National Academy of Sciences of the United States of America* 117 (17): 9466–76. https://doi.org/10.1073/PNAS.1912139117/SUPPL_FILE/PNAS.1912139117.SD14.XLSX.

Xiang, Menglan, Rubén Adrián Grosso, Akira Takeda, Junliang Pan, Tove Bekkhus, Kevin Brulois, Denis Dermadi, et al. 2020. "A Single-Cell Transcriptional Roadmap of the Mouse and Human Lymph Node Lymphatic Vasculature." *Frontiers in Cardiovascular Medicine* 7 (April): 523939. https://doi.org/10.3389/FCVM.2020.00052/BIBTEX.

Ximenes Filho, João Aragao, Domingos Hiroshi Tsuji, Paulo Hilario Saldiva Do Nascimento, and Luiz Ubirajara Sennes. 2003. "Histologic Changes in Human Vocal Folds Correlated with Aging: A Histomorphometric Study." *Annals of Otology, Rhinology and Laryngology* 112 (10): 894–98. https://doi.org/10.1177/000348940311201012.

Yamashita, Masaru, Diane M. Bless, and Nathan V. Welham. 2009a. "Surgical Method to Create Vocal Fold Injuries in Mice." *Annals of Otology, Rhinology and Laryngology* 118 (2): 131–38. https://doi.org/10.1177/000348940911800209.

Yamashita, Masaru, Diane M Bless, and Nathan V Welham. 2009b. "Surgical Method to Create Vocal Fold Injuries in Mice." *The Annals of Otology, Rhinology, and Laryngology* 118 (2): 131–38. https://doi.org/10.1177/000348940911800209.

Yin, Jun, and Zhaoyan Zhang. 2014. "Interaction between the Thyroarytenoid and Lateral Cricoarytenoid Muscles in the Control of Vocal Fold Adduction and Eigenfrequencies." *Journal of Biomechanical Engineering* 136 (11). https://doi.org/10.1115/1.4028428/371083.

You, Yingjian, Tao Huang, Edward J. Richer, Jens Erik Harboe Schmidt, Joseph Zabner, Zea Borok, and Steven L. Brody. 2004. “Role of F-Box Factor Foxj1 in Differentiation of Ciliated Airway Epithelial Cells.” *American Journal of Physiology. Lung Cellular and Molecular Physiology* 286 (4). https://doi.org/10.1152/AJPLUNG.00170.2003.

Zammit, Peter S., Frederic Relaix, Yosuke Nagata, Ana Pérez Ruiz, Charlotte A. Collins, Terence A. Partridge, and Jonathan R. Beauchamp. 2006. “Pax7 and Myogenic Progression in Skeletal Muscle Satellite Cells.” *Journal of Cell Science* 119 (Pt 9): 1824–32. https://doi.org/10.1242/JCS.02908.

Zaw-Tun, H. A., and A. R. Burdi. 1985a. “Reexamination of the Origin and Early Development of the Human Larynx.” *Acta Anat* 122 (3): 163–84. https://doi.org/10.1159/000145998.

Zaw-Tun, H A, and A R Burdi. 1985b. “Reexamination of the Origin and Early Development of the Human Larynx.” *Acta Anal* 122: 163–84.

Zhang, Zhaoyan. 2016a. “Mechanics of Human Voice Production and Control.” *J Acoust Soc Ame* 140 (4): 2614–35. https://doi.org/10.1121/1.4964509.

———. 2016b. “Mechanics of Human Voice Production and Control.” *The Journal of the Acoustical Society of America* 140 (4): 2614. https://doi.org/10.1121/1.4964509.

Zhao, Shancheng, Chao Deng, Zhen Wang, Liping Teng, and Jinghua Chen. 2015. “Heparan Sulfate 6-O-Sulfotransferase 3 Is Involved in Bone Marrow Mesenchymal Stromal Cell Osteogenic Differentiation.” *Biochemistry. Biokhimiia* 80 (3): 379–89. https://doi.org/10.1134/S000629791503013X.

Zheng, Xiao-Shuang, Qi Wang, Juan Min, Xu-Rui Shen, Qian Li, Qiu-Chen Zhao, Xi Wang, et al. 2022. “Single-Cell Landscape of Lungs Reveals Key Role of Neutrophil-Mediated Immunopathology during Lethal SARS-CoV-2 Infection.” *Journal of Virology* 96 (9).

https://doi.org/10.1128/JVI.00038-22.

Abbas, W., Kumar, A., & Herbein, G. (2015). The eEF1A Proteins: At the Crossroads of Oncogenesis, Apoptosis, and Viral Infections. *Frontiers in Oncology*, *5*(APR). https://doi.org/10.3389/FONC.2015.00075

Benoit, M. E., Clarke, E. V., Morgado, P., Fraser, D. A., & Tenner, A. J. (2012). Complement protein C1q directs macrophage polarization and limits inflammasome activity during the uptake of apoptotic cells. *Journal of Immunology (Baltimore, Md. : 1950)*, *188*(11), 5682. https://doi.org/10.4049/JIMMUNOL.1103760

Breiteneder-Geleff, S., Soleiman, A., Kowalski, H., Horvat, R., Amann, G., Kriehuber, E., Diem, K., Weninger, W., Tschachler, E., Alitalo, K., & Kerjaschki, D. (1999). Angiosarcomas express mixed endothelial phenotypes of blood and lymphatic capillaries: Podoplanin as a specific marker for lymphatic endothelium. *American Journal of Pathology*, *154*(2), 385–394. https://doi.org/10.1016/S0002-9440(10)65285-6

Brooks, M. D., Bennett, R. D., Weaver, A. L., Sebo, T. J., Eckert, S. E., Strehler, E. E., & Carr, A. B. (2013). Human Calmodulin-Like Protein CALML3: A Novel Marker for Normal Oral Squamous Mucosa That Is Downregulated in Malignant Transformation. *International Journal of Dentistry*, *2013*. https://doi.org/10.1155/2013/592843

Bruland, T., Beisvag, V., Erlandsen, S. E., Flatberg, A., Doseth, B., Sandvik, A. K., & Bakke, I. (2015). Genome-wide analysis of the oxyntic proliferative isthmus zone reveals ASPM as a possible gastric stem/progenitor cell marker over-expressed in cancer. *Journal of Pathology*, *237*(4), 447–459. https://doi.org/10.1002/PATH.4591

Carreon, T. A., Castellanos, A., Gasull, X., & Bhattacharya, S. K. (2017). Interaction of cochlin and mechanosensitive channel TREK-1 in trabecular meshwork cells influences the regulation of intraocular pressure. *Scientific Reports 2017 7:1*, *7*(1), 1–11. https://doi.org/10.1038/s41598-017-00430-2

Chapman, M. A., Meza, R., & Lieber, R. L. (2016). Skeletal Muscle Fibroblasts in Health and Disease. *Differentiation; Research in Biological Diversity*, *92*(3), 108. https://doi.org/10.1016/J.DIFF.2016.05.007

Chen, P., Zuo, N., Wu, C., Ma, J., Li, Y., Gu, J., Li, W., & Liu, S. (2022). MECOM promotes supporting cell proliferation and differentiation in cochlea. *Journal of Otology*, *17*(2), 59. https://doi.org/10.1016/J.JOTO.2021.11.002

Chengxiao, Z., & Ze, Y. (2015). Biological function and molecular mechanism of Twist2. *Yi Chuan = Hereditas / Zhongguo Yi Chuan Xue Hui Bian Ji*, *37*(1), 17–24. https://doi.org/10.16288/J.YCZZ.2015.01.003

De Araújo, R., Lôbo, M., Trindade, K., Silva, D. F., & Pereira, N. (2019). Fibroblast Growth Factors: A Controlling Mechanism of Skin Aging. *Skin Pharmacology and Physiology*, *32*(5), 275–282. https://doi.org/10.1159/000501145

De Leon-Oliva, D., Garcia-Montero, C., Fraile-Martinez, O., Boaru, D. L., García-Puente, L., Rios-Parra, A., Garrido-Gil, M. J., Casanova-Martín, C., García-Honduvilla, N., Bujan, J., Guijarro, L. G., Alvarez-Mon, M., & Ortega, M. A. (2023). AIF1: Function and Connection with Inflammatory Diseases. *Biology*, *12*(5). https://doi.org/10.3390/BIOLOGY12050694

Dozynkiewicz, M. A., Jamieson, N. B., MacPherson, I., Grindlay, J., vandenBerghe, P. V. E., vonThun, A., Morton, J. P., Gourley, C., Timpson, P., Nixon, C., McKay, C. J., Carter, R., Strachan, D., Anderson, K., Sansom, O. J., Caswell, P. T., & Norman, J. C. (2012). Rab25

and CLIC3 Collaborate to Promote Integrin Recycling from Late Endosomes/Lysosomes and Drive Cancer Progression. *Developmental Cell*, *22*(1), 131. https://doi.org/10.1016/J.DEVCEL.2011.11.008

Duynstee, M. L. G., Verwoerd-Verhoef, H. L., Verwoerd, C. D. A., & van Osch, G. J. V. M. (2002). The dual role of perichondrium in cartilage wound healing. *Plastic and Reconstructive Surgery*, *110*(4), 1073–1079. https://doi.org/10.1097/01.PRS.0000020991.10201.6C

Ferrari, M., Righi, M., Baldan, V., Wawrzyniecka, P., Bulek, A., Kinna, A., Ma, B., Bughda, R., Akbar, Z., Srivastava, S., Gannon, I., Robson, M., Sillibourne, J., Jha, R., El-Kholy, M., Amin, O. M., Kokalaki, E., Banani, M. A., Hussain, R., … Pule, M. (2024). Structure-guided engineering of immunotherapies targeting TRBC1 and TRBC2 in T cell malignancies. *Nature Communications 2024 15:1*, *15*(1), 1–16. https://doi.org/10.1038/s41467-024-45854-3

Foldi, J., Shang, Y., Zhao, B., Ivashkiv, L. B., & Hu, X. (2016). RBP-J is required for M2 macrophage polarization in response to chitin and mediates expression of a subset of M2 genes. *Protein & Cell*, *7*(3), 201–209. https://doi.org/10.1007/S13238-016-0248-7

Foote, A. G., Lungova, V., & Thibeault, S. L. (2022). Piezo1-expressing vocal fold epithelia modulate remodeling via effects on self-renewal and cytokeratin differentiation. *Cellular and Molecular Life Sciences : CMLS*, *79*(12). https://doi.org/10.1007/S00018-022-04622-6

Foote, A. G., & Thibeault, S. L. (2021). Sensory innervation of the larynx and the search for mucosal mechanoreceptors. *Journal of Speech, Language, and Hearing Research*, *64*(2), 371–391. https://doi.org/10.1044/2020_JSLHR-20-00350

Foote, A. G., Wang, Z., Kendziorski, C., & Thibeault, S. L. (2019). Tissue specific human fibroblast differential expression based on RNAsequencing analysis. *BMC Genomics 2019 20:1*, *20*(1), 1–19. https://doi.org/10.1186/S12864-019-5682-5

Frisdal, A., & Trainor, P. A. (2014). Development and evolution of the pharyngeal apparatus. *Wiley Interdisciplinary Reviews: Developmental Biology*, *3*(6), 403–418. https://doi.org/10.1002/WDEV.147

Fujiki, R. B., Olson-Greb, B., & Thibeault, S. L. (2024). Clinical Profiles of Children and Adolescents With Induced Laryngeal Obstruction (ILO) and Exercise Induced Laryngeal Obstruction (EILO). *The Annals of Otology, Rhinology, and Laryngology*, *133*(2), 136–144. https://doi.org/10.1177/00034894231190842

Fujiwara-Tani, R., Mori, S., Ogata, R., Sasaki, R., Ikemoto, A., Kishi, S., Kondoh, M., & Kuniyasu, H. (2023). Claudin-4: A New Molecular Target for Epithelial Cancer Therapy. *International Journal of Molecular Sciences*, *24*(6). https://doi.org/10.3390/IJMS24065494

Funk, S. D., Bayer, R. H., Malone, A. F., McKee, K. K., Yurchenco, P. D., & Miner, J. H. (2018). Pathogenicity of a human laminin β2 mutation revealed in models of alport syndrome. *Journal of the American Society of Nephrology*, *29*(3), 949–960. https://doi.org/10.1681/ASN.2017090997/-/DCSUPPLEMENTAL

Galvagni, F., Nardi, F., Maida, M., Bernardini, G., Vannuccini, S., Petraglia, F., Santucci, A., & Orlandini, M. (2016). CD93 and dystroglycan cooperation in human endothelial cell adhesion and migration adhesion and migration. *Oncotarget*, *7*(9), 10090–10103. https://doi.org/10.18632/ONCOTARGET.7136

Gao, J., Li, C., Li, W., Chen, H., Fu, Y., & Yi, Z. (2021). Increased UBE2L6 regulated by type 1 interferon as potential marker in TB. *Journal of Cellular and Molecular Medicine*, *25*(24), 11232. https://doi.org/10.1111/JCMM.17046

Gather, L., Nath, N., Falckenhayn, C., Oterino-Sogo, S., Bosch, T., Wenck, H., Winnefeld, M., Grönniger, E., Simm, S., & Siracusa, A. (2022). Macrophages Are Polarized toward an Inflammatory Phenotype by their Aged Microenvironment in the Human Skin. *Journal of Investigative Dermatology*, *142*(12), 3136-3145.e11. https://doi.org/10.1016/J.JID.2022.06.023

Goel, M., Sienkiewicz, A. E., Picciani, R., Wang, J., Lee, R. K., & Bhattacharya, S. K. (2012). Cochlin, intraocular pressure regulation and mechanosensing. *PloS One*, *7*(4). https://doi.org/10.1371/JOURNAL.PONE.0034309

Greaney, A. M., Adams, T. S., Brickman Raredon, M. S., Gubbins, E., Schupp, J. C., Engler, A. J., Ghaedi, M., Yuan, Y., Kaminski, N., & Niklason, L. E. (2020). Platform Effects on Regeneration by Pulmonary Basal Cells as Evaluated by Single-Cell RNA Sequencing. *Cell Reports*, *30*(12), 4250. https://doi.org/10.1016/J.CELREP.2020.03.004

Griffin, K., Pedersen, H., Stauss, K., Lungova, V., & Thibeault, S. L. (2021a). Characterization of intrauterine growth, proliferation and biomechanical properties of the murine larynx. *PLOS ONE*, *16*(1), e0245073. https://doi.org/10.1371/JOURNAL.PONE.0245073

Griffin, K., Pedersen, H., Stauss, K., Lungova, V., & Thibeault, S. L. (2021b). Characterization of intrauterine growth, proliferation and biomechanical properties of the murine larynx. *PLOS ONE*, *16*(1), e0245073. https://doi.org/10.1371/JOURNAL.PONE.0245073

Gvaramia, D., Kern, J., Jakob, Y., Zenobi-Wong, M., & Rotter, N. (2022). Regenerative Potential of Perichondrium: A Tissue Engineering Perspective. *Tissue Engineering - Part B:*

Reviews, *28*(3), 531–541. https://doi.org/10.1089/TEN.TEB.2021.0054/ASSET/IMAGES/TEN.TEB.2021.0054_FIGURE6.JPG

Han, C., Leonardo, T. R., Romana-Souza, B., Shi, J., Keiser, S., Yuan, H., Altakriti, M., Ranzer, M. J., Ferri-Borgogno, S., Mok, S. C., Koh, T. J., Hong, S. J., Chen, L., & DiPietro, L. A. (2023). Microfibril-associated protein 5 and the regulation of skin scar formation. *Scientific Reports 2023 13:1*, *13*(1), 1–15. https://doi.org/10.1038/s41598-023-35558-x

Hancock, L. A., Hennessy, C. E., Solomon, G. M., Dobrinskikh, E., Estrella, A., Hara, N., Hill, D. B., Kissner, W. J., Markovetz, M. R., Grove Villalon, D. E., Voss, M. E., Tearney, G. J., Carroll, K. S., Shi, Y., Schwarz, M. I., Thelin, W. R., Rowe, S. M., Yang, I. V., Evans, C. M., & Schwartz, D. A. (2018). Muc5b overexpression causes mucociliary dysfunction and enhances lung fibrosis in mice. *Nature Communications 2018 9:1*, *9*(1), 1–10. https://doi.org/10.1038/s41467-018-07768-9

Hewitt, R. J., & Lloyd, C. M. (2021a). Regulation of immune responses by the airway epithelial cell landscape. *Nature Reviews. Immunology*, *21*(6), 347. https://doi.org/10.1038/S41577-020-00477-9

Hewitt, R. J., & Lloyd, C. M. (2021b). Regulation of immune responses by the airway epithelial cell landscape. *Nature Reviews Immunology 2021 21:6*, *21*(6), 347–362. https://doi.org/10.1038/s41577-020-00477-9

Horowitz, A., Yu, H., Pandey, S., Mishra, B., Sahoo, D., & Lipschultz, J. (2024). C1QA is an invariant biomarker for tissue macrophages. *BioRxiv*, 2024.01.26.577475. https://doi.org/10.1101/2024.01.26.577475

Hu, N., Mo, X. M., Xu, S. N., Tang, H. N., Zhou, Y. H., Li, L., & Zhou, H. De. (2022). A novel antimicrobial peptide derived from human BPIFA1 protein protects against Candida albicans infection. *Innate Immunity*, *28*(2), 67. https://doi.org/10.1177/17534259221080543

Ito, S., & Nagata, K. (2017). Biology of Hsp47 (Serpin H1), a collagen-specific molecular chaperone. *Seminars in Cell & Developmental Biology*, *62*, 142–151. https://doi.org/10.1016/J.SEMCDB.2016.11.005

Ivanchenko, M. V., Hathaway, D. M., Klein, A. J., Pan, B., Strelkova, O., De-la-Torre, P., Wu, X., Peters, C. W., Mulhall, E. M., Booth, K. T., Goldstein, C., Brower, J., Sotomayor, M., Indzhykulian, A. A., & Corey, D. P. (2023). Mini-PCDH15 gene therapy rescues hearing in a mouse model of Usher syndrome type 1F. *Nature Communications*, *14*(1). https://doi.org/10.1038/S41467-023-38038-Y

Ji, J. J., & Fan, J. (2019). Discovering myeloid cell heterogeneity in the lung by means of next generation sequencing. *Military Medical Research*, *6*(1), 1–10. https://doi.org/10.1186/S40779-019-0222-9/FIGURES/1

Karalı, F. S., Azizli, E., Tadihan-Özkan, E., Eskioğlu, E., Sari, A., & Resuloglu, A. (2022). Voice Therapy Efficacy in Pediatric Professional Voice Users With Vocal Fold Nodules: A Preliminary Study. *Journal of Voice : Official Journal of the Voice Foundation*. https://doi.org/10.1016/J.JVOICE.2022.09.005

Karetsou, Z., Sandaltzopoulos, R., Frangou-Lazaridis, M., Lai, C. Y., Tsolas, O., Becker, P. B., & Papamarcaki, T. (1998). Prothymosin α modulates the interaction of histone H1 with chromatin. *Nucleic Acids Research*, *26*(13), 3111–3118. https://doi.org/10.1093/NAR/26.13.3111

Kelly, T. K., Miranda, T. B., Liang, G., Berman, B. P., Lin, J. C., Tanay, A., & Jones, P. A. (2010). H2A.Z Maintenance During Mitosis Reveals Nucleosome Shifting on Mitotically Silenced Genes. *Molecular Cell*, *39*(6), 901. https://doi.org/10.1016/J.MOLCEL.2010.08.026

Khandelwal, S., & Roche, P. A. (2010). Distinct MHC Class II Molecules Are Associated on the Dendritic Cell Surface in Cholesterol-dependent Membrane Microdomains. *Journal of Biological Chemistry*, *285*(46), 35303–35310. https://doi.org/10.1074/JBC.M110.147793

Kuo, C. S., Darmanis, S., de Arce, A. D., Liu, Y., Almanzar, N., Wu, T. T. H., Quake, S. R., & Krasnow, M. A. (2022). Neuroendocrinology of the lung revealed by single-cell RNA sequencing. *ELife*, *11*. https://doi.org/10.7554/ELIFE.78216

Kurita, T., Chitose, S. ichi, Sato, K., Sakazaki, T., Fukahori, M., Sueyoshi, S., & Umeno, H. (2019). Pathological mechanisms of laryngeal papillomatosis based on laryngeal epithelial characteristics. *Laryngoscope Investigative Otolaryngology*, *4*(1), 89. https://doi.org/10.1002/LIO2.242

La, L., Wang, L., Qin, F., Jiang, J., He, S., Wang, C., & Li, Y. (2018). Zhen-wu-tang ameliorates adenine-induced chronic renal failure in rats: regulation of the canonical Wnt4/beta-catenin signaling in the kidneys. *Journal of Ethnopharmacology*, *219*, 81–90. https://doi.org/10.1016/J.JEP.2017.12.013

Laitman, B. M., Charytonowicz, D., Zhu, A. J., Lynch, K., Varelas, E. A., Burton, M., Andreou, C., Kore, P., Kirke, D. N., Chen, Y. W., Beaumont, K. G., Sebra, R., Genden, E. M., & Courey, M. S. (2024). High-Resolution Profiling of Human Vocal Fold Cellular Landscapes With Single-Nuclei RNA Sequencing. *The Laryngoscope*. https://doi.org/10.1002/LARY.31334

Lee, J. M., Roy, N., Park, A., Muntz, H., Redmond, S. M., & Smith, M. (2022). Self-regulation in children with vocal fold nodules: A multilevel analysis. *Journal of Communication Disorders*, *97*. https://doi.org/10.1016/J.JCOMDIS.2022.106203

Lesourne, R., Uehara, S., Lee, J., Song, K. D., Li, L. Q., Pinkhasov, J., Zhang, Y., Weng, N. P., Wildt, K. F., Wang, L., Bosselut, R., & Love, P. E. (2009). THEMIS, a new T cell specific protein important for late thymocyte development. *Nature Immunology*, *10*(8), 840. https://doi.org/10.1038/NI.1768

Levendoski, E. E., Leydon, C., & Thibeault, S. L. (2014). Vocal Fold Epithelial Barrier in Health and Injury: A Research Review. *Journal of Speech, Language, and Hearing Research*, *57*(5), 1679–1691. https://doi.org/10.1044/2014_JSLHR-S-13-0283

Li, J., Li, E., Czepielewski, R. S., Cohen, P., Tsai, L., & Rosen Correspondence, E. D. (2021). Neurotensin is an anti-thermogenic peptide produced by lymphatic endothelial cells. *Cell Metabolism*, *33*, 1449-1465.e6. https://doi.org/10.1016/j.cmet.2021.04.019

Liu, Z., Jin, Y. Q., Chen, L., Wang, Y., Yang, X., Cheng, J., Wu, W., Qi, Z., & Shen, Z. (2015). Specific Marker Expression and Cell State of Schwann Cells during Culture In Vitro. *PLoS ONE*, *10*(4). https://doi.org/10.1371/JOURNAL.PONE.0123278

Liu, Z. Q., Dai, H., Yao, L., Chen, W. F., Wang, Y., Ma, L. Y., Li, X. Q., Lin, S. L., He, M. J., Gao, P. T., Liu, X. Y., Xu, J. X., Xu, X. Y., Wang, K. H., Wang, L., Chen, L., Zhou, P. H., & Li, Q. L. (2023). A single-cell transcriptional landscape of immune cells shows disease-specific changes of T cell and macrophage populations in human achalasia. *Nature Communications 2023 14:1*, *14*(1), 1–19. https://doi.org/10.1038/s41467-023-39750-5

Lunga, T., Thibeault, S. L., & Francis, D. O. (2022). Economic Burden Associated With Management of Paradoxical Vocal Fold Motion Disorder. *The Laryngoscope*, *132*(1), 142–147. https://doi.org/10.1002/LARY.29754

Lungova, V., Verheyden, J. M., Herriges, J., Sun, X., & Thibeault, S. L. (2015). Ontogeny of the mouse vocal fold epithelium. *Dev Biol*, *399*(2), 2. https://doi.org/10.1016/j.ydbio.2014.12.037

Lungova, V., Verheyden, J. M., Sun, X., & Thibeault, S. L. (2018a). β-catenin signaling is essential for mammalian larynx recanalization and the establishment of vocal fold progenitor cells. *Development (Cambridge)*, *145*(4). https://doi.org/10.1242/DEV.157677/264506/AM/BETA-CATENIN-SIGNALING-IS-ESSENTIAL-FOR-MAMMALIAN

Lungova, V., Verheyden, J. M., Sun, X., & Thibeault, S. L. (2018b). β-catenin signaling is essential for mammalian larynx recanalization and the establishment of vocal fold progenitor cells. *Development (Cambridge)*, *145*(4). https://doi.org/10.1242/DEV.157677/264506/AM/BETA-CATENIN-SIGNALING-IS-ESSENTIAL-FOR-MAMMALIAN

Marshall, H., Morrison, A., Studer, M., Pöpperl, H., & Krumlauf, R. (1996). Retinoids and Hox genes. *FASEB*, *10*(9), 969–978. https://doi.org/10.1096/fasebj.10.9.8801179

Martinez, F. O., Helming, L., Milde, R., Varin, A., Melgert, B. N., Draijer, C., Thomas, B., Fabbri, M., Crawshaw, A., Ho, L. P., Hacken, N. H. T., Jiménez, V. C., Kootstra, N. A., Hamann, J., Greaves, D. R., Locati, M., Mantovani, A., & Gordon, S. (2013). Genetic programs expressed in resting and IL-4 alternatively activated mouse and human

macrophages: similarities and differences. *Blood*, *121*(9), e57–e69. https://doi.org/10.1182/BLOOD-2012-06-436212

Maselli, R. A., Arredondo, J., Ferns, M. J., & Wollmann, R. L. (2012). Synaptic basal lamina–associated congenital myasthenic syndromes. *Annals of the New York Academy of Sciences*, *1275*(1), 36–48. https://doi.org/10.1111/J.1749-6632.2012.06807.X

Mattiola, I., Tomay, F., De Pizzol, M., Silva-Gomes, R., Savino, B., Gulic, T., Doni, A., Lonardi, S., Astrid Boutet, M., Nerviani, A., Carriero, R., Molgora, M., Stravalaci, M., Morone, D., Shalova, I. N., Lee, Y., Biswas, S. K., Mantovani, G., Sironi, M., … Locati, M. (2019). The macrophage tetraspan MS4A4A enhances dectin-1-dependent NK cell–mediated resistance to metastasis. *Nature Immunology*, *20*(8), 1012–1022. https://doi.org/10.1038/S41590-019-0417-Y

Miner, J. H., Cunningham, J., & Sanes, J. R. (1998). Roles for laminin in embryogenesis: Exencephaly, syndactyly, and placentopathy in mice lacking the laminin α5 chain. *Journal of Cell Biology*, *143*(6), 1713–1723. https://doi.org/10.1083/JCB.143.6.1713

Muhl, L., Mocci, G., Pietilä, R., Liu, J., He, L., Genové, G., Leptidis, S., Gustafsson, S., Buyandelger, B., Raschperger, E., Hansson, E. M., Björkegren, J. L. M., Vanlandewijck, M., Lendahl, U., & Betsholtz, C. (2022). A single-cell transcriptomic inventory of murine smooth muscle cells. *Developmental Cell*, *57*(20), 2426-2443.e6. https://doi.org/10.1016/J.DEVCEL.2022.09.015

Nguyen, T. T., Mitchell, J. M., Kiel, M. D., Kenny, C. P., Li, H., Jones, K. L., Cornell, R. A., Williams, T. J., Nichols, J. T., & Van Otterloo, E. (2024). TFAP2 paralogs regulate midfacial development in part through a conserved ALX genetic pathway. *Development*

(Cambridge), *151*(1). https://doi.org/10.1242/DEV.202095/336058/AM/TFAP2-PARALOGS-REGULATE-MIDFACIAL-DEVELOPMENT-IN

Niewiadomski, P., Niedziółka, S. M., Markiewicz, Ł., Uśpieński, T., Baran, B., & Chojnowska, K. (2019). Gli Proteins: Regulation in Development and Cancer. *Cells*, *8*(2). https://doi.org/10.3390/CELLS8020147

Ophir, M. J., Liu, B. C., & Bunnell, S. C. (2013). The N terminus of SKAP55 enables T cell adhesion to TCR and integrin ligands via distinct mechanisms. *The Journal of Cell Biology*, *203*(6), 1021–1041. https://doi.org/10.1083/JCB.201305088

Pascal, L. E., Goo, Y. A., Vêncio, R. Z. N., Page, L. S., Chambers, A. A., Liebeskind, E. S., Takayama, T. K., True, L. D., & Liu, A. Y. (2009). Gene expression down-regulation in CD90+ prostate tumor-associated stromal cells involves potential organ-specific genes. *BMC Cancer*, *9*, 317. https://doi.org/10.1186/1471-2407-9-317

Pavlakis, E., Chiotaki, R., & Chalepakis, G. (2011). The role of Fras1/Frem proteins in the structure and function of basement membrane. *The International Journal of Biochemistry & Cell Biology*, *43*(4), 487–495. https://doi.org/10.1016/J.BIOCEL.2010.12.016

Pickard, M. R., Mourtada-Maarabouni, M., & Williams, G. T. (2011). Candidate tumour suppressor Fau regulates apoptosis in human cells: an essential role for Bcl-G. *Biochimica et Biophysica Acta*, *1812*(9), 1146–1153. https://doi.org/10.1016/J.BBADIS.2011.04.009

Plasschaert, L. W., Žilionis, R., Choo-Wing, R., Savova, V., Knehr, J., Roma, G., Klein, A. M., & Jaffe, A. B. (2018). A single cell atlas of the tracheal epithelium reveals the CFTR-rich pulmonary ionocyte. *Nature*, *560*(7718), 377. https://doi.org/10.1038/S41586-018-0394-6

Ponichtera, H. E., Shainheit, M. G., Liu, B. C., Raychowdhury, R., Larkin, B. M., Russo, J. M., Salantes, D. B., Lai, C.-Q., Parnell, L. D., Yun, T. J., Cheong, C., Bunnell, S. C., Hacohen,

N., & Stadecker, M. J. (2014). CD209a Expression on Dendritic Cells is Critical for the Development of Pathogenic Th17 Cell Responses in Murine Schistosomiasis. *Journal of Immunology (Baltimore, Md. : 1950)*, *192*(10), 4655. https://doi.org/10.4049/JIMMUNOL.1400121

Qu, H., Jin, Q., & Quan, C. (2021). CLDN6: From Traditional Barrier Function to Emerging Roles in Cancers. *International Journal of Molecular Sciences*, *22*(24). https://doi.org/10.3390/IJMS222413416

Sadri, G., Fischer, A. G., Brittian, K. R., Elliott, E., Nystoriak, M. A., Uchida, S., Wysoczynski, M., Leask, A., Jones, S. P., & Moore, J. B. (2022). Collagen type XIX regulates cardiac extracellular matrix structure and ventricular function. *Matrix Biology*, *109*, 49–69. https://doi.org/10.1016/J.MATBIO.2022.03.007

Schulz, C., Perdiguero, E. G., Chorro, L., Szabo-Rogers, H., Cagnard, N., Kierdorf, K., Prinz, M., Wu, B., Jacobsen, S. E. W., Pollard, J. W., Frampton, J., Liu, K. J., & Geissmann, F. (2012). A lineage of myeloid cells independent of myb and hematopoietic stem cells. *Science*, *335*(6077), 86–90. https://doi.org/10.1126/SCIENCE.1219179/SUPPL_FILE/SCHULZGOMEZ1219179.AVI

Simmons Beck, R., Liang, O. D., & Klinger, J. R. (2023). Light at the ENDothelium-role of Sox17 and Runx1 in endothelial dysfunction and pulmonary arterial hypertension. *Frontiers in Cardiovascular Medicine*, *10*. https://doi.org/10.3389/FCVM.2023.1274033

Smits, P., Li, P., Mandel, J., Zhang, Z., Deng, J. M., Behringer, R. R., De Crombrugghe, B., & Lefebvre, V. (2001). The transcription factors L-Sox5 and Sox6 are essential for cartilage formation. *Developmental Cell*, *1*(2), 277–290. https://doi.org/10.1016/S1534-5807(01)00003-X

Sperber, S. M., & Dawid, I. B. (2008). barx1 is necessary for ectomesenchyme proliferation and osteochondroprogenitor condensation in the zebrafish pharyngeal arches. *Developmental Biology*, *321*(1), 101. https://doi.org/10.1016/J.YDBIO.2008.06.004

Sprenkeler, E. G. G., Zandstra, J., van Kleef, N. D., Goetschalckx, I., Verstegen, B., Aarts, C. E. M., Janssen, H., Tool, A. T. J., van Mierlo, G., van Bruggen, R., Jongerius, I., & Kuijpers, T. W. (2022). S100A8/A9 Is a Marker for the Release of Neutrophil Extracellular Traps and Induces Neutrophil Activation. *Cells*, *11*(2). https://doi.org/10.3390/CELLS11020236

Starkova, T., Polyanichko, A., Tomilin, A. N., & Chikhirzhina, E. (2023). Structure and Functions of HMGB2 Protein. *International Journal of Molecular Sciences*, *24*(9). https://doi.org/10.3390/IJMS24098334

Sun, X., & Kaufman, P. D. (2018). Ki-67: more than a proliferation marker. *Chromosoma*, *127*(2), 175. https://doi.org/10.1007/S00412-018-0659-8

Surmann-Schmitt, C., Dietz, U., Kireva, T., Adam, N., Park, J., Tagariello, A., Önnerfjord, P., Heinegård, D., Schlötzer-Schrehardt, U., Deutzmann, R., Von Der Mark, K., & Stock, M. (2008). Ucma, a Novel Secreted Cartilage-specific Protein with Implications in Osteogenesis. *Journal of Biological Chemistry*, *283*(11), 7082–7093. https://doi.org/10.1074/JBC.M702792200

Tabler, J. M., Rigney, M. M., Berman, G. J., Gopalakrishnan, S., Heude, E., Al-Lami, H. A., Yannakoudiadkis, B. Z., Fitch, R. D., Carter, C., Vokes, S., Liu, K. J., Tajbakhsh, S., Egnor, S. E. R., & Wallingford, J. B. (2017). Cilia-mediated hedgehog signaling controls form and function in the mammalian larynx. *ELife*, *6*, 1–26. https://doi.org/10.7554/elife.19153

Tuan, N. M., & Lee, C. H. (2020). Role of Anillin in Tumour: From a Prognostic Biomarker to a Novel Target. *Cancers*, *12*(6), 1–27. https://doi.org/10.3390/CANCERS12061600

van Kuijk, K., McCracken, I. R., Tillie, R. J. H. A., Asselberghs, S. E. J., Kheder, D. A., Muitjens, S., Jin, H., Taylor, R. S., Schreur, R. W., Kuppe, C., Dobie, R., Ramachandran, P., Gijbels, M. J., Temmerman, L., Kirkwoord, P. M., Luyten, J., Li, Y., Noels, H., Goossens, P., … Sluimer, J. C. (2023). Human and murine fibroblast single-cell transcriptomics reveals fibroblast clusters are differentially affected by ageing and serum cholesterol. *Cardiovascular Research*, *119*(7), 1509–1523. https://doi.org/10.1093/CVR/CVAD016

Vermot, J., Niederreither, K., Garnier, J. M., Chambon, P., & Dollé, P. (2003). Decreased embryonic retinoic acid synthesis results in a DiGeorge syndrome phenotype in newborn mice. *Proc Natl Acad Sci USA*, *100*(4), 1763–1768. https://doi.org/10.1073/pnas.0437920100

Walter, L. D., Orton, J. L., Fong, E. H. H., Maymi, V. I., Rudd, B. D., Elisseeff, J. H., & Cosgrove, B. D. (2023). Single-cell transcriptomic analysis of skeletal muscle regeneration across mouse lifespan identifies altered stem cell states associated with senescence. *BioRxiv*. https://doi.org/10.1101/2023.05.25.542370

Wendt, K. D., Brown, J., Lungova, V., Mohad, V., Kendziorski, C., & Thibeault, S. L. (2022). Transcriptome Dynamics in the Developing Larynx, Trachea, and Esophagus. *Frontiers in Cell and Developmental Biology*, *0*, 1319. https://doi.org/10.3389/FCELL.2022.942622

Wolbert, J., Li, X., Heming, M., Mausberg, A. K., Akkermann, D., Frydrychowicz, C., Fledrich, R., Groeneweg, L., Schulz, C., Stettner, M., Gonzalez, N. A., Wiendl, H., Stassart, R., & zu Hörste, G. M. (2020). Redefining the heterogeneity of peripheral nerve cells in health and autoimmunity. *Proceedings of the National Academy of Sciences of the United States of*

America, *117*(17), 9466–9476. https://doi.org/10.1073/PNAS.1912139117/SUPPL_FILE/PNAS.1912139117.SD14.XLSX

Xiang, M., Grosso, R. A., Takeda, A., Pan, J., Bekkhus, T., Brulois, K., Dermadi, D., Nordling, S., Vanlandewijck, M., Jalkanen, S., Ulvmar, M. H., & Butcher, E. C. (2020). A Single-Cell Transcriptional Roadmap of the Mouse and Human Lymph Node Lymphatic Vasculature. *Frontiers in Cardiovascular Medicine*, *7*, 523939. https://doi.org/10.3389/FCVM.2020.00052/BIBTEX

Xie, T., Wang, Y., Deng, N., Huang, G., Taghavifar, F., Geng, Y., Liu, N., Kulur, V., Yao, C., Chen, P., Liu, Z., Stripp, B., Tang, J., Liang, J., Noble, P. W., & Jiang, D. (2018). Single-Cell Deconvolution of Fibroblast Heterogeneity in Mouse Pulmonary Fibrosis. *Cell Reports*, *22*(13), 3625. https://doi.org/10.1016/J.CELREP.2018.03.010

Yamamoto, M., Legendre, N. P., Biswas, A. A., Lawton, A., Yamamoto, S., Tajbakhsh, S., Kardon, G., & Goldhamer, D. J. (2018). Loss of MyoD and Myf5 in Skeletal Muscle Stem Cells Results in Altered Myogenic Programming and Failed Regeneration. *Stem Cell Reports*, *10*(3), 956. https://doi.org/10.1016/J.STEMCR.2018.01.027

You, Y., Huang, T., Richer, E. J., Schmidt, J. E. H., Zabner, J., Borok, Z., & Brody, S. L. (2004). Role of f-box factor foxj1 in differentiation of ciliated airway epithelial cells. *American Journal of Physiology. Lung Cellular and Molecular Physiology*, *286*(4). https://doi.org/10.1152/AJPLUNG.00170.2003

Zammit, P. S., Relaix, F., Nagata, Y., Ruiz, A. P., Collins, C. A., Partridge, T. A., & Beauchamp, J. R. (2006). Pax7 and myogenic progression in skeletal muscle satellite cells. *Journal of Cell Science*, *119*(Pt 9), 1824–1832. https://doi.org/10.1242/JCS.02908

Zhang, L., Zhu, T., Miao, H., & Liang, B. (2021). The Calcium Binding Protein S100A11 and Its Roles in Diseases. *Frontiers in Cell and Developmental Biology*, *9*. https://doi.org/10.3389/FCELL.2021.693262

Zhang, Q., Pan, Y., Ji, J., Xu, Y., Zhang, Q., & Qin, L. (2021a). Roles and action mechanisms of WNT4 in cell differentiation and human diseases: a review. *Cell Death Discovery 2021 7:1*, *7*(1), 1–10. https://doi.org/10.1038/s41420-021-00668-w

Zhang, Q., Pan, Y., Ji, J., Xu, Y., Zhang, Q., & Qin, L. (2021b). Roles and action mechanisms of WNT4 in cell differentiation and human diseases: a review. *Cell Death Discovery*, *7*(1). https://doi.org/10.1038/S41420-021-00668-W

Zheng, X.-S., Wang, Q., Min, J., Shen, X.-R., Li, Q., Zhao, Q.-C., Wang, X., Jiang, R.-D., Geng, R., Chen, Y., Zhu, Y., Li, B., Zhang, W., Li, A., Xie, T.-T., Liu, M.-Q., Cheng, L., Shi, Z.-L., & Zhou, P. (2022). Single-Cell Landscape of Lungs Reveals Key Role of Neutrophil-Mediated Immunopathology during Lethal SARS-CoV-2 Infection. *Journal of Virology*, *96*(9). https://doi.org/10.1128/JVI.00038-22

Zhou, Y., Yang, Y., Guo, L., Qian, J., Ge, J., Sinner, D., Ding, H., Califano, A., & Cardoso, W. V. (2022). Airway basal cells show regionally distinct potential to undergo metaplastic differentiation. *ELife*, *11*, 80083. https://doi.org/10.7554/ELIFE.80083

Zuo, W. L., Rostami, M. R., LeBlanc, M., Kaner, R. J., O'Beirne, S. L., Mezey, J. G., Leopold, P. L., Quast, K., Visvanathan, S., Fine, J. S., Thomas, M. J., & Crystal, R. G. (2020). Dysregulation of club cell biology in idiopathic pulmonary fibrosis. *PLoS ONE*, *15*(9). https://doi.org/10.1371/JOURNAL.PONE.0237529